Quantification of Groundwater Recharge

Peter Cook and Philip Brunner

THE **GROUNDWATER** PROJECT

Quantification of

Groundwater Recharge

The Groundwater Project

Peter Cook

Professorial Research Fellow
National Centre for Groundwater Research and Training
Flinders University
Bedford Park, South Australia, Australia

Philip Brunner

Professor
Centre d'Hydrogéologie et de Géothermie (CHYN)
Université de Neuchâtel
Neuchâtel, Switzerland

Quantification of Groundwater Recharge

The Groundwater Project
Guelph, Ontario, Canada

The Groundwater Project relies on private funding for book production and management of the Project.

Please consider sponsoring the Groundwater Project so that our books will continue to be freely available. https://gw-project.org/donate/↗

Thank you.

Please consider signing up for the GW-Project mailing list to stay informed about new book releases, events, and ways to participate in the GW-Project. When you sign up for our email list it helps us build a global groundwater community. Sign up↗.

Table of Contents

The Groundwater Project Foreword

The United Nations (UN)-Water Summit on Groundwater, held from 7 to 8 December 2022, at the UNESCO headquarters in Paris, France, concluded with a call for governments and other stakeholders to scale up their efforts to better manage groundwater. The intent of the call to action was to inform relevant discussions at the UN 2023 Water Conference held from 22 to 24 March 2023 at the UN headquarters in New York City. One of the required actions is *strengthening human and institutional capacity*, for which groundwater education is fundamental.

The <u>UN-Water website</u>↗ states that *more than three billion people worldwide depend on water that crosses national borders*. There are 592 transboundary aquifers, yet most do not have an intergovernmental cooperation agreement in place for sharing and managing the aquifer. Moreover, while groundwater plays a key role in global stability and prosperity, it also makes up 99 percent of all liquid freshwater—accordingly, groundwater is at the heart of the freshwater crisis. *Groundwater is an invaluable resource*.

The Groundwater Project (GW-Project), a registered Canadian charity with its beginnings in 2018, pioneers in advancing understanding of groundwater and, thus, enables *building the human capacity for the development and management of groundwater*. The GW-Project is not government funded and relies on donations from individuals, organizations, and companies. The GW-Project creates and publishes high-quality books about *all-things-groundwater* that are scientifically significant and/or relevant to societal and ecological needs. Our books synthesize knowledge, are rigorously peer reviewed and translated into many languages. Groundwater is 'hidden' and, therefore, our books have a strong emphasis on visualizations essential to support the spatial thinking and conceptualization in space and time of processes, problems, and solutions. Based on *our philosophy that high quality groundwater knowledge should be accessible to everyone*, The GW-Project provides all publications for free.

The GW-Project embodies a new type of global educational endeavor made possible by the contributions of a dedicated international group of over 1000 volunteer professionals from a broad range of disciplines, and from 70 countries on six continents. Academics, practitioners, and retirees contribute by writing and/or reviewing books aimed at diverse levels of readers including children, youth, undergraduate and graduate students, groundwater professionals, and the general public.

The GW-Project started publishing books in August 2020; by the end of 2024, we have published 55 original books and 77 translations (55 languages). Revised editions of the books are published from time to time. In 2024, interactive groundwater education tools and groundwater videos were added to our website, <u>gw-project.org</u>↗.

We thank our individual and corporate sponsors for their ongoing financial support. Please consider sponsoring the GW-Project so we can continue to publish books free of charge.

The Groundwater Project *Board of Directors*, January 2025

Foreword

Knowledge of groundwater recharge is important for good environmental management. Recharge is the water from precipitation that infiltrates far enough below the ground surface to cross the water table where it is added to the groundwater zone. Groundwater recharge is one of the most important processes of the water cycle because this addition of water to the groundwater zone allows aquifers to sustain water supply to wells on which our civilization relies. Furthermore, this recharge water supplies the baseflow to streams and rivers as well as seepage to wetlands, peatlands and desert oases that support vital, sensitive ecological systems.

Although the concept of water infiltrating to the groundwater zone is readily visualized, the task of determining the amount of recharge over a period, such as annual recharge, is fraught with difficulties and uncertainty because many factors are involved. The timing of recharge varies from region to region. In some arid regions recharge occurs only when there is an exceptionally large precipitation event, perhaps only once every few years, while in humid regions recharge commonly occurs during many precipitation events throughout the year.

This book is global in its examination of recharge with emphasis on the circumstances of recharge, the processes that govern recharge, and the estimation of recharge rates. This book is a companion to a book previously published by the Groundwater Project, <u>Groundwater Resource Development: Effect and Sustainability</u>↗, that examines how recharge relates to sustainable and unsustainable use of groundwater resources.

The authors of this book have conducted recharge studies in many countries around the globe. Dr. Peter Cook is a Professional Research Fellow at Flinders University, Australia and Director of the Australia National Centre for Groundwater Research and Training. He also authored the Groundwater Project book titled <u>Introduction to Isotopes and Environmental Tracers as Indicators of Groundwater Flow</u>↗. Dr. Philip Brunner is a professor at the Centre for Hydrogeology at the University of Neuchatel, Switzerland, where he leads the Hydrogeological Processes group.

John Cherry, The Groundwater Project Leader

Guelph, Ontario, Canada, February 2025

Preface

Hydrogeologists should understand how groundwater recharges aquifers, the methods available for quantifying this component of the water budget, and the strengths and weaknesses of the different methods. Understanding the sources of recharge can be important for predicting the impacts of land use change and climate change on groundwater resources and for determining the vulnerability of groundwater resources to contamination by human activity. Recharge rates are also important input parameters for many groundwater models—models that are essential tools for predicting the impacts of groundwater extraction.

Changes in recharge rates can have important implications for groundwater resources and groundwater dependent ecosystems. Decreases in recharge rates—for example, during drought or due to climate change—can lead to declines in groundwater levels, leading to reductions in spring and river flows and adverse impacts on groundwater-dependent ecosystems. Increases in recharge rates—such as those due to urban developments, land clearance or the development of irrigated agriculture—are often linked to rising groundwater levels, groundwater flooding, and the development of land and river salinity. In arid regions, increases in recharge can cause leaching of salts stored in deep unsaturated profiles, which can increase groundwater salinity. Quantifying rates of recharge and the timescale between changes in land use and changes in groundwater recharge are key to predicting impacts on groundwater systems.

This book begins by describing the relevant recharge processes, some of the principal methods for estimating recharge, and how the recharge rate is affected by precipitation, snowmelt, evapotranspiration, soil type, and land use. It also examines the spatial and temporal variability of recharge, and the spatial and temporal scales at which recharge can be measured. Case studies from around the globe are presented to illustrate the diversity of approaches used to understand and quantify recharge processes. The final chapter discusses climate change impacts on recharge.

Acknowledgments

We deeply appreciate the thorough and useful reviews of and contributions to this book by the following individuals:

- ❖ Randy Stotler (University of Waterloo, Waterloo, Ontario, Canada);
- ❖ Ferdinando Manna (University of Guelph, Ontario, Canada);
- ❖ John Molson (Université Laval, Quebec City, Canada);
- ❖ Roger Diamond (University of Pretoria, Pretoria, South Africa); and
- ❖ Russell Crosbie (CSIRO, Urrbrae, South Australia, Australia).

We are grateful for Amanda Sills and the Formatting Team of the Groundwater Project for their oversight and copyediting of this book. We thank Eileen Poeter (Colorado School of Mines, Golden, Colorado, USA) for reviewing, editing, and producing this book.

1   Introduction

Groundwater recharge is the addition of water to an aquifer. Over most of the earth's land surface, groundwater recharge occurs from infiltration of precipitation and its downward movement through the soil and unsaturated zone into the underlying saturated zone. Groundwater recharge also occurs through infiltration of irrigation water, seepage from rivers, lakes and dams, and deliberate injection of water into the aquifer through injection wells.

Information on recharge processes and rates of groundwater recharge is important across many areas of hydrology. Understanding the sources of recharge can be important for predicting the impacts of land use change and climate change on groundwater resources and for determining the vulnerability of groundwater resources to contamination by human activity. Through groundwater recharge, chemicals can be transported from the land surface to underlying unconfined aquifers, and the rate of recharge controls the rate of this transport. Recharge rates are important input parameters for many groundwater models—models that are often used for predicting impacts of groundwater development and contaminant transport.

Changes in recharge rates can have important implications for groundwater resources and ecosystems dependent on groundwater. Decreases in recharge rates—for example, during drought or due to climate change—can lead to declines in groundwater levels, leading to reductions in spring and river flows and adverse impacts on groundwater-dependent ecosystems. Increases in recharge rates—such as those due to urban developments, land clearance or the development of irrigated agriculture—are often linked to rising groundwater levels, groundwater flooding (Gotkowitz et al., 2014),and the development of land and river salinity (Allison et al., 1990). In arid regions, increases in recharge can cause leaching of salts stored in deep unsaturated profiles, which can increase groundwater salinity (Suarez, 1989).

Estimates of groundwater recharge are often a key consideration in determining the maximum volume of groundwater that is permitted to be extracted across a region. Traditionally, extraction limits for unconfined aquifers were set to be equal to the volume of recharge—a practice referred to as *safe yield* (Meyland, 2011). Today, it is more common to allocate a fraction of recharge with the remaining volume representing a notional allocation to the environment and/or a conservative factor that acknowledges uncertainty of our knowledge of the groundwater system (Meyland, 2011; MDBA, 2020). Thus, for example, if an aquifer receives 200×10^6 m^3 of recharge, water managers may decide to allocate 150×10^6 m^3 and reserve the remaining 50×10^6 m^3 for natural environmental purposes. While it is recognized that management of regional extraction volumes cannot prevent impacts on groundwater-dependent ecosystems (GDEs) (Bredehoeft 1997; Devlin and Sophocleous, 2005), regional limits on groundwater pumping are an important

management tool, and recharge rates provide a sensible starting point for determining such limits (Cook et al., 2022).

This book introduces the topic of groundwater recharge. Section 1 discusses the importance of studying groundwater recharge. Section 2 describes the different recharge processes. Sections 3 and 4 describe some of the principal methods for estimating recharge. Section 5 summarizes typical values of recharge in different environments, as well as how recharge is affected by precipitation, soil type and land use. Section 6 describes the spatial and temporal variability of recharge and the spatial and temporal scales at which recharge can be measured. Section 7 discusses the impacts of climate change on recharge.

2   Recharge Processes

2.1   Infiltration, Deep Drainage and Recharge

The *infiltration rate* is the amount of water that moves from the land surface into the soil profile per unit area over a given time (Figure 1). It is usually measured in mm/hour, cm/hour or m/day. However, much of this water may subsequently evaporate or be extracted by plant roots; so, the mean rate of downward water movement below the root zone of the vegetation will be less than the mean infiltration rate.
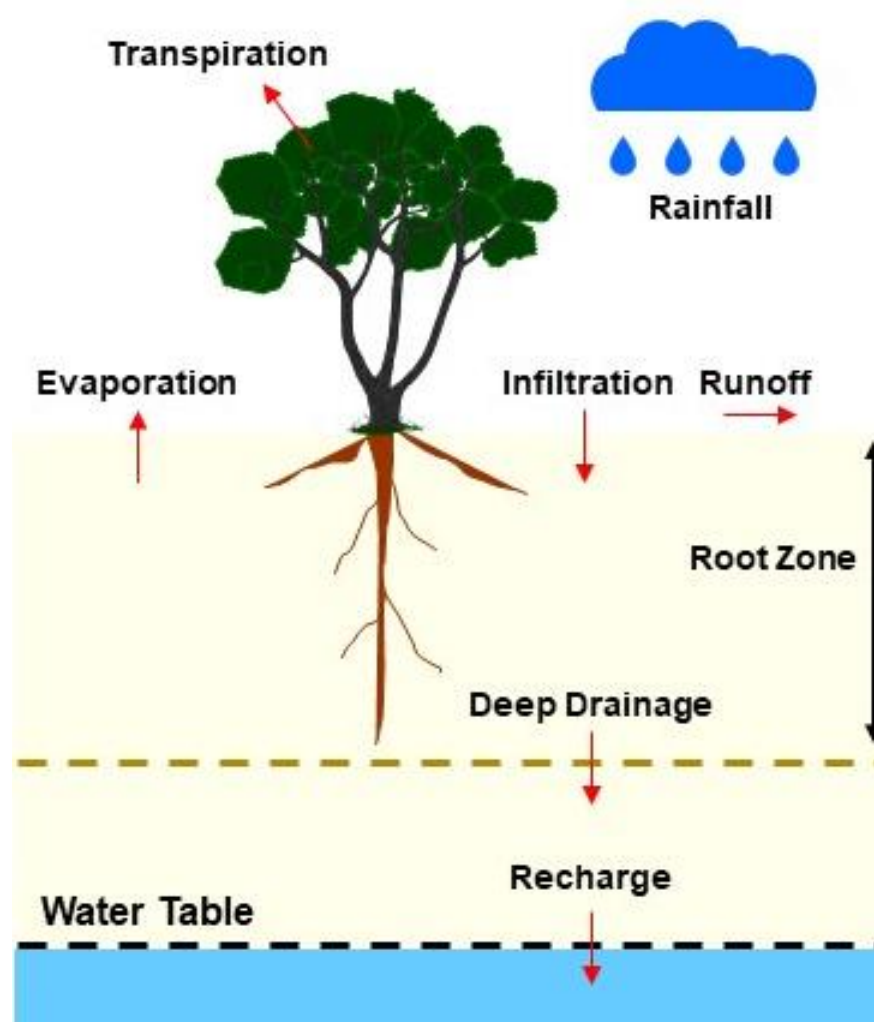
Figure 1 - Conceptual model of infiltration, deep drainage, and recharge processes through a uniform soil in a temperate climate.

Deep drainage is the water that has moved past the evaporative and root zones and is no longer available to plants. The upper part of the soil profile where water can be lost to evapotranspiration is referred to as the *plant root zone*. Below this zone water moves downward under the influence of gravity and pressure gradients induced by infiltration events. Importantly, the plant root zone will usually extend beyond the maximum depth of plant roots, because soil water can move upwards to replenish water removed by

3

The GROUNDWATER PROJECT   ©The Authors   Free download from gw-project.org

Anyone may use and share gw-project.org links. Direct distribution of the book is strictly prohibited.

evaporation and transpiration. The *deep drainage rate* is the rate of downward water movement below the base of the plant root zone.

Recharge is the downward water flux that reaches the water table. Both deep drainage and recharge rates are usually measured in mm/year or m/year. If there are no impediments to the downward flow of water through the unsaturated zone, then all deep drainage will eventually become groundwater recharge. The average rate of groundwater recharge that occurs at any location will depend upon numerous factors, including the climate, vegetation type, land use, geology and soil type (particularly their hydraulic properties), and topography (which affects surface runoff).

If the climate and land use do not change, then—if there are no impediments to the downward flow of water within the profile—the average rate of deep drainage over time should equal the average rate of groundwater recharge. Thus, if we are interested in average fluxes over time, distinguishing between *deep drainage* and *recharge* may not be important. However, it will take time for water to move from the base of the plant root zone to the water table. Under piston flow conditions (as described in Section 2.2) with steady infiltration and recharge, the travel time (t) of water from the base of the plant root zone to the water table is given in Equation (1):

$$t = \frac{(z_{WT} - z_R)\theta}{R} \tag{1}$$

where (parameter dimensions are dark green font with mass as M, length as L, time as T):

z_{WT} = water table depth (L)

z_R = maximum depth from which plants are able to extract water (L) (i.e., the base of the root zone)

θ = average volumetric soil water content between these two depths (dimensionless)

R = recharge rate (LT^{-1})

Equation (1) states that the travel time is the volume of water (per horizontal area, L^2) stored between the base of the root zone and the water table, divided by water flux.

The travel time of water through the root zone (between the land surface and z_R) is more difficult to calculate because it depends upon the rate of water uptake at different depths. It can be calculated if the rate of water extraction as a function of depth is assumed, as shown by the example in Figure 2. The travel time of water through the unsaturated zone provides a minimum travel time for contaminants applied at the land surface (e.g., pesticides and nitrates applied to agricultural fields). Many dissolved contaminants have longer travel time than the travel time of water because contaminants are subject to geochemical processes that may retard their transport by temporarily attaching solutes to solid particles (sorption) of the vadose zone.
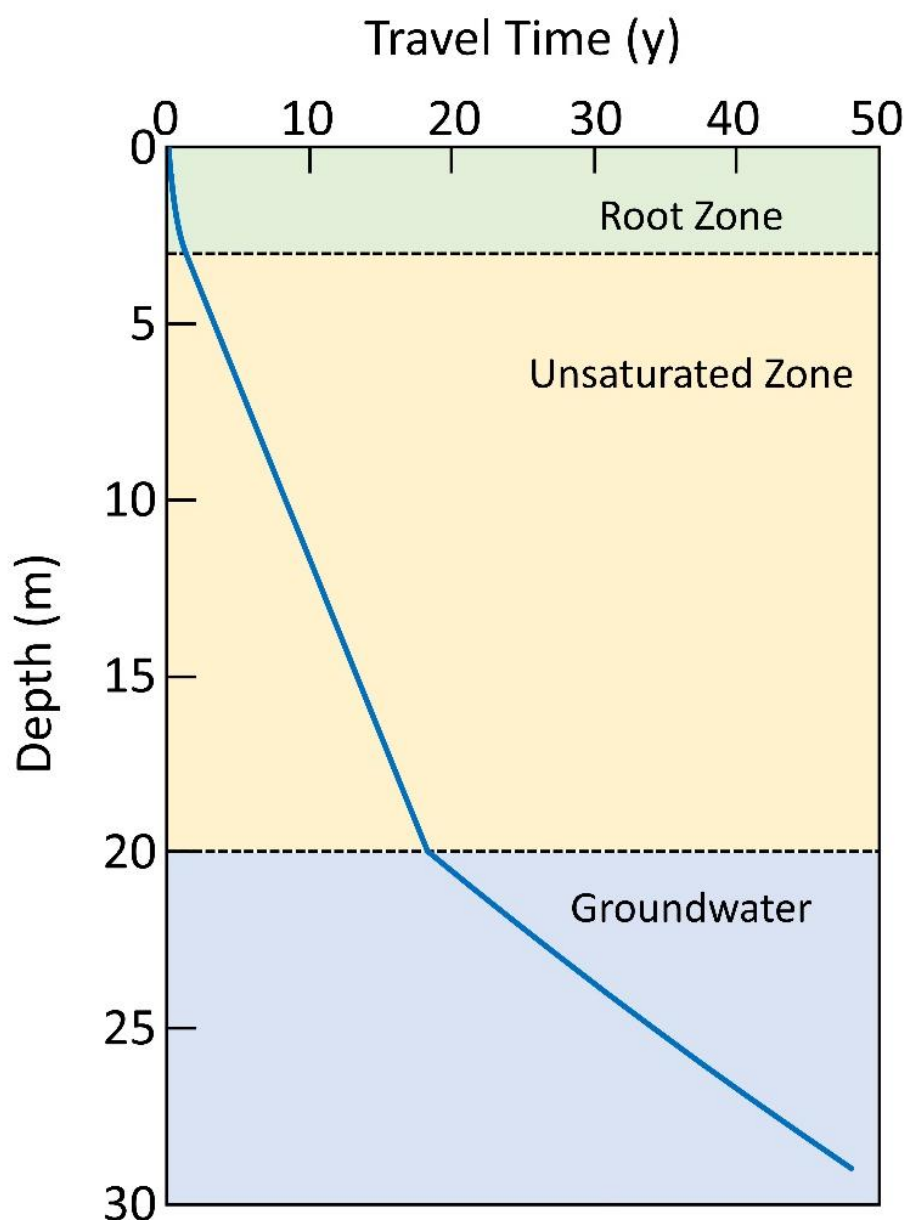
Figure 2 - Travel time of water within the unsaturated zone and shallow groundwater. In a homogeneous soil, the downward velocity of water—the slope of the line in this figure—is most rapid through the root zone, slower through the unsaturated zone below the root zone, and even slower below the water table. The velocity in the root zone is related to the recharge rate, the soil water content, and to the pattern of soil water uptake by vegetation. In the unsaturated zone, the velocity is related to the recharge rate and the soil water content. Below the water table, the vertical velocity is related to the recharge rate, the aquifer porosity, and the aquifer geometry. This figure uses a uniform root uptake function (Tyler & Walker, 1994) for the rate of movement within the root zone, the rate described by Equation (1) for movement within the unsaturated zone below the root zone, and an equation that is discussed in Section 3.6 for the rate of movement below the water table. Parameters used to calculate the rates are: root zone depth $z_R = 3$ m, water table depth $z_{WT} = 20$ m, aquifer thickness $H = 50$ m, soil water content $\theta = 0.1$, aquifer porosity $\varepsilon = 0.3$, precipitation $P = 500$ mm/y, and recharge $R = 100$ mm/y (after Cook & Bohlke, 2000).

Because of the time delay for water to move through the unsaturated zone, at any particular time, the deep drainage rate and recharge rate may be different. Where a change

5

in climate or land use has occurred, then the deep drainage rate will change to reflect this new system before the recharge rate changes. Importantly, Equation (1) cannot be used to estimate the time between a change in deep drainage and a change in recharge, because this is determined by the propagation of pressure through the unsaturated zone, which will depend on the magnitude of the change in deep drainage and the soil moisture characteristic curve (Hillel, 1982) as discussed in Section 5.7.

The discussion in this section assumes that water will percolate unimpeded through the unsaturated zone to the underlying groundwater. This will be the case if the rate of *deep drainage* is less than the minimum value of the saturated hydraulic conductivity of the soil between the base of the plant root zone and the water table. However, if the saturated hydraulic conductivity at some depth is less than the deep drainage rate, then the downward movement of water will be impeded, and a perched aquifer will develop. Recharge will occur through leakage across the low hydraulic conductivity layer, but it can occur at a rate less than the deep drainage rate. Water may also flow laterally on top of the low hydraulic conductivity layer and may recharge the water table at some other location, for example where the low hydraulic conductivity layer is absent (Figure 3).
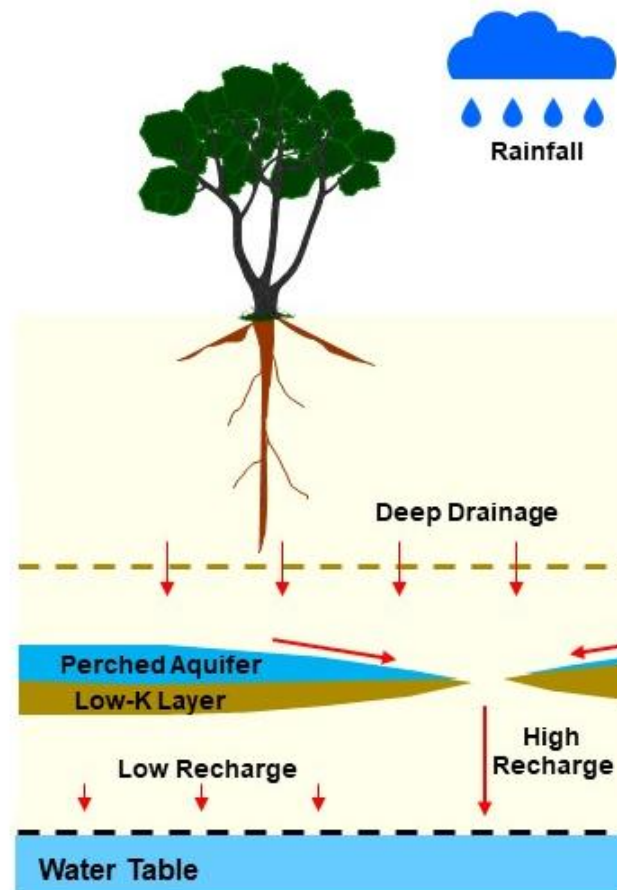
Figure 3 - Schematic illustration of the formation of a perched aquifer on top of a low hydraulic conductivity (Low-K) layer and deep drainage below this layer to recharge the regional water table aquifer. The figure illustrates the case when the low hydraulic conductivity layer is below the base of the root zone.

2.2   Piston Flow and Preferential Flow

Piston flow—sometimes referred to as *interstitial flow* or *matrix flow*—refers to soil water movement where the new infiltration water uniformly pushes the pre-existing soil water ahead of it. This creates a soil profile which is layered, with the younger water closer to the soil surface overlying older water deeper in the profile (Figure 4). In contrast, *preferential flow*—sometimes called *macropore flow*—involves bypassing of older water by younger infiltrating water. Preferential flow may involve movement through cracks, fractures, solution cavities, animal burrows, and root channels.
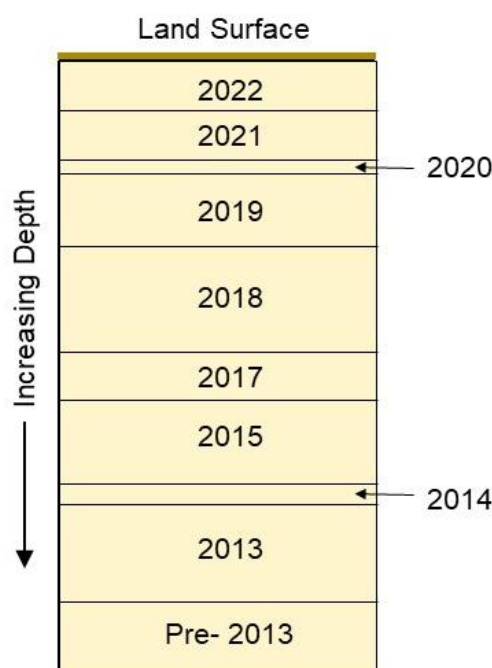
Figure 4 - Conceptual illustration of layered soil water in the unsaturated zone due to piston flow. Piston flow involves new infiltration pushing older, existing soil water ahead of it, meaning that water age increases with depth in the profile. Numerals in the diagram denote the year of infiltration.

Whether soil water movement occurs through *piston flow* or *preferential flow* is important because it determines which methods are likely to be most successful for estimating recharge (methods are discussed in Chapters 3 and 4). It is also important because it affects the rates of solute transport through the unsaturated zone. Preferential flow allows solutes dissolved in recharge water to reach the water table faster, due to higher water velocities, but also because the contact area between the water and sediment particles is reduced and so there is less opportunity for sorption and other chemical reactions to impact dissolved concentrations (Wood et al., 1997). On the other hand, piston flow results in more complete leaching of solutes already stored within the soil profile, while preferential flow may bypass this solute store. In Australia and North America, clearing of native vegetation has resulted in leaching of salt that had accumulated in soil profiles over

thousands of years (Cook et al., 1989; Scanlon et al., 2007). This leaching is reduced if preferential flow is the dominant transport process.

Water movement by preferential flow is commonly observed where recharge occurs through fractured hard rocks, but it can also occur through cracking clay soil, root channels, and macropores created by burrowing organisms in sands and loams. Macropores can also form as a result of repeated freeze–thaw processes (Qi et al., 2006). Preferential flow is most likely to occur in environments characterized by high precipitation or by large, intense precipitation events that cause water to pond on the surface because macropores are full only at high saturation levels. Where soils are dry, macropores are likely to be empty and so will not contribute to soil water flow. Preferential flow is most likely to be an important recharge mechanism in areas with shallow water tables, where saturated conditions occurring in soil macropores extend to the water table (Johnson et al., 2001). It is more likely to occur in areas of focused recharge, where surface runoff ponds on the soil surface.

In areas of deep groundwater tables, preferential flow can be indicated by the rapid rise of groundwater levels following precipitation events (Lee et al., 2006) or from the rapid appearance of agricultural chemicals or pathogens at the water table following precipitation (Johnson et al., 2001). The existence of preferential flow can also be inferred from the movement of environmental or artificial tracers through the soil profile (Allaire et al., 2009). In general, root channels, worm holes and other macropores that result from biological activity are most common within the upper layers of the soil profile and occur less frequently at greater depths. They are most active during periods of saturation, when macropores are filled with water. Infiltration experiments using ponded water or tension infiltrometers and dye tracers have been used to observe preferential flow through soils (Cey & Rudolph, 2009). However, such tests create artificial conditions that are conducive to preferential flow and so are difficult to extrapolate to natural conditions. Environmental tracers—e.g., tritium—have proven useful for evaluating the role of preferential flow under natural conditions and have been used for investigating vertical water movement through cracks in clay-rich glacial till deposits in southern Ontario (Ruland et al., 1991; Cook, 2020), through root channels in sandy soils in southern Australia (Allison & Hughes, 1983) and through fractures in chalk in southern UK (Smith et al., 1970).

2.3   Diffuse and Focused Recharge

Groundwater recharge is often divided into *diffuse* recharge and *focused* recharge. *Diffuse recharge* is recharge that occurs throughout the landscape, following infiltration of precipitation. Diffuse recharge is essentially a one-dimensional process with water recharging the aquifer where the precipitation fell. *Focused recharge* (sometimes called *point* or *localized* recharge) results from infiltration below streams, lakes, and depressions in the landscape. In this case, water moves laterally as surface runoff from where the precipitation falls to the point where recharge occurs (Figure 5). Focused recharge can also occur if water

moves laterally on subsurface soil layers to recharge the aquifer somewhere other than its point of infiltration (Figure 3). Both diffuse and focused recharge can occur in landscapes, but rates of focused recharge will usually be higher. Focused recharge will also have short travel times through the unsaturated zone, and so it can be an important pathway for contaminant transport to aquifers (Hartmann et al., 2021; Salley et al., 2022). Focused recharge can occur in all environments but is particularly prevalent in karst environments where rapid recharge through sinkholes is often directly observed (Fryar et al., 2023; Kuniansky et al., 2022).
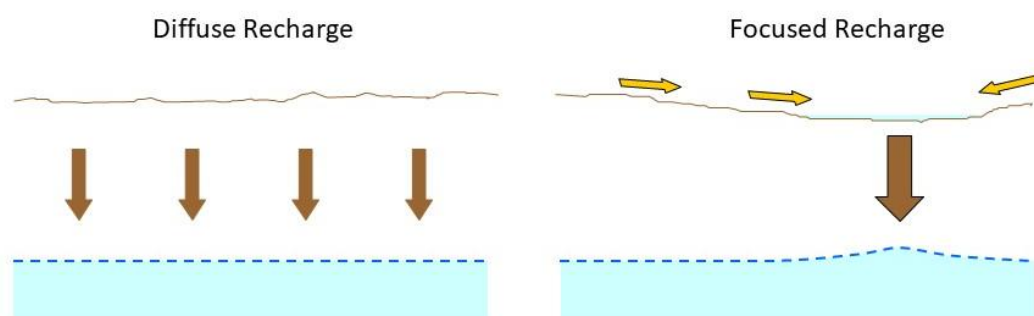
Figure 5 - Conceptual illustration of diffuse recharge and focused recharge. Focused recharge occurs where rainfall or snowmelt flows across the land surface to depressions in the landscape where it infiltrates to groundwater. Focused recharge also occurs where water moves laterally on subsurface soil layers to recharge groundwater somewhere other than its area of infiltration, as shown in Figure 3.

It is generally accepted that focused recharge is the dominant recharge process in arid areas, and diffuse recharge dominates in most temperate environments. Under arid conditions, rates of diffuse recharge beneath native vegetation are often very low, because the vegetation tends to have deep roots, and precipitation events rarely produce enough infiltration to penetrate below the depth of the roots. Thus, infiltration is often extracted before the next precipitation event. High evaporation rates also contribute to low rates of diffuse recharge. In arid areas, high rates of recharge therefore occur only where surface runoff results in water ponding in low areas of the landscape. Focused recharge through playa lakes (Figure 6) has been shown to dominate the groundwater balance under native vegetation in the semi-arid High Plains of the United States. For example Scanlon and Goldsmith (1997) estimated that focused recharge through playas accounted for 97% of total areal recharge prior to agricultural development but only 8% of areal recharge since development due to the large increase in diffuse recharge beneath dryland and especially irrigated agriculture (Crosbie et al., 2013). In humid regions, the importance of focused recharge is likely to depend on climatic and geological conditions. In some areas, while rates of focused recharge exceed rates of diffuse recharge, the contribution of focused recharge to the regional water balance may be small because areas of focused recharge tend also to be small (e.g., Herczeg et al., 1997).

9
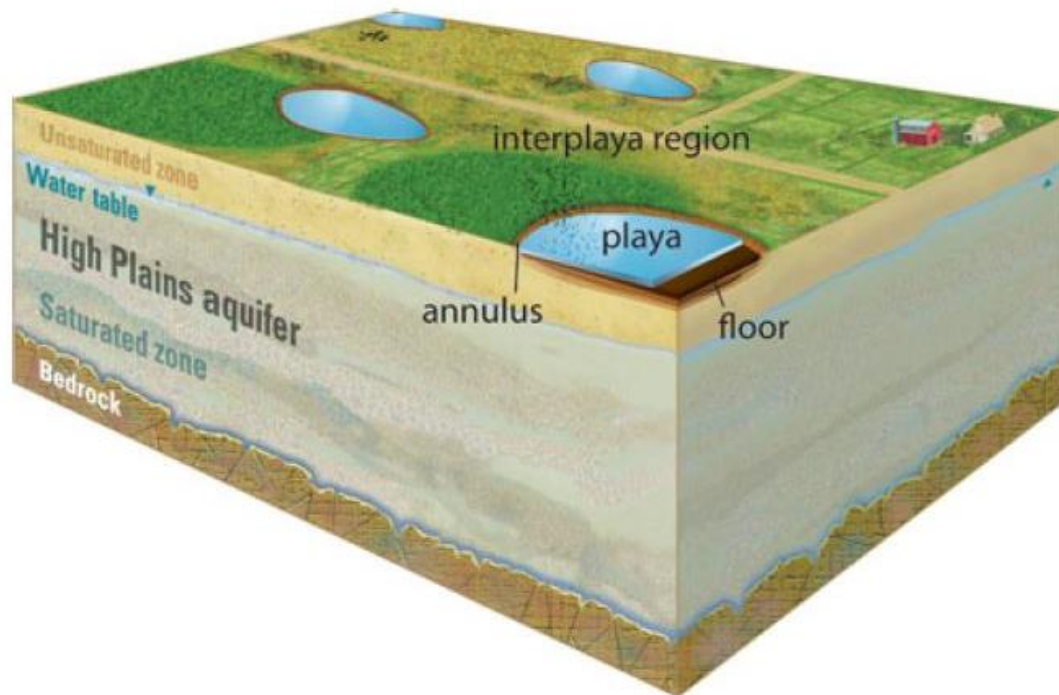
Figure 6 - Principal features of playa lakes of the High Plains aquifer in the USA. Playas are shallow closed basins that are separated from the water table by a thick unsaturated zone but receive runoff from surrounding areas and intermittently contain ponded surface water. They provide important habitat for bird species and other wildlife, as well as a water source for irrigation and livestock. They are also important sites of focused recharge to the underlying groundwater system and have been extensively studied. The playa floor is typically flat and is surrounded by an annulus which slopes towards the playa floor. Sediments in the playa annulus may be coarser than those in the playa floor, and it has been suggested that this may also be a focus of recharge on the perimeter of the lakes. The inter-playa region surrounds the playa and includes upland areas that drain into playas (Reproduced from Gurdak & Roe, 2010).

Permanent lakes can be sites of focused recharge, although most often they will be either groundwater discharge sites or throughflow lakes that simultaneously receive groundwater inflow but also recharge aquifer systems (Zlotnik et al., 2009). Examples of lakes that recharge local aquifers (at least episodically) include Lake Chad, Africa (Isiorho et al., 1996), some of the kettle lakes in northeastern Ontario, Canada (Boreux et al., 2021), and Coongie Lakes in southern Australia (Costelloe et al., 2009). Focused recharge associated with streams and runoff from mountain ranges is discussed in Sections 2.3 and 2.4, respectively.

Exercise 1⮡ provides an opportunity to calculate diffuse and focused recharge.

2.4   Recharge from Rivers

Under natural conditions, perennial rivers will often receive groundwater inflow. In fact, the flow of groundwater into these rivers is the reason that they flow all year. Such rivers are often referred to as *gaining rivers*. Sometimes, though, groundwater levels are lower than river levels, causing rivers to leak water into the underlying aquifer; hence, they recharge the groundwater and are referred to as *losing rivers*. Many rivers will have some reaches that are gaining and others that are losing. It is also possible for river reaches to

10

change from losing to gaining and back to losing through the year as the water table rises and falls. Gaining and losing conditions can also be affected by changes in the water level of the river.

Classification of rivers as gaining or losing is relatively straightforward, based on the relationship between the water level in the river and the water table level in the aquifer adjacent to the river. However, for losing rivers, it is important to distinguish between *losing connected rivers* and *losing disconnected rivers* (Figure 7). Losing connected rivers occur where the subsurface is fully saturated beneath the river. For losing connected rivers, the infiltration flux is determined by the hydraulic gradient between the river and the groundwater (Brunner et al., 2009). For these rivers, lowering the water table will increase the infiltration rate, as it increases this hydraulic gradient. Losing disconnected rivers occur where there is an unsaturated zone beneath the river. In losing disconnected rivers, lowering the water table does not change the infiltration rate. However, the length of the disconnected section of river can increase (Fox & Durnford, 2003). Ephemeral rivers are often losing disconnected and can represent a significant source of groundwater recharge.
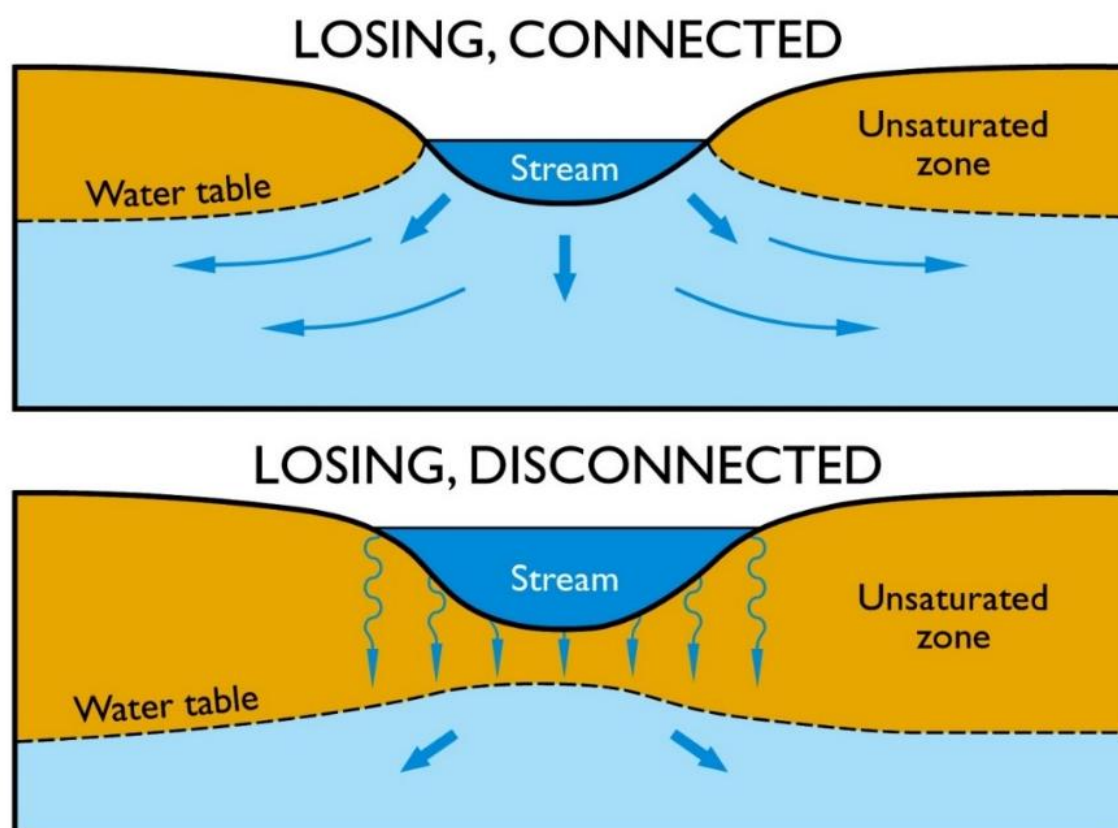
Figure 7 - Losing rivers recharge underlying aquifers. This schematic shows two different types of losing rivers. Losing connected rivers occur where there is no unsaturated zone beneath the river such that the water table is hydraulically connected to the surface water. Losing disconnected rivers have an unsaturated zone between the river and the underlying unconfined aquifer (After Brunner et al., 2009).

Few studies have estimated the relative proportions of stream recharge versus diffuse recharge in a catchment. In arid and semi-arid environments, diffuse groundwater

11

The GROUNDWATER PROJECT   ©The Authors   Free download from gw-project.org

Anyone may use and share gw-project.org links. Direct distribution of the book is strictly prohibited.

recharge is often assumed to be very low, and recharge from ephemeral rivers is often assumed to dominate the groundwater budget. In the Ti Tree Basin in arid central Australia, for example, recharge through ephemeral stream beds contributes approximately 90% of the total recharge to the basin which is estimated to average approximately 2 mm/year (Harrington et al., 2002; Villeneuve et al., 2015). However, recharge from rivers can also be important in more humid environments. A predevelopment water budget for the California Central Valley, USA estimated that annual recharge was approximately 2.5×10^9 m^3/y. Of this, 75% (1.9×10^9 m^3/y) was diffuse precipitation recharge and 25% (0.6×10^9 m^3) was recharge from rivers as shown in Figure 8 (Faunt, 2009). For part of the San Joaquin Valley which lies within the Central Valley, Visser and others (2018) used water chemistry to estimate that 74% of groundwater recharged before 1950 was diffuse recharge and 26% was river recharge. This is consistent with the predevelopment Central Valley budget.
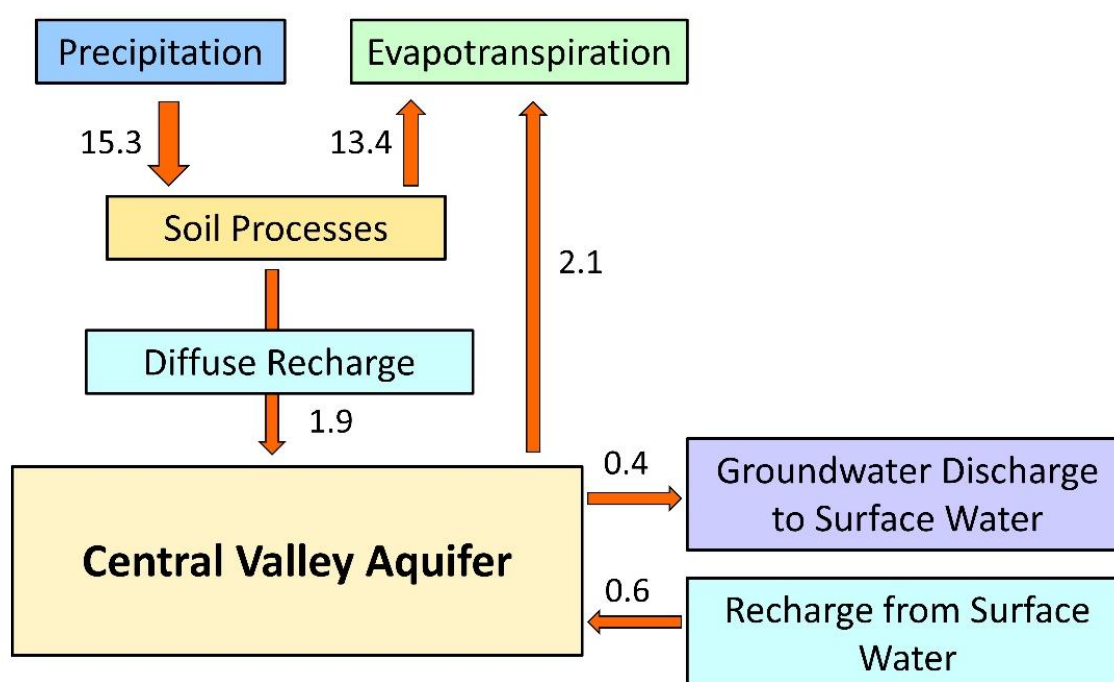
Figure 8 - Predevelopment water budget for the Central Valley, California, USA. Values are in 10^9 m^3 per year. Annual precipitation averaged approximately 15.3x10^9 m^3/y, of which 13.4x10^9 m^3/y was lost to evapotranspiration from the unsaturated zone and 1.9x10^9 m^3/y was diffuse aquifer recharge. Evapotranspiration from groundwater accounted for 2.1x10^9 m^3 giving a total of 15.5x10^9 m^3/y evapotranspiration. An average 39.1x10^9 m^3/y of surface water flowed annually into the Central Valley, of which 0.6x10^9 m^3/y infiltrated to recharge the aquifer and 0.4x10^9 m^3/y of groundwater flowed from the groundwater into the surface water. Stream recharge thus represents 25% of total estimated recharge (i.e., 0.6/(1.9+0.6)) to the Central Valley aquifer (after Faunt, 2009).

In Australia, the proportion of diffuse recharge and focused recharge from rivers has been estimated for 21 regions that have groundwater models as shown in Figure 9 (Barron et al., 2012). Calibration of these groundwater models to groundwater and river levels has resulted in estimates of both diffuse and focused recharge. In some cases, model-derived recharge estimates have been constrained by more direct estimates. For the

12

modelled areas, mean annual precipitation ranges from less than 400 mm/y—Lower Murrumbidgee and Lower Lachlan—to more than 900 mm/y—South Perth Basin, Daly Basin, Howard East, Mella-Togari. Sites with high annual precipitation tend to have higher proportions of diffuse recharge. For example, diffuse recharge averages approximately 30% of total recharge for sites with less than 400 mm/y annual precipitation, but more than 80% of total recharge for sites with more than 900 mm/y annual precipitation.
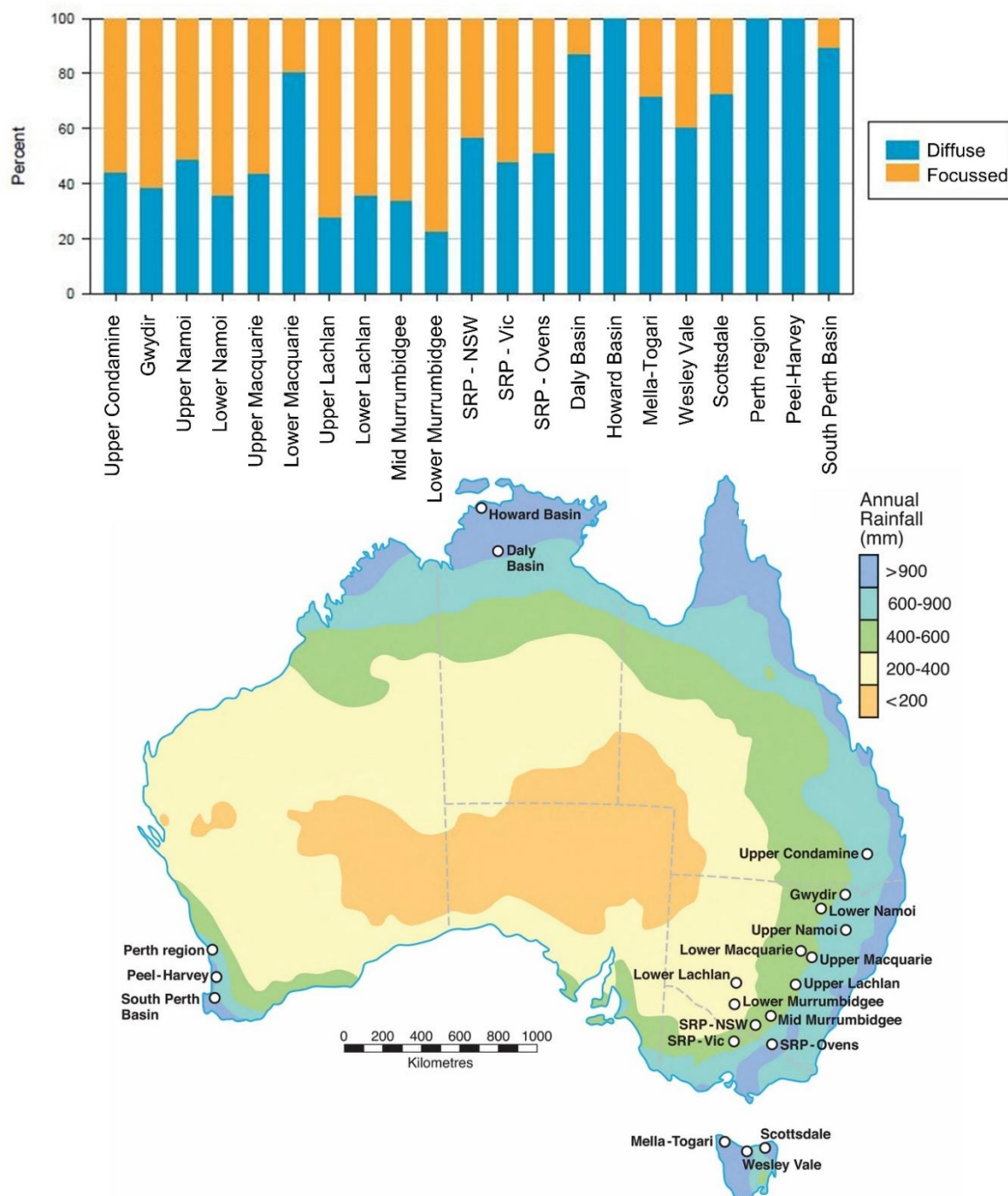
Figure 9 - Proportion of diffuse and focused recharge from rivers as inputs to groundwater models of Australian catchments under fitted historical conditions (After Barron, et al., 2012).

13

For some of the aquifers shown in Figure 9, the proportion of focused recharge has increased since development, as groundwater pumping has lowered water tables and hence increased recharge from rivers and streams—e.g., Lower Namoi. Reduction in the level of the water table near a river will either reduce the groundwater discharge to the river or increase groundwater recharge from the river. If the river was originally gaining, then either the rate of groundwater flow to the river will decrease or, if the water table drops below the surface water level, the river will change from gaining to losing. If the river was originally losing connected, then the rate of loss will increase. The reduction in groundwater flow to rivers or increase in groundwater recharge from rivers because of groundwater pumping is sometimes referred to as *stream capture* or *stream depletion*. Analytical and numerical approaches have been developed for predicting the change in groundwater flow to streams due to groundwater pumping near rivers, and this is discussed in Groundwater Resource Development↗ by Konikow and Bredehoeft (2020).

Recharge from rivers can provide a pathway for contaminants to move into aquifers. Examples of groundwater contamination due to recharge from losing rivers have been described by Böhlke and others (1997) as well as by Jurado and others (2019).

2.5   Mountain Block and Mountain Front Recharge

Some basins in arid and semi-arid regions receive most of their recharge from precipitation in adjacent mountains. Diffuse recharge within the basin is often limited due to low precipitation and high evapotranspiration. In contrast, adjacent mountains often receive more precipitation because of orographic effects. They also have lower temperatures so that less precipitation is lost to evapotranspiration (Wilson & Guan, 2004). Recharge to the basin aquifer can thus be concentrated in the piedmont area. Two different recharge mechanisms are often distinguished. *Mountain front recharge* occurs when ephemeral rivers flow from the mountains onto the plains, and recharge occurs as stream infiltration. *Mountain block recharge* occurs when precipitation recharges aquifers within the mountain range, and the recharge flows into aquifers on the plains (Figure 10). In many regions, both processes will occur, but one or the other may be dominant.

a) Mountain front recharge

b) Mountain block recharge
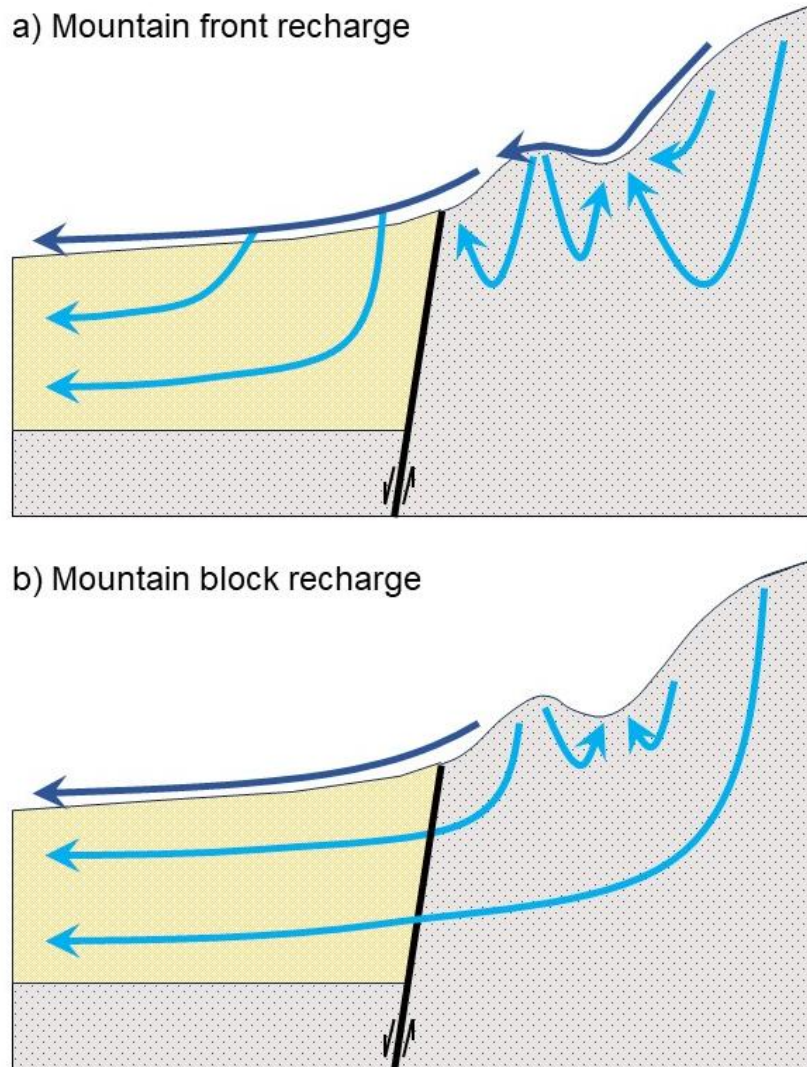
Figure 10 - a) Mountain front and b) mountain block recharge. Light blue lines represent groundwater flow paths and dark blue lines are surface water flow paths. The sub-vertical black line denotes a fault separating the mountain block from the plains (redrawn from Bresciani et al., 2018).

Characterizing mountain front recharge and mountain block recharge can be difficult because the mountain blocks are often characterized by high heterogeneity and an absence of suitable wells for sampling. The dominance of crystalline rocks and fracture flow can make application of Darcy's Law for estimation of flow rates difficult. Where fault zones separate the mountain block and plain zones, large head differences may be observed across the fault zones. Quantifying flow across these faults is difficult. For these reasons, geochemical methods are often useful for identifying recharge processes in mountainous terrains (Manning & Solomon, 2005). Noble-gas and isotopic methods allow temperature and elevation of recharge to be estimated, which helps identify the location of groundwater recharge and assists the development of conceptual flow models in these systems (as discussed in Section 3.7).

2.6   Recharge under Snow, Ice, and Permafrost

Mountain snowmelt supports a billion people worldwide (Dozier et al., 2016) thus a quantitative understanding of snow-related recharge processes is crucial. Compared to available field approaches in humid or arid regions, field studies of recharge in cold regions are limited (Iwata et al., 2010). Recharge processes in cold climatic regions are influenced by numerous processes (Figure 11) and by extreme seasonal variability. Snowfall, snowmelt, and freeze-thaw cycles affect groundwater recharge in numerous ways and bring many additional challenges to estimating groundwater recharge. During the snow-accumulation phase, infiltration and subsequent groundwater recharge are halted; while during snowmelt periods, melting snow and ice can contribute to recharge. However, soils may freeze during cold periods, reducing the hydraulic conductivity at the ground surface and hence reducing infiltration (Bayard et al., 2005). In areas with permafrost, the low hydraulic conductivity of the soil can prevent groundwater recharge from occurring (Lemieux et al., 2020). Thawing of permafrost can thus increase groundwater recharge. Moreover, Young and others (2020) found that with the thawing permafrost, major changes in landcover occur, notably a shift from tundric vegetation to shrubland forests which can further increase groundwater recharge.
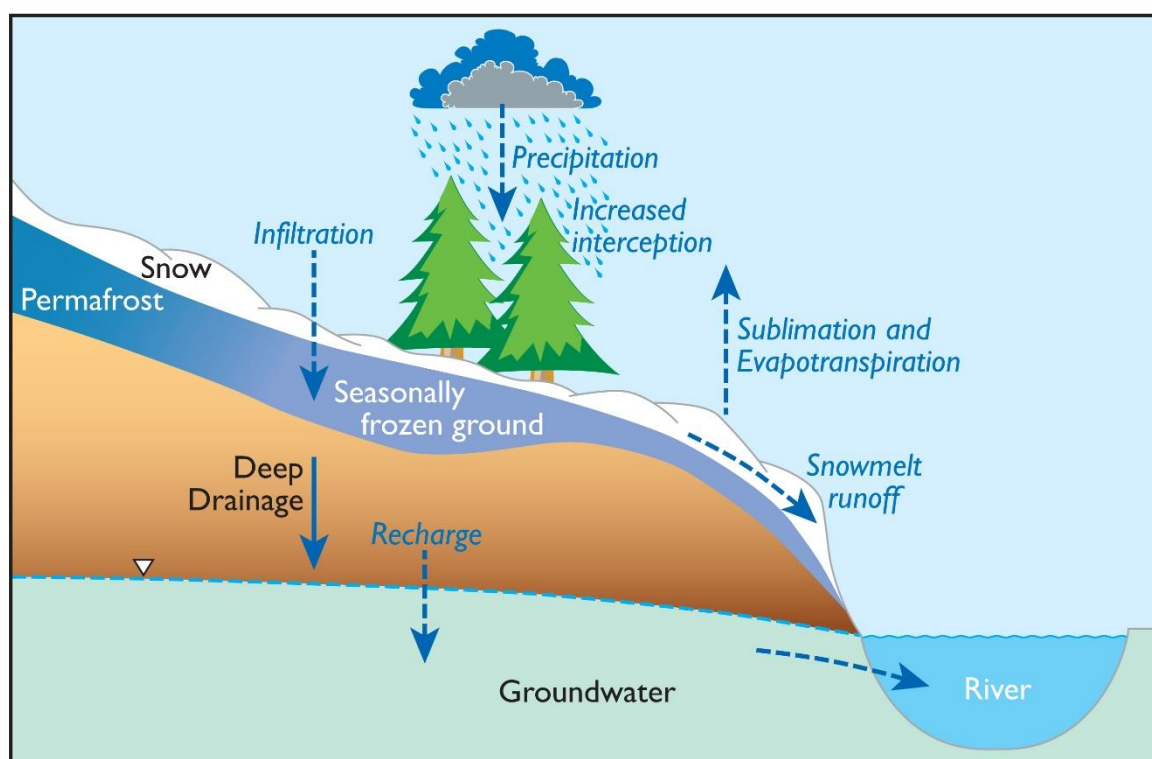
Figure 11 - Conceptual diagram of recharge in cold regions (modified from Ala-Aho, et al. 2021).

The first important aspect related to snow is the increased interception rate, especially in forested catchments. For example, Storck and others (2002) observed interception rates of up to 60% through the forest canopy in the Umpqua National Forest,

16

Oregon, USA—elevation 1200 m. The intercepted snow is exposed to sublimation which can significantly reduce the total amount of water retained by the vegetation cover. Interception and sublimation processes should thus be considered in the water-balance based assessment of groundwater recharge (as discussed in Section 3.2).

To estimate the amount of water stored in the snow cover, the snow water equivalent and the spatial distribution of snow depth are required. The snow water equivalent (SWE) represents the amount of water stored in the snow cover. Monitoring the spatial and temporal dynamics of snow is vital for predicting infiltration rates. The extent of snow cover can, in principle, be assessed through remote sensing (Sun et al., 2018). However, there are significant differences in snow accumulation and ablation under the forest canopy (Pomeroy et al., 2002). These sub-canopy dynamics cannot be monitored through air- or space-borne multispectral sensors. In steep, forested catchments, mapping the spatial distribution of snow remains a major challenge (Koutantou et al., 2022). Emerging alternatives are plane- and drone-based LiDAR approaches (Harder et al. 2020, Koutantou et al., 2021).

Estimating the water equivalent stored in a snow-covered area is not straightforward. SWE can be calculated from the snow depth if the bulk snow density is known. Because the direct measurement of SWE in the field is time-consuming, models have been proposed to estimate it. For example, Jonas and others (2009) proposed a model based on season, snow depth, altitude, and the snow-climatic region. A wide range of available approaches for estimating SWE is discussed by Dozier and others (2016).

Above-zero temperatures will trigger snowmelt and thus the potential onset of infiltration. Then the infiltration capacity of the soil becomes the determining factor for recharge. Frost will generally reduce the infiltration capacity of a soil, and the magnitude of this reduction is influenced by antecedent moisture conditions, the presence of preferential flow paths such as macropores, and the saturated hydraulic conductivity. However, infiltration through macropores can play a crucial role in rapidly recharging groundwater during snowmelt, even while the surrounding soil remains frozen (Sanchez-Rodriguez et al., 2025).

2.7   Human Impacts on Groundwater Recharge

Human development has changed recharge rates and processes. It has altered the land use and land cover over large areas of the Earth. Native vegetation has been cleared and replaced with annual or perennial crops, pastures for grazing of domesticated animals, or forest plantations. In some areas, crops and pastures are irrigated with water that is drawn from an aquifer and/or from river networks. Sometimes canals are constructed to move water to urban centers or to supply irrigation areas, and drainage ditches have been dug to remove surplus water and drain waterlogged land. Sometimes irrigation involves changes to land surface topography, such as leveling or construction of stepped terraces.

Urbanization fundamentally changes not only the landscape modifying drainage patterns, but also covers soils with roads, pavements, and buildings. All these changes impact rates and processes of groundwater recharge, as well as water quality.

Land use and land cover exert a major control on rates of groundwater recharge. Native vegetation has deeper roots than most crops and pasture grasses, giving them the ability to extract water from deep in the soil profile. The maximum average rooting depth of cropland is approximately 2 m, but it is 3–4 m for temperate forest vegetation, 5 m for sclerophyllous shrubland and forest, 9–10 m for desert vegetation, and 7–15 m for tropical grassland/savanna and evergreen forest (Canadell et al., 1996). As well as having greater rooting depth than crop and pasture grasses, native vegetation in arid and semi-arid climates is adapted to a low water environment; hence, it is more water efficient and can extract water from drier soils compared to most crop species.

In general, recharge rates beneath native vegetation are less than under rangelands and dryland (rainfed) crops, and recharge beneath dryland crops is less than beneath irrigated agriculture (as discussed in Section 5). Recharge rates beneath dryland crops are a function of soil type and crop type, precipitation and climate, and crop management. Seasonality of recharge also depends on cropping practices, being strongly affected by precipitation patterns immediately before and shortly after sowing—when root systems are not well developed—and by periods of bare soil or fallow. In some areas, a rotation of crops and a rotation between crops and pasture is common; the nature of this rotation also affects recharge rates. Recharge rates beneath irrigated areas are also a function of soil type and crop type, precipitation and climate, and irrigation management practices. Irrigation practices that affect groundwater recharge include the method of water application, the volume of applied water, and the frequency, duration and timing of application. Flood irrigation is generally considered to produce the most recharge with less recharge resulting from sprinkler and drip irrigation methods (Vallet-Coulomb et al., 2017). Leakage from irrigation channels can also be an important source of recharge in irrigation areas. Recharge beneath agricultural areas can transport contaminants into unconfined aquifers (Böhlke, 2002), with higher recharge rates beneath irrigated areas likely to have shorter travel times and hence less potential for chemical reactions to impact dissolved concentrations. Typical rates of recharge under different vegetation covers and in different climates are discussed in Section 5.

Recharge rates can be affected by groundwater extraction. In the short term, groundwater extraction may simply reduce the volume of water stored within an aquifer; although, eventually any groundwater extraction must be balanced by an increase in groundwater recharge, a decrease in groundwater discharge, or a change in groundwater flow between aquifers. Reductions in groundwater discharge due to groundwater pumping are common and occur where a reduction in the water table elevation reduces groundwater discharge to rivers, lakes, wetlands, and/or springs. In some cases,

18

groundwater extraction can lead to an increase in diffuse recharge. If the aquifer is fully saturated (i.e., the water table is at, or near, the land surface) so it cannot accept additional recharge, all precipitation is lost to either evapotranspiration or runoff (this is sometimes referred to as *rejected recharge*; Theis, 1940). In these situations, a decrease in the water table elevation reduces loss of groundwater to evapotranspiration and increases infiltration, such that areas of groundwater discharge become areas of diffuse recharge. For losing streams, a decrease in the water table can result in an increase in groundwater recharge. For rivers that were originally gaining, a decrease in the water table elevation can cause discharge to cease completely and instead cause groundwater recharge to occur. Increases in groundwater recharge from rivers due to groundwater extraction is discussed in Section 2.4. Impacts of groundwater pumping are discussed in more detail by Konikow and Bredehoeft (2020) in <u>Groundwater Resource Management</u>↗.

The impact of urbanization on groundwater recharge is discussed in Section 2.8. Another human impact on the rate of groundwater recharge includes managed aquifer recharge, which is deliberate surface water ponding to enhance recharge or deliberate injection of water into aquifers through wells as discussed in Section 2.9. Another significant human impact is climate change as discussed in Section 7.

2.8   Urban Recharge

Historically, there has been some controversy over whether urban development increases or decreases groundwater recharge (Lerner, 1990). A reduction in permeability of ground surfaces—roads and pavements—is likely to lead to a decrease in diffuse recharge, particularly if runoff from these surfaces leaves the urban area via a stormwater collection system (Figure 12). However, it is now generally accepted that, overall, urban recharge is higher than natural recharge, principally due to leakages in water delivery and wastewater collection systems (Lerner, 1990; Wakode et al., 2018). Also, there is often significant importation of water into urban areas, which contributes to higher recharge rates (Wakode et al., 2018). Recharge from water delivery systems is usually much greater than recharge from wastewater collection systems because pressures in delivery pipes are higher. Leakage of delivery pipes results in water moving from the pipe network into the surrounding soil, whereas leaky sewer pipes recharge the groundwater system when they are above the water table and receive discharge from the groundwater system when they are below the water table. Other sources of recharge in urban areas include leakage from septic tanks and over-irrigation of sport fields, parks, and gardens (Lerner, 1990). In some areas stormwater runoff is diverted into *soakaways*, or engineered runoff ponds, whereas in other areas it may be directly injected into aquifers as discussed in Section 2.9, both contribute to increased recharge in urban areas. Permeable pavements are being increasingly used to reduce stormwater runoff in urban areas, which also usually increases diffuse recharge (Lerner, 1990).
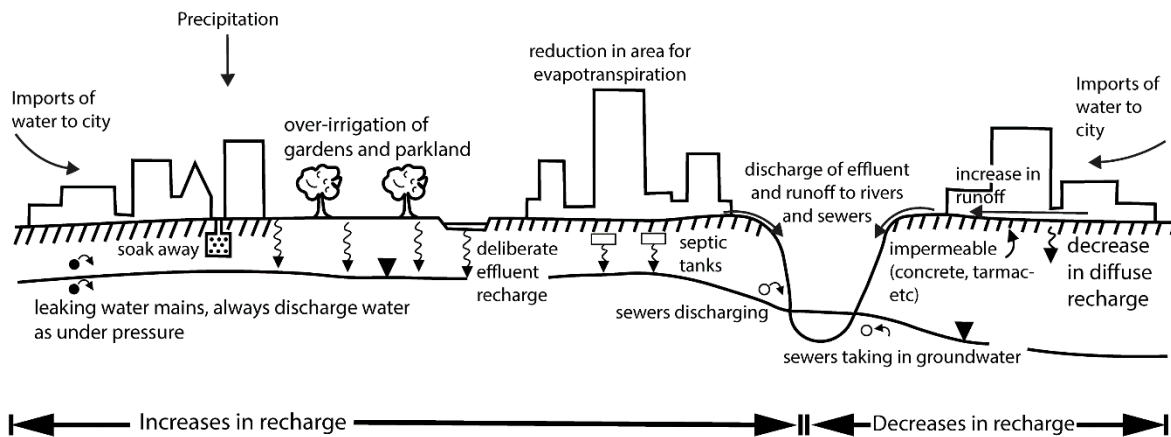
Figure 12 - Schematic illustration of recharge processes in urban environments (after Lerner, 1990).

Relatively few studies have quantified recharge in urban areas; most of the available studies show an increase in recharge over pre-development conditions with leakage from the water delivery system often a major component of the recharge. A geochemical study in Barcelona, Spain (Figure 13), suggested that 22% of the total urban recharge was from the water supply network, 30% from wastewater, 17% from precipitation recharge, 11% was recharge from the Besos River, and 20% was from runoff infiltration (Vásquez-Sũné et al., 2010). More commonly, though, water balances carried out at various points on water delivery and wastewater collection systems are used to estimate recharge (Wakode et al., 2018). In Caracas, Venezuela, 40% of the total recharge is attributed to leakage from the water delivery system. In Hat Yai, Thailand, 40% of the urban recharge component was from leakage of the water delivery system, 20% was from precipitation on non-paved areas, 16% was leakage from cesspits, and 24% from wastewater disposal in areas without sewerage systems (Lerner, 2002). Total recharge beneath urban environments was estimated to be approximately 40% greater than natural recharge in Wolverhampton, UK, and approximately double the natural recharge in Perth, Australia. In the latter case, the increase in recharge was attributed to the clearing of native vegetation, import of water, and infiltration of stormwater (Lerner, 2002). In Hyderabad, India, urban recharge is more than ten times the natural recharge (Wakode et al., 2018). Of the urban recharge, 49% was estimated to be leakage from the water supply system with the remainder (51%) derived from wastewater. The high figure for wastewater occurs because only 35% of the population in Hyderabad is served by the sewerage network; so, most of the wastewater recharge is due to leakage from surface reservoirs containing wastewater, on-site sanitation, latrines, or soakaways. Less than 5% of the wastewater recharge is attributed to leakage from the sewerage network.
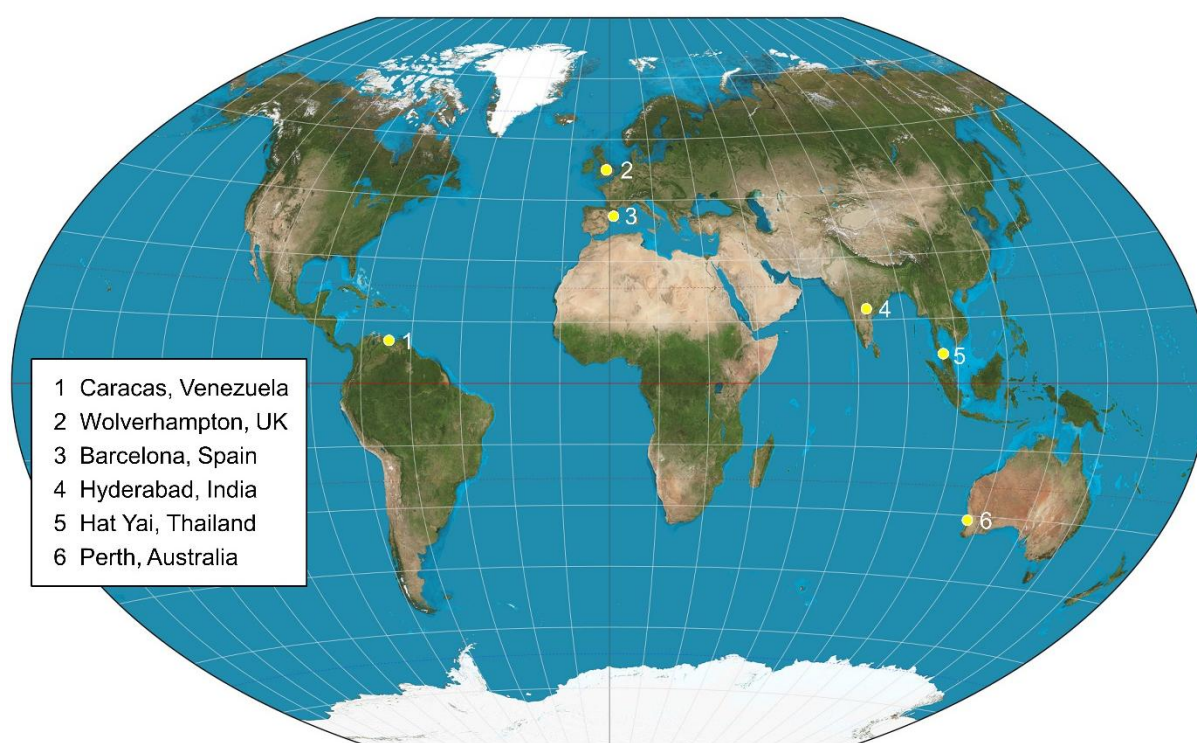
Figure 13 - Locations of urban recharge study sites referred to in the text (basemap is from https://en.wikipedia.org/wiki/World_map↗).

Urban recharge provides a pathway for contamination of groundwater, and results in poor water quality beneath many urban areas. This topic is discussed by Howard (2023).

2.9   Managed Aquifer Recharge

Managed aquifer recharge (MAR) is the intentional augmentation of groundwater recharge. It is usually carried out to replenish depleted aquifers and hence allow continued or increased extraction, or to preserve ecosystems that are or may be threatened by aquifer depletion. MAR can be particularly valuable when periods of peak water availability and water demand are not concurrent. MAR uses the aquifer as a reservoir and filter and allows water to be stored until it is needed without requiring land surface area and with minimal evaporation.

MAR is usually carried out by directly injecting water into wells, or pumping water into infiltration ponds or channels from which it infiltrates (Figure 14). However, other forms of recharge augmentation are also possible, including streambed channel modification which usually involves construction of dams or shallow excavations in ephemeral streams that hold surface water during river flows, allowing subsequent infiltration (Standen et al., 2020).

21
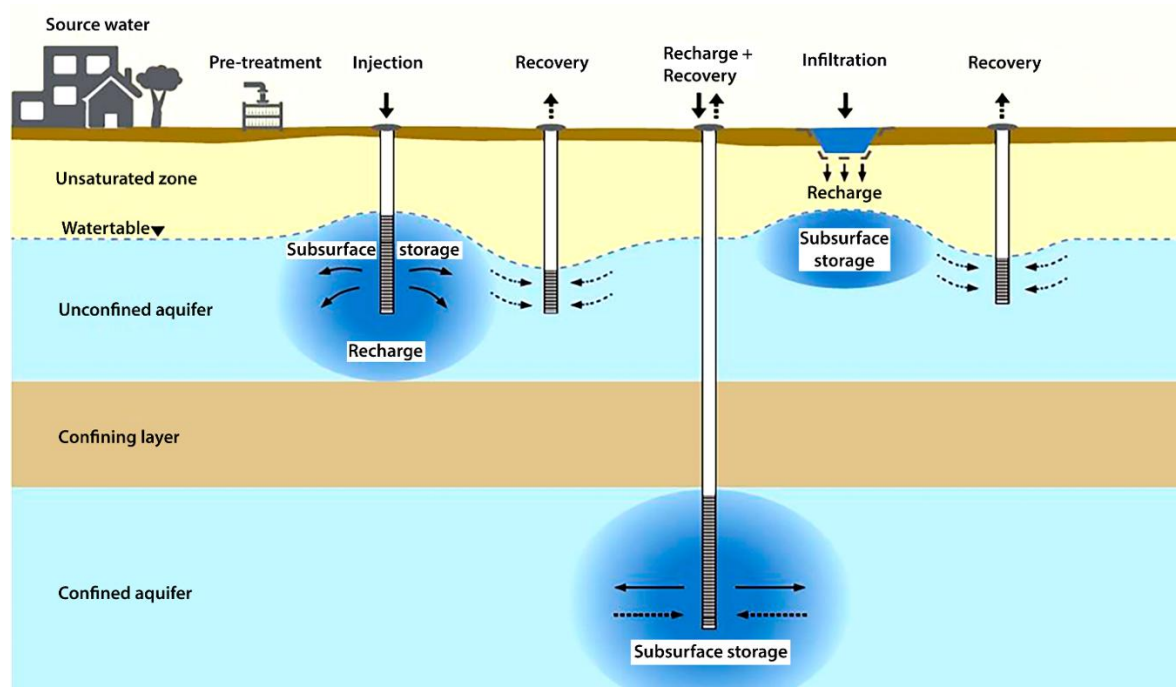
Figure 14 - Schematic illustration of managed aquifer recharge (Reproduced from Government of Western Australia, 2021).

MAR was first recorded in China prior to 200 BC, where river water was directed into channel networks and allowed to infiltrate, thus raising groundwater levels and improving groundwater quality (Zhang et al., 2020). It is now widely practiced in urban environments, where stormwater runoff or treated wastewater is first collected in detention basins where it is either allowed to naturally infiltrate or from which it is pumped into nearby injection wells (Moeck et al., 2017; Dillon et al., 2019). Some of the water quality issues associated with managed aquifer recharge are discussed by Edwards and others (2022), Dillon and others (2019) and by Díaz-Cruz and Barceló (2008).

MAR is becoming common in mining environments, where it is used to reduce environmental impacts of water table drawdown resulting from mine dewatering (Baquero et al., 2016). There is potential for MAR to be used to improve mine closure outcomes by hastening water table recovery after mine operations cease thus reducing the time that rock is exposed to oxidation which leads to acid mine drainage (Cook et al., 2022). Aquifer injection to dispose of wastewater—e.g., co-produced water for shale gas—is not usually considered to be MAR as its focus is disposal of waste not beneficial use.

3   Assessment of Diffuse Recharge

3.1   Introduction

Several methods are available for estimating rates of diffuse groundwater recharge, and some of the most widely applied techniques are described in this section. More extensive descriptions of these and other methods can be found in Healy (2010), Healy and Cook (2002), Scanlon and others (2002), and Seiler and Gat (2007). The methods described here are: water balance approaches (Section 3.2); hydrograph analysis (Section 3.3); chloride mass balance (Section 3.4); unsaturated zone tracers (Section 3.5); and groundwater dating (Section 3.6). Stable isotopes of water and noble gases cannot usually be used for quantifying recharge but can provide important information on recharge processes, so these methods are described in Section 3.7. Other methods (including geophysics and remote sensing) can be used for spatially extrapolating field measurements of recharge, or identifying landscape characteristics that influence recharge rates. These approaches do not directly estimate recharge rates, and so are not discussed here, rather these methods of *recharge mapping* are discussed in Section 6.

Methods for quantifying recharge can be classified into areal-based methods (water balance), soil-based methods (unsaturated zone tracers), or groundwater-based methods (hydrograph analysis, groundwater dating). The chloride mass balance can be applied either as an unsaturated zone method or as a groundwater method, depending on whether chloride concentrations are measured in the soil or in the aquifer. The type of method is linked to the spatial and temporal scales of the derived fluxes, as discussed in Section 6. This means that the methods provide an average estimate over a period of time and for a particular area of land. In general, soil-based methods provide recharge estimates over very small spatial scales (< 1 m^2), whereas areal-based and groundwater-based methods provide more regional estimates. Soil-based methods, therefore, need to be replicated to provide information over larger regions. This is discussed in more detail in Section 6.4. Areal- and soil-based methods usually estimate *deep drainage*, rather than *recharge* as defined in Section 2.1; although, soil-based methods may estimate recharge if the data collected are close to the water table. Groundwater-based methods estimate *recharge*. These are key considerations in choosing which method(s) to apply in a particular study.

Another consideration is the temporal scale of the different measurement methods. Some methods estimate recharge over the period of the study, while others provide longer-term estimates. If the recharge rate has changed, then it is necessary to consider whether the unsaturated zone and groundwater system have adjusted to the new recharge rate both in terms of hydraulics and geochemistry. For example, in southern Australia, geochemical measurements on groundwater samples were used to estimate rates of groundwater recharge prior to the clearing of native vegetation and the development of dryland agriculture, even though this land use change had occurred many decades prior to the

23

study (Leaney & Allison, 1986). This was possible because deep groundwater tables and low rates of recharge meant that infiltration since the change in land use had not yet reached the water table (Katz et al., 2016). The temporal scales of the different methods are discussed in Section 6.4.

Another consideration is the accuracy of each method. It is difficult to quantitatively compare the accuracy of most of the methods for estimating recharge because each method relies on different assumptions, and they represent different spatial and temporal scales. However, some methods are more accurate when recharge rates are high (e.g., water balance), and others are more accurate when recharge rates are low (e.g., chloride mass balance). The expected recharge rate at the site should therefore be considered when selecting the most appropriate method(s). In all cases, it is recommended that multiple methods are used and that the assumptions of each method are carefully considered (Healy & Cook, 2002).

3.2   Water Balance Approaches

One of the simplest approaches for estimating groundwater recharge rates uses water balance models. These models typically track changes in water storage over time, and the water balance as illustrated in Figure 15 is expressed by Equation (2).
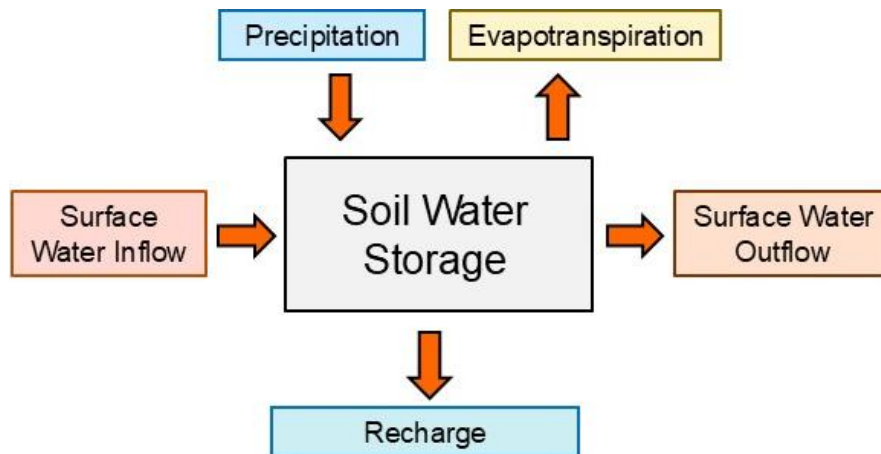
Figure 15 - Schematic representation of water balance models for estimating recharge. These models track changes in soil water storage over time. Over long time periods, changes in soil water storage will be zero, and recharge is equal to *precipitation* plus net *surface water inflow* minus *evapotranspiration*.

$$\Delta S = P + Q_{in} - Q_{out} - ET - R \tag{2}$$

where (parameter dimensions are dark green font with mass as M, length as L, time as T):

     ΔS =   change in moisture storage per unit area (LT^{-1})

     P =   precipitation, plus irrigation if appropriate (LT^{-1})

     Q_{in} =   inflow from surface *runoff* (LT^{-1})

Q_{out} =   outflow from surface *runoff* (LT^{-1})

ET =   actual evapotranspiration (LT^{-1})

R =   recharge (LT^{-1})

The water balance is best calculated using a daily timestep and can significantly underestimate recharge if much longer timesteps are used (Dripps & Bradbury, 2007; Rushton & Ward, 1979). When averaged over long periods of time, the change in water storage should be zero (i.e., inflow equals outflow), and so recharge is given by Equation (3). The water balance method is less accurate when recharge is a small fraction of precipitation because small errors in precipitation, runoff and evapotranspiration can produce large errors in recharge.

$$R = P + Q_{in} - Q_{out} - ET \tag{3}$$

Many different water balance models have been used. They principally differ in how they estimate the components of the water budget and whether they represent the soil as a single storage layer or multiple layers. For example, some models specifically include interception of precipitation by the plant canopy (e.g., Dripps & Bradbury, 2007), whereas others include this in the evapotranspiration term. In cold-climate areas, it is necessary to consider snowpack processes and ground freezing. Cold-climate models thus distinguish between rain and snow, with the precipitation term in Equation (3) partitioned into rain and snow—expressed as snow water equivalent (as discussed in Section 2.6) – and temperature data used to determine the form of the precipitation (Dripps & Bradbury, 2007). A simple and widely used approach for estimating snowmelt is the degree-day method (Tobin et al., 2013). In this approach, melt is estimated based on air temperature, average snowpack temperature, and a range of empirical factors. While more accurate methods are available, they require data that are often not available at meteorological stations (Avanzi et al., 2016; Meeks et al., 2017). If the soil is frozen, infiltration may not occur, and all rain and snowmelt may become surface runoff (Dubois et al., 2021).

In the simplest one-layer water balance models, the plant root zone can be envisioned as a bucket (or reservoir). The water in the bucket represents the water in soil moisture storage. Each day, precipitation is added to the soil moisture storage until a threshold value is reached. Additional precipitation above this threshold value becomes surface runoff (i.e., the bucket overflows). The threshold value is sometimes linked to the soils saturation water content (Finch, 1998). *Actual* evapotranspiration is removed from the bucket. Actual evapotranspiration is difficult to measure so, in the simplest models, actual evapotranspiration is assumed to be a fraction of potential evapotranspiration with the value of the fraction based on the amount of soil moisture storage at that time (e.g., Kennett-Smith et al., 1994). Potential evapotranspiration is the rate that plants can transpire, if unlimited water is available, given the prevailing environmental conditions (e.g., solar

25

radiation, temperature, humidity, wind speed, dew point). Actual evapotranspiration is zero when the wilting point is reached. Recharge occurs as long as the water level in the bucket exceeds some minimum value – a value that is often linked to the soil field capacity.

The maximum value for the soil water storage (S) is called the *plant available water capacity* (PAWC), which can be defined as in Equation (4).

$$PAWC = (\theta_{fc} - \theta_{WP})z_R \tag{4}$$

where (parameter dimensions are dark green font with mass as M, length as L, time as T):

$PAWC$ =   plant available water capacity (L)

θ_{FC} =   volumetric soil water content at field capacity (dimensionless) - often defined as the content to which an initially saturated soil drains after 1 to 2 days

θ_{WP} =   volumetric soil water content at the wilting point (dimensionless) - when the plant cannot access the remaining soil water and therefore wilts

z_R =   thickness of the plant root zone (L)

Recharge occurs when the maximum soil moisture storage ($PAWC$) is exceeded (i.e., the soil moisture storage exceeds the field capacity within the root zone). Multi-reservoir models have also been developed in which the soil is separated into several vertically stacked layers representing different depth zones (e.g., Finch, 2001). Water then moves from upper layers into lower layers when the storage capacity of the upper layers is exceeded. In these more complex models, recharge occurs when the storage capacity of the deepest soil layer is exceeded.

Some models estimate actual evapotranspiration using an energy balance approach, and water uptake is distributed between different layers according to their soil matric potential and plant root content. The soil matric potential is the force with which water is held by the soil matrix (Hillel, 1982). Soil water is preferentially extracted by the vegetation where water is most available and where plant roots are concentrated. Such models typically use the Richards Equation (Hillel, 1982) to simulate soil water movement. In these models, the rate of soil water movement depends on the unsaturated hydraulic conductivity of the soil, which in turn depends on the soil water content at that time. If plant roots extend to the water table, models based on the Richards Equation are able to simulate the time lag between infiltration and recharge (as discussed in Section 5.7). A few models simulate dynamic plant growth as a function of the availability of water, nutrients, and light (Crosbie et al., 2013; Zhang et al., 1999). As plants grow, transpiration increases, and the root distribution can change depending on the availability of water within the soil. Many models are one-dimensional (Kennett-Smith et al., 1994), but some are quasi-three-dimensional and route surface runoff to adjoining model cells using a digital elevation

model (Dripps & Bradbury, 2007). Routing runoff to other cells based on topography is necessary to simulate focused recharge through topographic depressions.

Examples of the use of reservoir-type water balance models to estimate recharge include Rushton and Ward (1979), Kennett-Smith and others (1994), Dripps and Bradbury (2007), and Dubois and others (2021). Models that simulate water movement through the soil profile using the Richards Equation include Zhang and others (1999), Keese and others (2005), Kendy and others (2003), and Crosbie and others (2013).

The accuracy of water balance models is improved if they are calibrated to field data. Some models are calibrated to stream data, assuming that all surface runoff and groundwater recharge enters streams within a relatively short time period as illustrated in Figure 16 (Dubois et al., 2021). Models that simulate water movement through the soil profile are sometimes calibrated to soil water content data (e.g., Kendy et al., 2003). Models that simulate plant growth can be calibrated to leaf area index (Zhang et al., 1999). One-dimensional reservoir models are usually uncalibrated but may be validated by comparison with recharge estimates obtained using other methods. One of the advantages of water balance models is that they can be used in a hypothetical, predictive mode, such as to examine how changes in precipitation might impact groundwater recharge. This is discussed in Section 7.
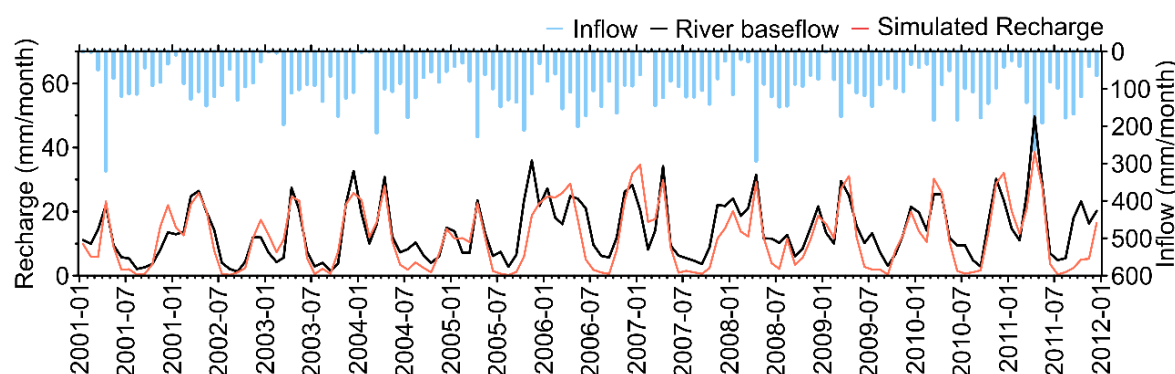
Figure 16 - Monthly potential groundwater recharge simulated for the Yamaska watershed, a catchment of the St Lawrence River, Canada. Recharge estimates were obtained from a daily water balance model and aggregated to monthly values (red line) for comparison with river baseflow estimates derived from a baseflow filter applied to stream gauge data (black line). Inflow (blue bars) is the sum of precipitation and snowmelt (reproduced from Dubois et al., 2021).

Recently, global scale water balance models—sometimes called *global hydrological models*—have been used to construct global recharge maps as illustrated in Figure 17 (Döll & Fiedler, 2008; Wada et al., 2010). These models typically use global precipitation and evaporation datasets, but a relatively simple model of surface water, soil, and groundwater systems. The models simulate river flow and groundwater discharge to rivers, and are usually calibrated using river flow data. However, the models do not explicitly include recharge from rivers or lakes, and so represent diffuse recharge rather than total recharge (Döll and Fiedler, 2008).

27
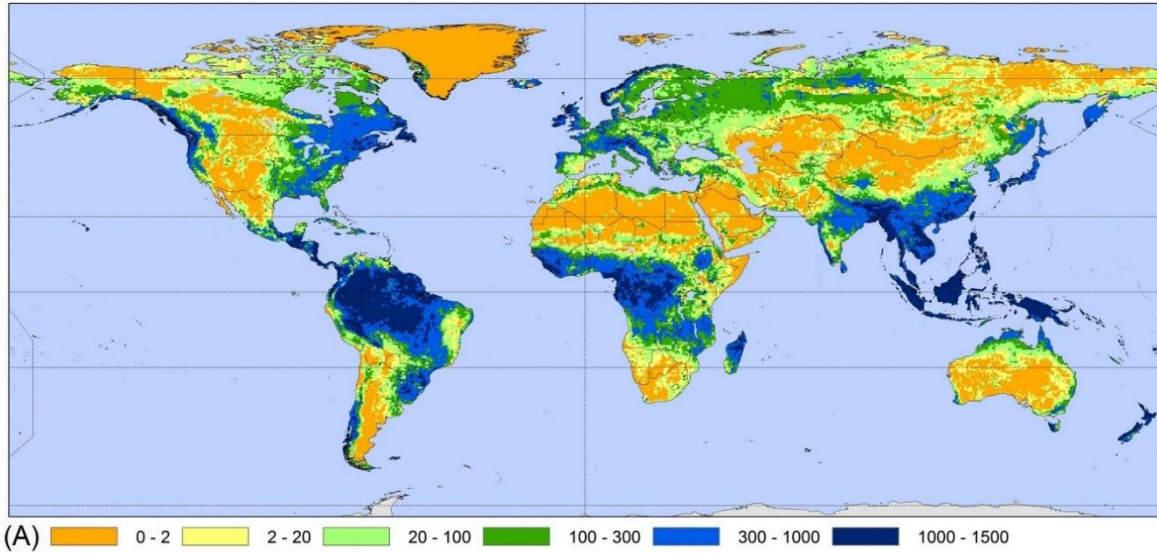
Figure 17 - Global map of groundwater recharge, based on the global hydrological model PCR-GLOBWB (reproduced from Wada et al., 2010).

3.3   Hydrograph Analysis

Analysis of groundwater levels is perhaps the most widely used method for estimating recharge. It is based on the premise that increases in groundwater levels in unconfined aquifers are primarily due to aquifer recharge. Recharge is then calculated from the rate of water table rise as shown in Equation (5).

$$R = S_y \frac{dh}{dt} \tag{5}$$

where (parameter dimensions are dark green font with mass as M, length as L, time as T):

R = recharge rate (LT^{-1})

S_y = specific yield (dimensionless)

h = water table height (L)

t = time (T)

This method is often referred to as the *water table fluctuation* (WTF) method (Healy & Cook, 2002). The application of the method, however, needs to be undertaken with care, as Equation (5) is incomplete. A more complete description of the change in water storage within the aquifer at any location of interest is given by Equation (6). As defined here, Δ*S* is the change in saturated zone water storage, whereas in Equation 2 it refers to the change in water storage above the water table.

$$\Delta S = S_y \frac{dh}{dt} = R - D + (Q_{gwin} - Q_{gwout}) \tag{6}$$

where (parameter dimensions are dark green font with length as L, time as T):

R = groundwater recharge rate for the region of interest (LT^{-1})

28

D	=	vertical discharge rate per unit area for the region of interest (e.g., evapotranspiration loss of groundwater, or downward leakage to an underlying confined aquifer) (LT^{-1})
Q_{gwin}	=	horizontal groundwater flow per unit area into the region of interest (LT^{-1})
Q_{gwout}	=	horizontal groundwater flow per unit area out of the region of interest (LT^{-1})

Equation (5) will be correct if, for the period of interest, discharge is negligible and the horizontal groundwater flow out equals the horizontal groundwater flow in. Thus, for example, Equation (5) will not be correct if any increase in groundwater recharge is balanced by an equivalent increase in groundwater flow away from the location. In general, a rise in the water table caused by groundwater recharge, **will** cause an increase in groundwater flow away from the site. However, where a sudden pulse of recharge occurs over a relatively large spatial area, the flow of water away from this location will be delayed. If most of the increase in groundwater flow occurs after the recharge event has occurred, water table monitoring with a fine temporal resolution can sometimes be used to estimate the amount of recharge that occurred based on the magnitude of the initial water table rise. This is the basis of the water table fluctuation method. In contrast, if groundwater recharge occurs continually and at a constant rate, then no water table rise would be expected (as Q_{gwout} would equal R), and so the water table fluctuation method would incorrectly estimate zero recharge. To calculate the recharge rate over long time periods it is usually necessary to calculate the recharge for each individual recharge event and to sum these values.

Defining the increase in water table elevation for each event usually involves first calculating what the water table elevation would have been in the absence of the recharge event. Where the water table elevation was stable prior to the recharge event, this is relatively straightforward, but often it involves extrapolating the observed water table decline following the previous recharge event (Figure 18) and this imposes some subjectivity to the method. This occurs because $Q_{gwout} > Q_{gwin}$ in Equation (6), and so the water level change from the pre-existing horizontal groundwater flow needs to be accounted for.
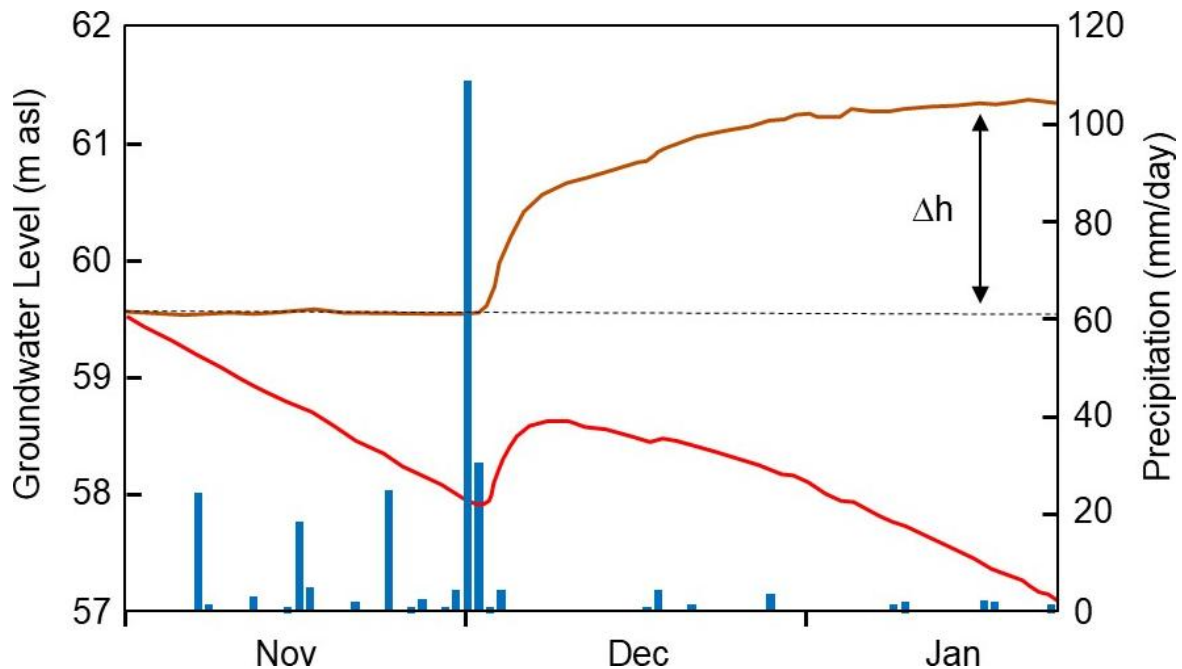
Figure 18 - Illustration of the water table fluctuation method for estimation of recharge. At this site in southern France, the water table was declining prior to a large rainfall in early December 2003. The observed water table is shown by the red curve (meters above sea level), and the brown curve depicts the inferred water table, Δh, after removing the initial linearly declining trend. While the increase in the water table immediately following the rain event was less than 1 m, the authors calculated that after 50 days the water table was 1.79 m above where it would have been if there had been no recharge and the declining trend had continued. For this extreme recharge event, the authors assumed that all precipitation from the event (141 mm) became recharge, and thus calculated a specific yield of 0.079 (141 mm / 1790 mm). This value of specific yield was then used to calculate the volumes of recharge from smaller rainfall and irrigation events (reproduced from Vallet-Coulomb et al., 2017).

Another uncertainty with the water table fluctuation method is estimation of the specific yield value to be used in Equation (5). Healy and Cook (2002) list specific yield values between 0.02 for a clay and 0.27 for a coarse sand, based on a compilation of studies by Johnson (1967). The specific yield can be calculated from laboratory determination of the soil moisture retention curve, soil drainage experiments, or from field pumping tests, but none of these methods are without uncertainty (Healy & Cook, 2002). While laboratory analyses might yield precise values and measurements might be repeatable (for particular soil types), the value required for Equation (5) to be correct is not constant and not easily measured. Rather, the specific yield will change depending on the water table depth below the land surface, the rate and duration of water table rise (Figure 19), as well as the geological formation at and immediately above the water table.

30
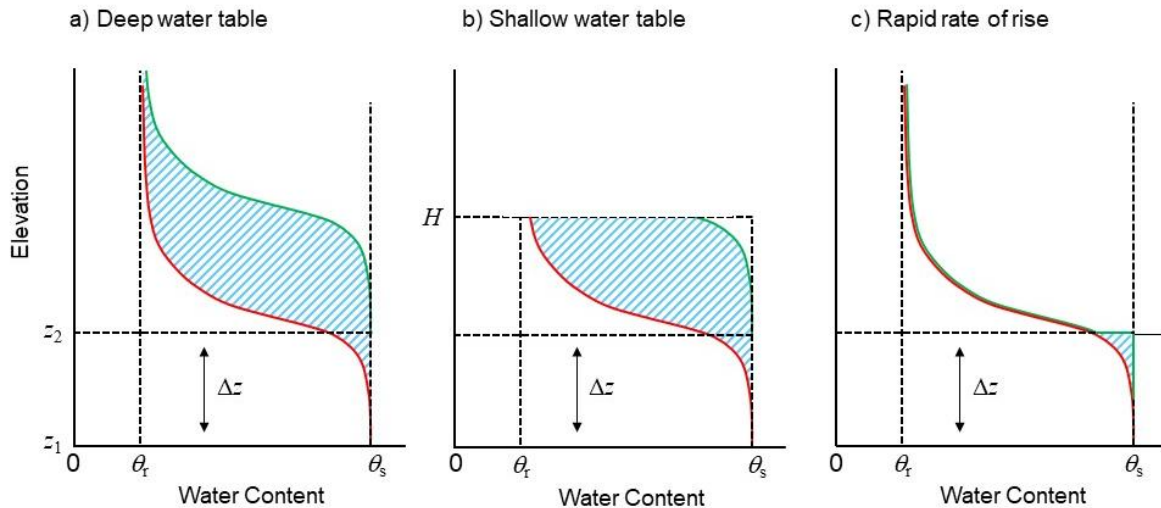
Figure 19 - Conceptual illustration of the specific yield in a homogeneous soil. a) Deep groundwater table. In the case of a static water table, the water content will be at saturation (θ_s) below the water table and for a short distance above the water table (capillary fringe). Above the top of the capillary fringe, the soil water content will decrease with height and will approach a constant value as the distance above the water table increases—sometimes called the residual water content, θ_r. The water content profile above a water table at z_1 is depicted by the red line. If the water table rises (from z_1 to z_2) sufficiently slowly for the water content profile to re-equilibrate, then the entire soil water content profile moves upward—the red curve is replaced by the green curve. The specific yield is the difference in the amount of water stored in the soil (the blue shaded area) divided by the change in water table height (Δz). b) If the water table is shallow—i.e., the land surface is at H in the diagram—then the water content curves become truncated, and the volume of water between these two curves is also reduced. The specific yield is therefore less. c) If the water table rises very rapidly, then there is insufficient time for the water content profile to equilibrate with the new water table position. In the extreme case, if there is no re-equilibration (green line), then the volume of water between the two curves becomes very small, giving a small value for specific yield. Of course, the downward flow of water through the unsaturated zone towards the water table is likely to modify the soil water content profile in the unsaturated zone. This is not depicted in this diagram and will further complicate calculation of specific yield (after Crosbie et al., 2005; Duke, 1972; and Healy & Cook, 2002).

Another complication with the water table fluctuation method is that other processes also induce changes in water levels. These include atmospheric pressure changes, evapotranspiration, and air entrapment during groundwater recharge. These processes are further discussed in Healy and Cook (2002).

The water table fluctuation method is best applied in areas with shallow water tables where recharge occurs in discrete events so that groundwater hydrographs display sharp water-level rises and declines. Sharp rises may not occur in areas of deep groundwater tables, because wetting fronts tend to disperse as they move through the unsaturated zone (Healy & Cook, 2002). Thus, while infiltration may be episodic, rates of recharge may be more-or-less continuous. As discussed above, under conditions of steady recharge, the rate of drainage away from the water table may be the same as the recharge rate so that the water table will be stable, and the water table fluctuation method would estimate that recharge is zero. Often, the water table fluctuation method will underestimate the recharge rate, as there will usually be some attenuation of the recharge pulses during passage through the unsaturated zone.

The time between a precipitation event and its response at the water table can also be analyzed; this can provide information on recharge processes, including the occurrence

31

The GROUNDWATER PROJECT   ©The Authors   Free download from gw-project.org

Anyone may use and share gw-project.org links. Direct distribution of the book is strictly prohibited.

of preferential flow. Preferential flow is usually inferred when deep groundwater tables respond rapidly to precipitation events (Johnston, 1987; Lee et al., 2006). However, quantification of recharge in areas of preferential flow is difficult, as the value of specific yield is highly uncertain.

3.4   Chloride Mass Balance

As precipitation evaporates, the salt present in the precipitation is concentrated in the remaining water. The salt concentration therefore increases in the remaining water. If we know the concentration of salt in precipitation, and there are no other significant sources or sinks of salt, then we can calculate the evapotranspiration rate by measuring the salinity of the remaining water. Chloride is usually measured rather than total salts, or total dissolved solids (TDS) because chloride input from weathering and fertilizers is usually small, uptake by vegetation is minimal, and chloride is less reactive than the other major ions. Consequently, chloride concentration in soil and groundwater can usually be directly linked to the concentration originally present in precipitation (Figure 20). This is the principle of the chloride mass balance approach for estimating recharge. If the system is at steady state, runoff is negligible, and precipitation is the only source of dissolved chloride, then the chloride input at the soil surface must equal the chloride output at the base of the unsaturated zone as indicated by Equation (7) (Allison & Hughes, 1978).
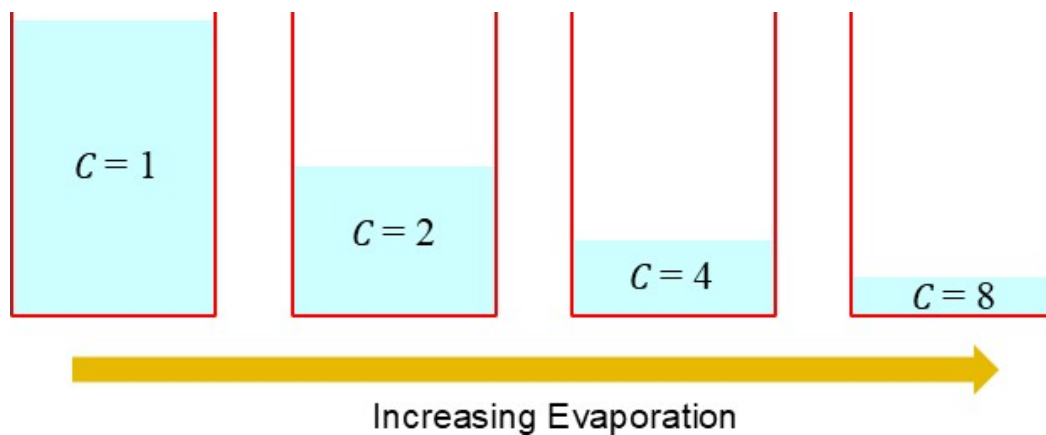
Figure 20 - Progressive increase in chloride concentration, C, in a bucket of water undergoing progressive evaporation. When the water volume reduces to half of the initial volume, the concentration will be double that in the original volume. Similarly, when a quarter of the water remains, the concentration will be four-times the initial value, and when one eighth of the water remains, the concentration will be eight-times the initial value. This is the principle of the chloride mass balance approach for estimating recharge. If the chloride concentration in recharge is double that in precipitation, then the recharge rate will be half of the precipitation rate with the remaining half having been lost to evapotranspiration.

$$C_P P = C_R R \qquad\qquad\qquad (7)$$

where (parameter dimensions are dark green font with mass as M, length as L, time as T):

C_P = chloride concentration of precipitation (including dust particles ($\mathrm{ML^{-3}}$)

C_R = chloride concentration of groundwater recharge ($\mathrm{ML^{-3}}$)

32

P = precipitation rate (LT^{-1})

R = recharge rate (LT^{-1})

The left-hand side of Equation (7) is the chloride input, and the right-hand side is the chloride output. The chloride input includes both the chloride dissolved in precipitation and dry deposition (e.g., windblown salts), and it is usually assumed that open rain gauges collect both components. Strictly speaking, C_P is the measured concentration of chloride in water that is collected in the rain gauge, which is not necessarily the same as that in precipitation. The chloride concentration in recharge (C_R) will be greater than that in precipitation (C_P) due to evapotranspiration, which removes water but does usually not remove salt. The recharge rate can then be calculated as in Equation (8).

$$R = \frac{C_P P}{C_R} \tag{8}$$

The chloride concentration in groundwater recharge can be estimated by measuring the Cl concentration of water within the unsaturated soil profile or in groundwater. Where chloride is measured in soil water, the *deep drainage* rate is estimated, although this is often equated with the recharge rate (as discussed in Section 2.1). In this case, it is most common to obtain vertical profiles of soil water content and chloride concentration, and these profiles need to extend below the root zone for deep drainage to be estimated. The chloride concentration in soil water typically increases through the root zone, as plant roots extract water for transpiration and the remaining chloride becomes progressively concentrated (Figure 21). This zone of increasing chloride concentration thus indicates the depth over which most soil water uptake occurs. Below this depth, chloride concentrations are often relatively stable, particularly in areas with deep groundwater tables. The chloride concentration in this zone is used to estimate the deep drainage rate. In some cases, variations in chloride concentration with depth can be used to estimate historical changes in recharge rates (e.g., Edmunds and Tyler, 2002). In areas with deep groundwater tables, changes in recharge over timescales extending back thousands of years and with resolutions of tens of years are sometimes possible (Stone & Edmunds, 2016).
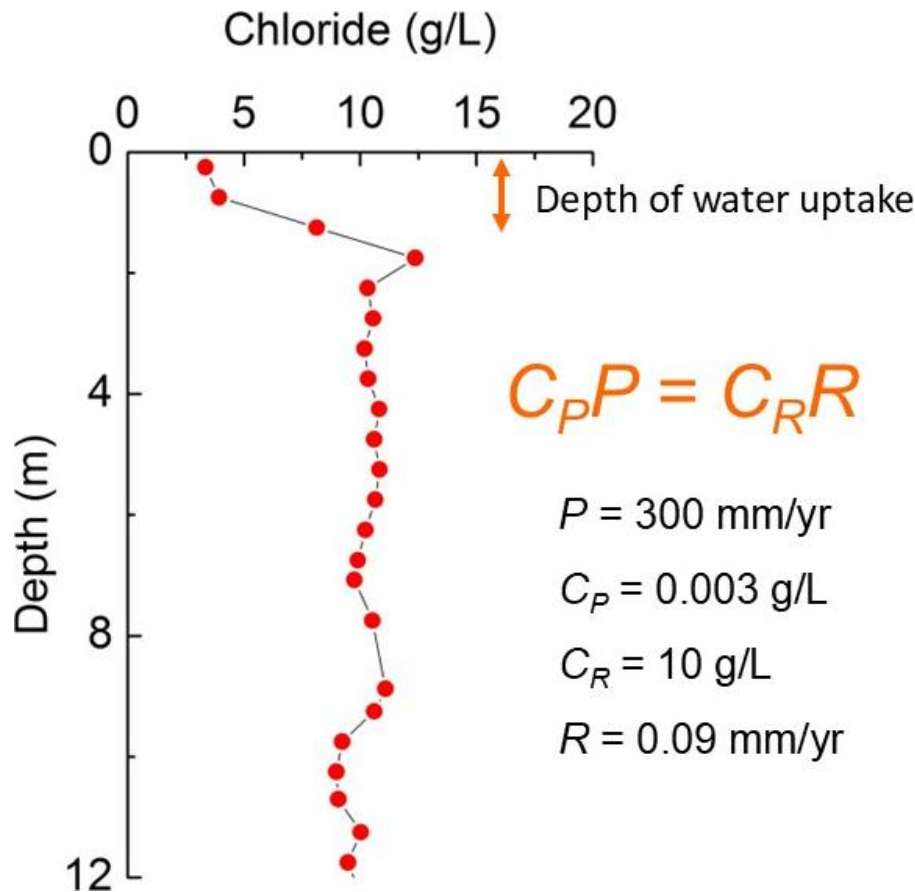
Figure 21 - Example of the application of the chloride mass balance approach to an unsaturated soil profile. This soil profile was obtained from beneath native *Eucalyptus* vegetation in southeastern Australia where the water table is at approximately 60 m depth. The vegetation is known to extend roots to more than 20 m depth, although the increase in chloride concentration in the upper 2 m of the profile indicates that most of the water is extracted in this part of the profile. The chloride concentration is constant at approximately 10 g/L (10,000 mg/L) below this depth (C_R), which is approximately 3300 times greater than the chloride concentration measured in precipitation (C_P). The recharge rate is therefore estimated to be 3300 times less than precipitation, or approximately 0.09 mm/y (redrawn from data in Jolly et al., 1989).

The chloride concentration in the groundwater may also be used as C_R in Equation (8) and used to estimate the *recharge* rate. In this case, the chloride concentration at the water table will indicate the current recharge rate, and concentrations at greater depth will indicate historic recharge rates (more discussion on this is provided in Section 6.4). Exercise 2⤸ provides an opportunity to work with data and apply the chloride mass balance method.

Some studies have estimated the relative contributions of preferential flow and piston flow recharge by comparing chloride concentrations in the unsaturated zone with those in underlying groundwater. The chloride concentration in the unsaturated zone is assumed to represent the piston flow contribution and the chloride concentration in groundwater to reflect the total recharge (sum of piston flow and preferential flow). In southern California, this approach was used to determine that preferential flow constituted approximately 20% of total recharge through a sandstone, with piston flow accounting for the remaining 80% as shown in Figure 22 (Manna et al., 2017). In contrast, a preferential flow proportion of 87% was estimated for China's Loess Plateau (Li et al., 2017). It should

34

be noted that preferential flow in this context includes flow through cracks, fractures, solution cavities, animal burrows, and root channels (as discussed in Section 2.2), as well as focused recharge (as discussed in Section 2.3). It should be noted that care must be taken using this approach, because chloride concentrations in groundwater reflect recharge that has occurred upgradient of the sampling site. It is therefore necessary to ensure that differences between chloride concentrations in the unsaturated zone and those in groundwater are not due to spatial variations in recharge.
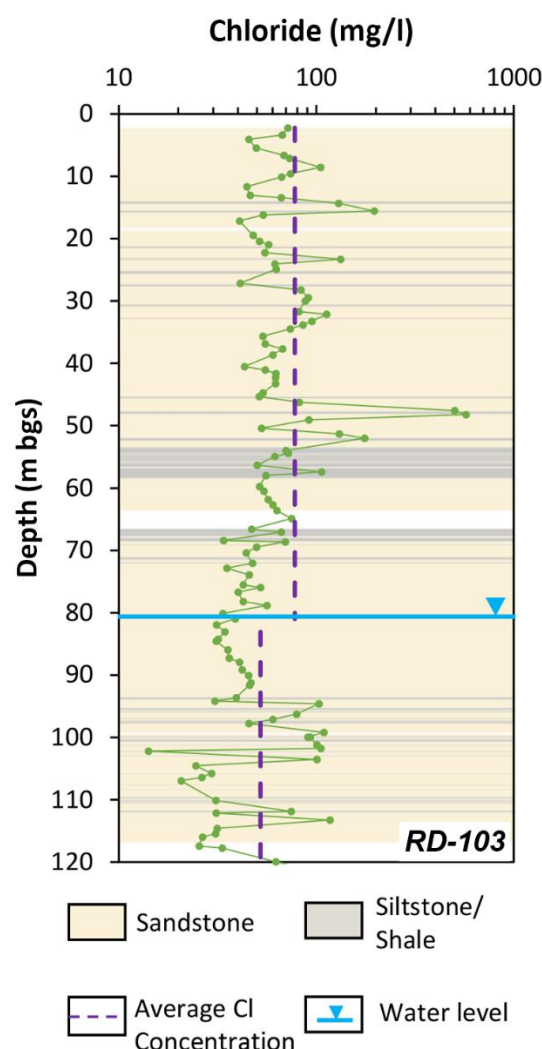
Figure 22 - Comparison of chloride concentrations in soil water and groundwater used to estimate the contribution of preferential flow to total recharge. At this site, the chloride concentration in soil water averages 79 mg/L, while that in the aquifer averages 52 mg/L. Based on a mean annual rainfall of 451 mm/y with chloride concentration of 2.6 mg/L, this gives recharge rates of 14.8 and 22.7 mm/y based on soil water and groundwater concentrations, respectively. Since preferential flow is assumed to bypass the soil water, the higher recharge rate obtained from the chloride concentration in the groundwater is believed to reflect total recharge, and the difference between the two values (22.7-14.8 = 7.9 mm/y) is believed to reflect preferential recharge. At this site, preferential flow is therefore believed to account for 35% of total recharge, although a lower figure of 20% was obtained by applying this approach to bores across the region (after Manna et al., 2017).

35

Several important assumptions are made when the chloride mass balance method is applied. The two most important of these are that 1) there is no source of chloride in the soil or aquifer and 2) the system is in steady state. In the case of sediments of marine origin, it is assumed that there has been sufficient time to flush out connate salts (Herczeg et al., 2001). Other possible chloride sources that need to be considered include the dissolution of minerals, fertilizer input, use of salt on nearby roads, and pollution sources—e.g., wastewater. Chloride/bromide ratios can sometimes be used to assess possible chloride sources (e.g., Manna et al., 2017; Marei et al., 2010; Marrero-Diaz et al., 2015). The chloride mass balance method is best applied in areas with deep groundwater tables, so that evapotranspiration loss of water from the water table does not occur.

Where there has been a change in land use, the chloride concentration in the unsaturated zone and groundwater may not reflect the current recharge rate because of the time required for water to move through the unsaturated zone and groundwater (this is discussed in Section 5.5). In this case, chloride concentrations may reflect the recharge rate under the previous land use. For the special case where the water that has infiltrated since the change in land use has not yet reached the water table, the chloride mass balance method may be modified to estimate the deep drainage rate under the new land use despite the new steady state not having been reached. The method estimates the new deep drainage rate based on unsaturated zone chloride profiles; the recharge rate under the original land use can be estimated from the chloride concentration in groundwater as discussed in Section 3.5 and by Walker and others (1991).

Equations (7) and (8) do not include water loss or gain through surface runoff, so the chloride mass balance is most commonly applied in areas where runoff is a relatively small component of the water balance. If surface water inflow occurs and is not considered, then estimates of recharge obtained from the chloride mass balance will usually be minimum values (Allison et al., 1985). The method may be modified to incorporate water and chloride input lost or added through surface runoff; although, in these cases the volumes of the water added or removed and its chloride concentration must be known (Manna et al., 2016). The chloride mass balance method has also been applied to arid areas where groundwater recharge is dominated by focused recharge from an ephemeral stream or *wadi* (Bazuhair & Wood, 1996; Marei et al., 2010), by measuring chloride concentrations in groundwater and without explicitly accounting for surface runoff ([Box 1⏎](#)). The assumption here is that the mean chloride concentration measured in the groundwater will represent the mean recharge rate within the region and that the chloride mass balance approach can be applied without needing to know about the processes and rates of redistribution of water and chloride. However, quantification of recharge through specific focused recharge features requires estimation of runoff volumes and chloride concentrations. Thus while it may be possible to quantify total recharge across a region based on the mean chloride concentration in the regional groundwater, this does not allow estimation of the fraction of recharge that occurs through focused recharge or the recharge

rate through specific focused recharge features. The chloride mass balance method can also be applied in irrigation areas if the irrigation rate and chloride concentration of irrigation water are known.

One of the main advantages of the chloride mass balance method is its simplicity. The method has been extensively applied in arid and semi-arid regions. In these areas recharge rates are usually very low and evaporation rates are high; so, chloride concentrations in soil water and groundwater are high. This means that they can be measured easily, and other contributions of chloride can usually be ignored. The approach fails, however, if salt concentrations exceed mineral solubility limits, and salt begins to precipitate.

Aside from the assumptions, one of the key sources of uncertainty is estimating the chloride input at the land surface. The chloride concentration in precipitation changes with the precipitation amount and sometimes with the wind direction and origin of storm systems. For this reason, long-term measurements of several years are recommended. Several studies have measured concentrations of different ions in precipitation (e.g., Freydier et al., 1998; Junge & Werby, 1958), that can be used to determine chloride input ($C_P P$). However, the challenge is estimating long-term chloride input, particularly if the chloride mass balance is used to estimate recharge over thousands of years (as discussed in Section 6.4). Over these time periods, the impacts of changes in sea-level and weather patterns on chloride concentrations in precipitation and precipitation volumes can be difficult to determine and current day concentrations may be very different than those of the past thousands of years.

3.5   Unsaturated Zone Tracers

Deep drainage can be estimated by monitoring the downward movement of applied or environmental tracers through the unsaturated zone. Environmental, or natural, tracers are deposited on the soil surface by precipitation—and sometimes as dry deposition as particles carried by the wind—while applied tracers can either be applied to the soil surface or at depth in the profile. Profiles of measured tracer concentrations can also be used to evaluate models of soil water flow and to assess mechanisms of groundwater recharge.

The steady state mass balance approach for estimating recharge from unsaturated zone chloride profiles is discussed in Section 3.4. Where a change in land use has led to an increase in deep drainage, the increased rate of drainage causes the leaching of salt from the soil profile. The boundary between the saline water (below) and the fresher water (above) forms a marker, and its rate of movement reflects the downward water velocity (this is discussed in Section 5.7). If the time of the change in land use is known, then the extent of the leaching can be used to estimate the deep drainage rate (Walker et al., 1991; Scanlon et al., 2007).

Several environmental tracers other than chloride have been used as unsaturated zone tracers for measuring rates of deep drainage leading to groundwater recharge. The two most widely used have been tritium (^{3}H) and chlorine-36 (^{36}Cl). Both ^{3}H and ^{36}Cl concentrations in precipitation were high during the 1950s and 1960s due to thermonuclear bomb testing, and they provide markers of precipitation from that time. Their depth in the soil profile can be used to estimate the downward water velocity (Cook et al., 1994). Both ^{3}H and ^{36}Cl are radioactive. Since the half-life of ^{3}H is 12.3 years, much of the ^{3}H that was deposited during the 1950s and 1960s has since been lost to radioactive decay. However, while the concentration of ^{3}H in the soil is decreasing, it remains a useful tracer of soil water processes. The half-life of ^{36}Cl is approximately 300,000 years, and so there has been insignificant radioactive decay of ^{36}Cl since the period of high fallout.

In its simplest form, the deep drainage rate is determined from the rate of downward movement of the peak (or maximum) concentration of the tracer (in the case of ^{3}H, ^{36}Cl or an artificial tracer) or the freshwater – saline water boundary (following an increase in recharge). The velocity of the tracer (v) is estimated from, as in Equation (9):

$$v = \frac{z_2 - z_1}{t_2 - t_1} \tag{9}$$

where (parameter dimensions are dark green font with mass as M, length as L, time as T):

z_1 = application depth of the tracer (L)

z_2 = observed tracer depth at time t_2 (L)

t_1 = application time (T)

t_2 = observation time (T)

The recharge rate is then in Equation (10):

$$R = (t_2 - t_1)^{-1} \int_{z_1}^{z_2} \theta(z) dz \tag{10}$$

where (parameter dimensions are dark green font with mass as M, length as L, time as T):

$\int_{z_1}^{z_2} \theta(z) dz$ = volume of water stored between depths z_1 and z_2 per square meter of land surface (L^{3}L^{-2} that is, L)

For a surface-applied tracer, including one that is naturally applied in precipitation, $z_1 = 0$. Some errors are introduced if the tracer has not moved significantly past the base of the plant root zone, as fluxes within the root zone will be higher than through the remainder of the unsaturated zone (as shown in Figure 2). As discussed in Section 2.1, under steady state conditions and if there are no impeding layers, the flux below the root zone can be equated with the recharge rate.

For both ^3H and ^{36}Cl, the derived deep drainage rate represents an average value over the time between peak levels of the tracer in precipitation and when the soil sampling occurred. Thus, since the peak ^3H concentration in precipitation occurred in about 1963; then if soil samples for ^3H analysis were collected in 2013, the derived deep drainage rate would be an average value over the 50-year period prior to sampling. An example of the use of environmental ^3H to estimate recharge is provided in Box 2. Other examples of the use of environmental ^3H to estimate recharge include the Gambier Plain in south-eastern Australia (Allison & Hughes, 1978), the High Plains aquifers of the USA (Wood & Sanford, 1995), and the Loess Plateau, northern China (Huang et al., 2019). Examples of the use of ^{36}Cl include south-eastern Australia (Cook et al., 1994) and the south-western USA (Phillips et al., 1988; Scanlon, 1992).

In the case of ^3H, an independent estimate of the recharge rate can also be obtained by comparing the total amount of ^3H in the soil profile with the total ^3H in precipitation, corrected for radioactive decay (Allison & Hughes, 1978). Since ^3H is lost from the profile when water is evaporated or transpired, the ratio of the total ^3H in the soil profile to the ^3H in precipitation provides an estimate of the deep drainage rate as a fraction of precipitation. There are some important differences in how the two methods of estimating recharge from ^3H profiles are affected by different hydrological processes. The use of the peak displacement approach assumes that water moves by piston flow—hence all the water above the ^3H peak has infiltrated since the time of maximum ^3H in precipitation (piston flow is discussed in Section 2.2). The mass balance approach does not assume piston flow and is not invalidated by preferential flow processes (preferential flow is discussed Section 2.2), but it does assume that the soil profile contains all ^3H that has infiltrated and that there has not been significant transport beyond the sampled depth. The mass balance method assumes that there is no runoff from, or to, the sampling site, or that such lateral inputs of ^3H are accounted for in the calculation of the ^3H input from precipitation. In the study described in Box 2⤵, the two deep drainage estimates (340 and 260 mm/y) differ by approximately 25%, which provides some indication of the uncertainty of the method at this site.

Applied tracers that have been used to estimate rates of deep drainage leading to groundwater recharge include ^3H (Athavale et al., 1980), deuterium (Beyer et al., 2015), bromide and chloride (Rugh & Burbey, 2008; Slater et al., 1997). Of course, all these tracers can also occur naturally; so, artificial applications need to be at concentrations that greatly exceed those that may occur naturally, and/or corrections need to be made for ambient concentrations. Importantly, artificial tracers only provide information on deep drainage rates over the period between application and observation—usually no more than a few years, and often much less. The method is therefore most suitable in areas with high rates of recharge, where significant movement of the tracer will occur in a relatively short time.

39

The GROUNDWATER PROJECT   ©The Authors   Free download from gw-project.org

Anyone may use and share gw-project.org links. Direct distribution of the book is strictly prohibited.

Even so, extrapolating from short-term recharge to long-term rates can be difficult as discussed in Section 6.4.

A key advantage of environmental and artificial tracers is that the measured profile also provides important information on flow processes, and particularly on the role of preferential flow (e.g., Beyer et al., 2015). The movement of saline tracers such as chloride and bromide can sometimes be detected using geophysical imaging to provide a more complete picture of flow processes (Rugh & Burbey, 2008; Slater et al., 1997).

3.6   Groundwater Age

In an unconfined aquifer receiving diffuse groundwater recharge, the groundwater close to the water table will be younger than groundwater from deeper within the aquifer. The groundwater age is usually considered to be zero at the water table. If the recharge rate is high, then the age will increase slowly with depth, and if the recharge rate is low, age will increase rapidly with depth (Figure 23). Assuming piston flow, the recharge rate can be estimated if the rate at which groundwater age increases with depth can be measured.
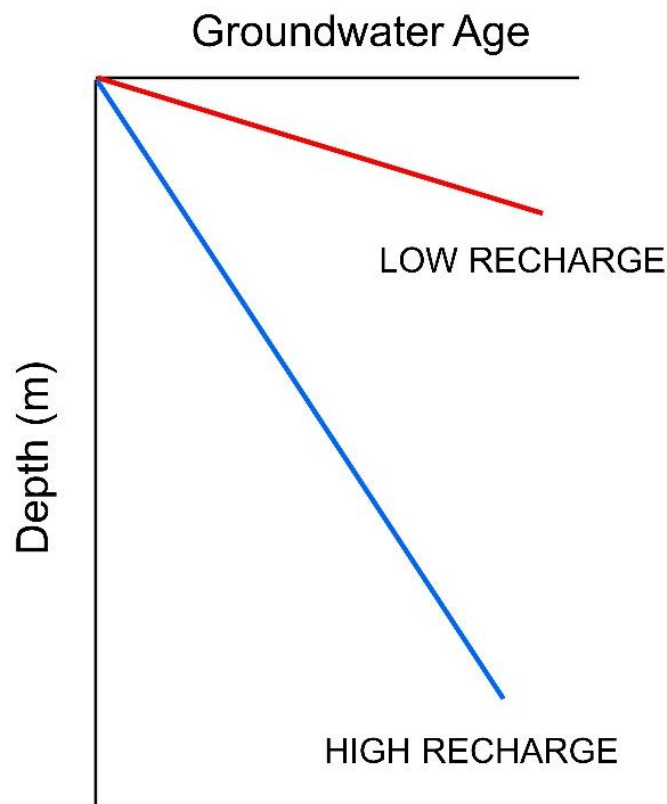
Figure 23 - Conceptual representation of the use of groundwater age tracers for estimating recharge. The groundwater age will increase rapidly with depth if the recharge rate is low and will increase slowly with depth if the recharge rate is high. If samples are collected close to the water table, then the rate of increase in age with depth will be proportional to the recharge rate.

Because aquifers are not infinitely deep, groundwater age does not continually linearly increase with depth. Rather, the rate at which age increases with depth becomes

40

faster towards the base of the aquifer. For an aquifer of uniform geology, constant thickness, that is receiving constant recharge, the groundwater age increases exponentially with depth below the water table, and is given by Equation (11) (Vogel, 1967).

$$t = \frac{H\varepsilon}{R} \ln \left(\frac{H}{H-z} \right) \tag{11}$$

where (parameter dimensions are dark green font with mass as M, length as L, time as T):

t = groundwater age (T)

H = aquifer thickness (L)

ε = porosity (dimensionless)

R = recharge rate (LT^{-1})

z = depth below the water table (L)

However, in the top part of the aquifer—where piezometers are often installed—the exponential rate of increase of the groundwater age can be approximated by a linear rate, and written as Equation (12).

$$t = \frac{z\varepsilon}{R} \tag{12}$$

The age of groundwater—defined as the time since water entered the saturated zone—can be estimated from measurements of water chemistry <u>as discussed by Cook (2020) in his Section 3.2</u>↗. In an unconfined aquifer, measurement of the age of water at discrete depths within the aquifer therefore allows the rate of groundwater recharge to be determined, if the aquifer porosity is known. The estimated recharge rate reflects the mean recharge over a period of time corresponding to the estimated groundwater age. Thus, using Equation (12), if the aquifer porosity is 0.10, and a groundwater sample collected at a depth of 5 m below the water table is estimated to be 50-years old, then the recharge rate is estimated to be 10 mm/y (i.e., 5000 mm (0.1)) / 50 y). This recharge rate is an average over the past 50 years. In this same case, if the aquifer thickness were 20 m and the more accurate Equation (11) was used, then the recharge rate would be estimated as 11 mm/y.

Figure 24 shows a vertical profile of groundwater age obtained from a multi-level well in the shallow, sand aquifer on Cape Cod, Massachusetts, USA, as part of an investigation into the transport of organic contaminants (Solomon et al., 1995). The exponential increase in age with depth at this site is revealed by the data, because some samples were collected close to the base of the aquifer. The observed increase in groundwater age with depth can be reproduced using Equation (11) with a recharge rate of R = 115 mm/y (also discussed in Section 3.2 of Cook (2020)).
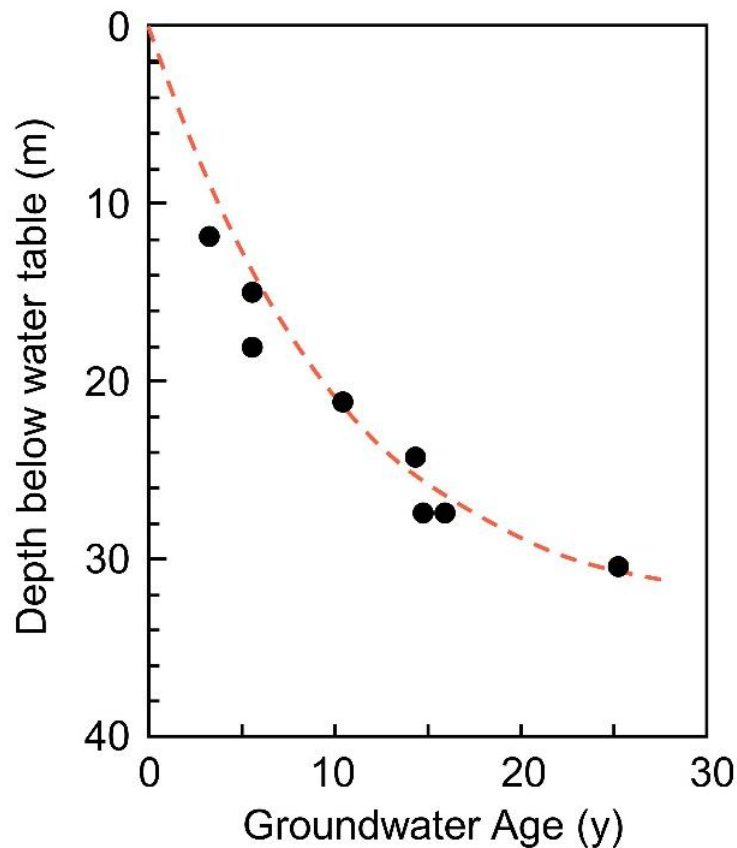
Figure 24 - Groundwater ages measured in 1992–93 at a field site in Cape Cod, Massachusetts, US using tritium (^{3}H) and helium isotopes. Closed circles represent field measurements from samples collected by piezometers screened at different depths, and the broken line represents the age profile predicted for an unconfined aquifer using Equation (11) with constant aquifer thickness of $H = 33$ m, porosity $\varepsilon = 0.35$ and recharge rate $R = 115$ mm/y (after Solomon et al., 1995).

It is important to recognize that estimation of recharge using vertical profiles of groundwater age does not require that groundwater flow is vertical. Groundwater samples collected from below the water table will have entered the aquifer upgradient of the sampling location, and the estimated recharge rate relates to the area upgradient of the sampling site. Deeper samples will provide estimates of recharge over longer time periods and greater upgradient distances. This is discussed further in Section 6.4. Recharge estimation using groundwater dating is most accurate when wells with short screen intervals can be sampled, so that the depth from which the groundwater samples are obtained (z in Equations (11) and (12)) is accurately known. It also requires that the groundwater age can be accurately determined, which will depend upon the methods used to estimate the groundwater age and the geochemical conditions in the aquifer (as discussed in Section 5 of Cook (2020)↗).

Exercise 3↳ provides an opportunity to calculate the time required for water to move from the surface to the water table.

3.7   Water Isotopes and Noble Gases

Measurement of the stable isotope ratios of hydrogen and oxygen atoms in water molecules, or concentrations of noble gases dissolved in water, are not usually used for estimating rates of groundwater recharge, but can be useful for determining recharge processes.

Isotopes are chemical elements that have the same atomic number but differ in their mass number due to different numbers of neutrons in their nucleus (Cook, 2020). Hydrogen, for example, the lightest element, has an atomic number of one. Most hydrogen atoms have a mass number of one—written ^1H—but some atoms have a mass number of two (^2H) and a very small number have a mass number of three (^3H). Hydrogen with a mass number of two is called *deuterium*. Hydrogen with a mass number of three is called *tritium* (^3H) and is discussed in Section 3.5. Since hydrogen is part of the water molecule (H_2O), some water molecules have an atom of deuterium (^2H) rather than both atoms being common hydrogen (^1H). Similarly, most oxygen molecules have a mass number of 16 but some have a mass number of 18. The ratios of $^2H/^1H$ and $^{18}O/^{16}O$ in the water molecule are referred to as the *stable isotope ratios* of water, and processes that cause this ratio to change are referred to as *isotopic fractionation* processes.

Evaporation and condensation are two processes that result in isotopic fractionation of $^2H/^1H$ and $^{18}O/^{16}O$ ratios of precipitation (Cook, 2020; Diamond, 2022). Sometimes these variations can be used to identify conditions under which groundwater recharge occurred. Other factors being equal, the isotopic composition will be more depleted in heavy isotopes—lower $^2H/^1H$ and $^{18}O/^{16}O$ ratios—during heavy rainstorms than during lighter storm events. If groundwater recharge primarily occurs during large rain events, it may cause the mean isotopic composition of groundwater to be more depleted than mean precipitation. Also, precipitation at higher elevations is more depleted than precipitation at lower elevations, and precipitation during cold climatic periods is more depleted than precipitation during warmer periods (Ingraham, 1998). After a precipitation event, the $^{18}O/^{16}O$ and $^2H/^1H$ composition of water may be further modified by evaporation from the soil or from surface water bodies. Thus, measurement of the isotopic composition of groundwater recharge sometimes may be used to determine the elevation at which precipitation leading to recharge occurred or the extent of evaporation before recharge. Stable isotopes are also sometimes used to distinguish irrigated recharge from recharge beneath dryland agriculture and native vegetation, and to identify irrigation canal leakage (Harvey and Sibray, 2001). This is most straightforward when the signature of irrigation water is different from local precipitation and groundwater, such as where irrigation water is sourced from rivers draining adjacent mountain areas (Vallet-Coulomb et al., 2017). Stable isotopes have also been used to identify sites of focused recharge (Vogt et al., 2024),

estimate the intensity of precipitation leading to groundwater recharge (<u>as discussed by Cook (2020) in his Section 3.4</u>↗), and the seasonality of recharge (Cherry et al., 2019).

Noble gases (<u>discussed by Cook (2020) in his Section 2.7</u>↗) are a group of chemical elements that are unreactive. The six naturally occurring noble gases are the chemical elements helium (He), neon (Ne), argon (Ar), krypton (Kr), xenon (Xe), and radon (Rn). Radon and helium are produced predominantly from radioactive decay of other elements. For the other noble gases—Ne, Ar, Kr, and Xe—atmospheric concentrations are constant and differences in their concentrations in natural waters are principally due to differences in gas solubility in water, which is a function of temperature, pressure, and salinity. Concentrations of these gases in water therefore provide information on the temperature and pressure at the time of recharge. Recharge temperature and pressure can be used to infer seasonality of recharge, or recharge elevation in mountainous regions (Peters et al., 2018).

4   Assessment of Focused Recharge

4.1   Introduction

Some of the methods that are used for quantifying rates of diffuse recharge can also be used for assessment of focused recharge. The water balance approach (Section 3.2) includes a term for water that enters a site as surface runoff (e.g., Equations (2) and (3), and the chloride mass balance (Section 3.4) can be similarly modified (e.g., Salley et al., 2022). However, this requires accurately estimating this additional water and/or chloride input, which can be difficult. The ^{36}Cl and tritium peak displacement method (Section 3.5) can be used without any modification to estimate focused recharge rates using samples collected from the unsaturated zone beneath playas (e.g., Wood and Sanford, 1995; Salley et al., 2022). The tritium mass balance method could be used but would require information on runoff contributions.

Different methods have been used for quantifying rates of recharge from rivers and lakes (Kalbus et al., 2006; Rosenberry & LaBaugh, 2008). Amongst the more widely used techniques are seepage meters (Lee, 1977; Murdoch & Kelly, 2003), measurement of heat propagation into the subsurface (Constantz, 1998) and hydraulic calculations using mini-piezometers located beneath the stream or lakebed (Chen et al., 2009; Kennedy et al., 2010). These methods are not used for estimating diffuse recharge either because they require saturated flow (and hence cannot be applied where an unsaturated zone occurs above the water table), or because they are only accurate at high recharge fluxes. Recharge fluxes beneath losing streams are usually much higher than diffuse recharge fluxes. However, all these methods provide estimates of the exchange flux over spatial scales of less than a few square meters of river or lakebed. Very high spatial variability in hydraulic conductivity and seepage flux beneath streams have been observed on scales of meters to tens of meters (Cey et al., 1998; Conant, 2004; Genereux et al., 2008; Kennedy et al., 2009), and so methods that estimate aquifer recharge from rivers over small spatial scales are difficult to extrapolate to catchments or aquifer systems. While these methods are useful for understanding processes, they are not discussed in this section. Methods that have been used for estimating stream recharge over larger scales include hydraulic head gradients, differential flow gauging, and groundwater chemistry. These are described in Sections 4.2 through 4.4.

4.2   Hydraulic Head Gradients

If stream recharge is an important component of total groundwater recharge, then a groundwater mound will usually occur beneath the stream (as discussed in Box 3↴). In connected losing streams (as discussed in Section 2.4), exchange flux can be estimated from Darcy's Law, based on observed hydraulic gradients between the river and nearby monitoring wells and estimates of aquifer transmissivity (Figure 25). However, for this

45

The GROUNDWATER PROJECT   ©The Authors   Free download from gw-project.org

Anyone may use and share gw-project.org links. Direct distribution of the book is strictly prohibited.

approach to be reliable, accurate estimation of transmissivity is critical. This is especially challenging for the case of Figure 25a where the transmissivity value should reflect the properties of both the riverbed and the aquifer. The hydraulic conductivity of the riverbed can be highly variable (Calver, 2001), and this can make accurate estimation of the transmissivity at the required scale difficult. If the riverbed material has a very low hydraulic conductivity, then this may significantly affect the mean transmissivity value, even though the thickness of the streambed sediments may be small. For this reason, this approach for estimating exchange flux is subject to high uncertainty (Cook, 2015). For a disconnected river, the head gradient within the groundwater perpendicular to the river should be used—measured between two wells—rather than the mean gradient between the groundwater and the river (Figure 25b). In this case, the riverbed sediments will not contribute to the transmissivity. The approach shown in Figure 25b is also applicable to a connected losing river, thus is the preferred approach if data from such bores are available. This approach assumes that focused recharge is the dominant process, and so diffuse recharge does not significantly affect the head gradient near the river.
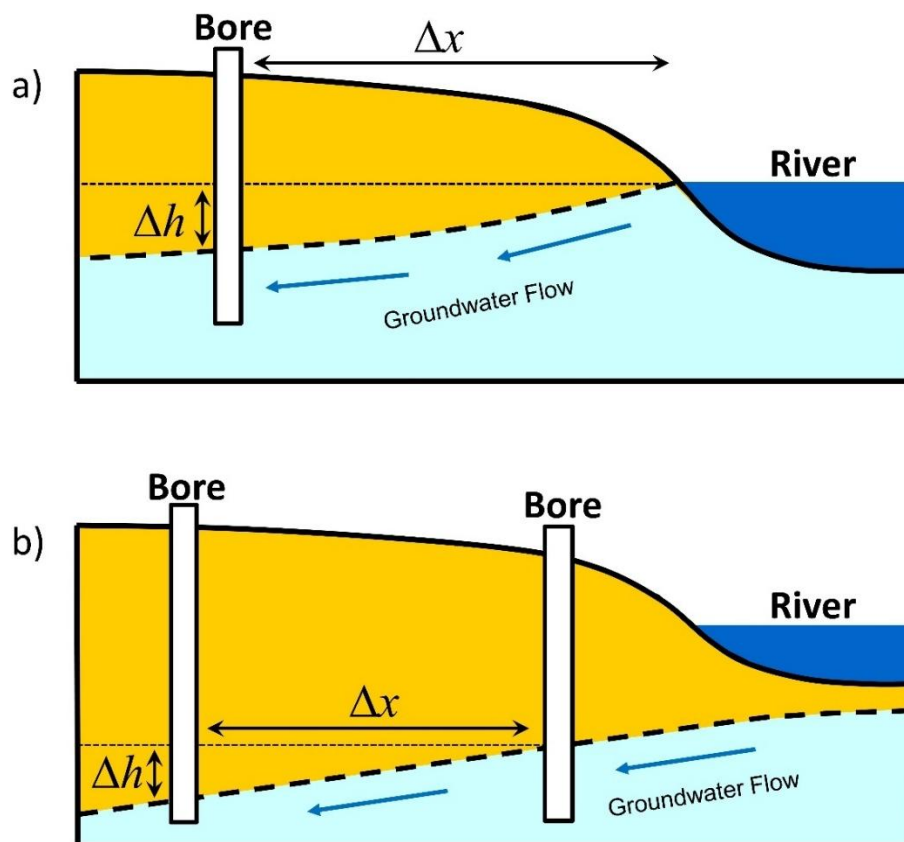
Figure 25 – Estimation of aquifer recharge from a river using the hydraulic gradient method: for a) a losing connected river and b) a losing disconnected river. In both cases, the exchange flux is given by $Q = T\ \Delta h/\Delta x$, where Q is the flux (per meter length of river, T is transmissivity, and $\Delta h/\Delta x$ is the head gradient. In (b), the transmissivity is that of the aquifer between the observation bores, whereas in (a) it is a weighted harmonic mean transmissivity that includes the aquifer transmissivity weighted by the distance from the bore to the riverbed and the riverbed transmissivity weighted by the bed thickness. In very thin aquifers, it may be necessary to consider how the transmissivity varies with aquifer thickness.

46

The GROUNDWATER PROJECT   ©The Authors   Free download from gw-project.org

Anyone may use and share gw-project.org links. Direct distribution of the book is strictly prohibited.

The exchange flux measured by this method most closely reflects the exchange flux over a length of river approximately equal to the distance of the piezometer from the river (Noorduijn et al., 2014). Thus, if piezometers are located 10 m from the stream, the method only provides an estimate of the exchange flux over the adjacent 10 m reach of river. Therefore, piezometers need to be located hundreds of meters from the river to measure regional rather than local fluxes. However, as the distance of the piezometer from the river increases, it becomes more likely that significant recharge or discharge will occur between the piezometer and the river, so that the head difference may no longer reflect only the stream recharge rate. For all these reasons, this approach is unlikely to yield accurate estimates of stream recharge at the regional scale, but the technique is very useful for initial stream recharge estimates, and for examining recharge processes and temporal trends in stream recharge fluxes.

The same approach can be used for quantifying recharge from lakes and other surface water bodies.

4.3   Differential Flow Gauging

Rates of groundwater flow into rivers and river flow into aquifers—recharge—have been estimated from differences between upstream and downstream river flows. If flow gauging takes place during steady flow conditions, then net recharge from the river into the underlying aquifer can be calculated as the difference between river flows measured at two points along the river, after other gains—e.g., tributaries—and losses—e.g., diversions, evapotranspiration—are accounted for. The water balance of any given stream reach can be expressed by Equation (13) (McCallum et al., 2014).

$$\frac{\Delta S}{\Delta t} = (Q_u + Q_t) - (Q_d + Q_p + E_a) + Q_f \tag{13}$$

where (parameter dimensions are dark green font with mass as M, length as L, time as T):

$\frac{\Delta S}{\Delta t}$ = change in water storage within the stream reach (L^3T^{-1})

Q_u = upstream flow (L^3T^{-1})

Q_t = inflow from tributaries or surface runoff (L^3T^{-1})

Q_d = downstream flow (L^3T^{-1})

Q_p = diversions from the stream (L^3T^{-1})

E_a = evapotranspiration (L^3T^{-1})

Q_f = surface water—groundwater exchange (L^3T^{-1})

Positive values of Q_f represent groundwater inflow, and negative values indicate stream loss. For steady flow conditions, $\frac{\Delta S}{\Delta t} = 0$, and so Q_f can be estimated as the difference between the other inflow and outflow terms (terms in the first and second parentheses, respectively).

If stream reaches without tributary inflow and pumping losses (diversions) are selected, often Q_t, Q_p and E_a can also be neglected; therefore, aquifer recharge can be estimated simply as $(Q_u - Q_d)$.

Errors arise from the measurement of river flows and estimation of other components of the water balance, and these errors have proven to be the main limitation of the technique (Cey et al., 1998; Harte & Kiah, 2009). Estimates of surface water—groundwater exchange will only be accurate in reaches where the net exchange flow is significantly greater than this uncertainty. The technique is very useful when aquifer recharge rates are high. Examples of estimation of aquifer recharge based on differential flow gauging include Konrad (2006) and McCallum and others (2014).

In ephemeral streams, flow is rarely stable, and river loss rates (often referred to as *transmission losses*) are determined by integrating the flow rate from the upstream and downstream stations across an entire flow event (Abdulrazzak, 1995). Estimating flow rates of ephemeral streams can be much more difficult than for perennial streams because accessing the river and carrying out manual gauging can be difficult or impossible during flow events (Shanafield & Cook, 2014). However, loss rates of ephemeral streams can be much larger than loss rates of perennial streams—sometimes approaching 100% of streamflow. Where river loss is a high proportion of streamflow, estimates of loss will be less sensitive to measurement errors in flow rate.

While numerous studies have estimated ephemeral river losses, relatively few studies have quantified recharge from ephemeral rivers. The difference between transmission losses and groundwater recharge rates can be very large, as water that infiltrates during flow events can evaporate from the dry riverbed or can be used for transpiration by riparian vegetation during intervening periods—term E_a in Equation (13). Very large floods that inundate floodplain areas produce large transmission losses but proportionally less aquifer recharge due to greater evapotranspiration losses. The water depth and duration of flows within the active streambed would appear to be more important for recharge than overbank flows (Benito et al., 2010). Identifying the proportion of transmission losses that result in aquifer recharge would usually require soil moisture sensors to track infiltration, piezometers to measure the water table rise, and/or climate and vegetation monitoring to quantify evapotranspiration losses. A good example of estimation of recharge using differential flow gauging took place in the Walnut Gulch Experimental Watershed, southeastern Arizona, USA (Goodrich et al., 2004). This study measured the difference in flow between upstream and downstream gauging stations over a two-year period and combined this with a runoff model to calculate runoff that entered the river between the gauging stations, sap flow and eddy covariance measurements to estimate transpiration of riparian vegetation, and monitoring of wells to detect changes in the water table. Other examples of differential flow gauging combined with other monitoring approaches to measure recharge from ephemeral rivers include the Kuiseb River, Namibia

(Benito et al., 2001; as discussed in <u>Box 4</u>↳) and the Tabalah Wadi, Saudi Arabia (Sorman and Abdulrazzak, 1993; as discussed in <u>Box 5</u>↳).

4.4   Groundwater Chemistry

In arid environments, where focused recharge from rivers often dominates total recharge, groundwater beneath streams may have lower total dissolved salts than groundwater further from the streams (as discussed in Box 3). This occurs because diffuse recharge will usually have higher salt concentrations than focused recharge due to greater evaporative enrichment (as discussed in Section 3.4). Stream recharge occurs more rapidly and so there is less opportunity for evapo-concentration of dissolved salts. However, while salinity may be used to infer high stream recharge, it does not usually permit quantification of stream recharge rates. Instead, the rate of stream recharge can sometimes be determined by measuring groundwater age at different distances from the river using environmental tracers. If focused recharge dominates the near-stream water balance, then measurements of groundwater age at different distances from the river allow calculation of the groundwater velocity. This can be converted to a flux by multiplying by the aquifer porosity, length of river and aquifer thickness.

A good example of this approach is a study of the Danube River in Hungary (Stute et al., 1997). In this study, groundwater age was estimated using ^{3}H/^{3}He dating, which permits estimation of water ages up to approximately 50 years as discussed by Cook (2020). Since the river dominates recharge to adjacent coarse-grained alluvial aquifers, groundwater flow away from the river is essentially horizontal, and plots of groundwater age versus distance away from the river appear as straight lines (Figure 26). The slope of these lines is the rate of increase in age with distance, which is the inverse of the groundwater velocity—steeper lines indicate lower velocities. For the shallow wells—screened 5 to 15 m below the land surface—the groundwater age increased from about 1 year at 2 km from the river to 25 years at 21 km from the river, giving an increase in age of approximately 24 years in 19 km. This represents a groundwater velocity of approximately 800 m/y. In deeper wells (screened 50 to 100 m below surface), the groundwater age increased more rapidly with distance, and so the groundwater velocity is calculated to be lower, at around 530 m/y. To calculate a recharge flux, we assume an aquifer thickness of 300 m and porosity of 0.2. We also assume that the shallow wells reflect the velocity in only the top 30 m of the aquifer. This gives a recharge flux of (800 m/y) (30 m) (0.2) + (530m/y) (270 m) (0.2) = 33420 m^2/y, or approximately 33x10^6 m^3/km length of river per year for the studied section. If we also assume that the groundwater velocity is the same on both sides of the river, this gives a recharge flux of 66x10^6 m^3/km/y (2 m^3/km/s). Over the 5 km river reach representative of this flux, this gives a river recharge rate of approximately 50 m^3/s, which is significantly less than the 2050 m^3/s discharge of the Danube at Bratislava (25 km upstream of this reach).
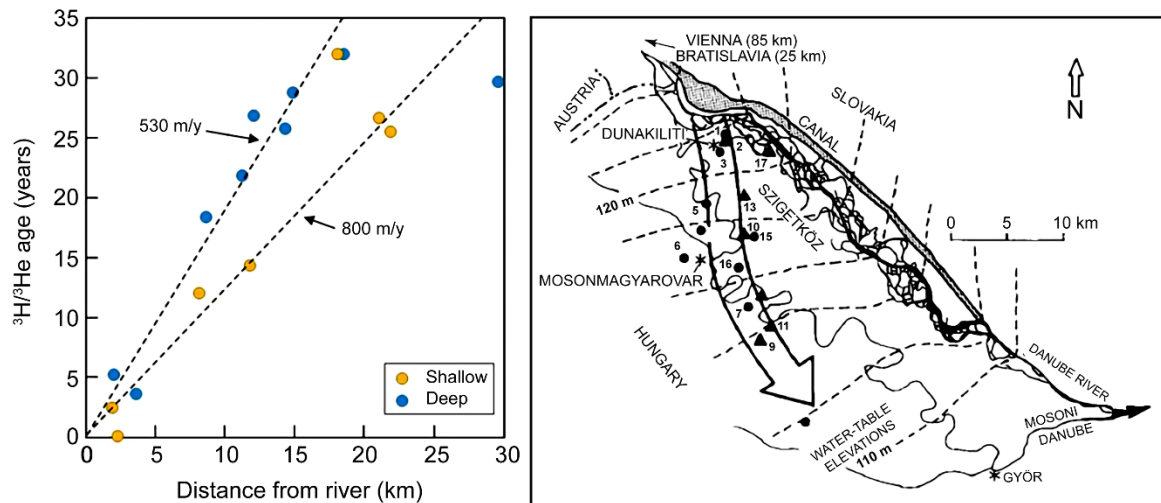
Figure 26 - Groundwater age versus distance from the Danube River in Hungary, measured along the inferred groundwater flow path away from the river. Groundwater velocity appears to be greater in shallow wells (800 m/y) than in deeper wells (530 m/y) (modified after Stute et al., 1997; also discussed by Cook (2020)).

Other environmental tracers have been used to estimate aquifer recharge from rivers, including radon (Bertin & Bourg, 1994; Hoehn & Von Gunten, 1989), and ^{14}C (Drury et al., 1984; Fulton, 2012). In all cases, the tracers are used to estimate the increase in water age with distance from the river. The choice of tracer will depend upon the distance of available wells from the river relative to the likely rate of river loss. If the rate of river loss (i.e., aquifer recharge) is expected to be high then tracers that can estimate ages of young water are preferred (e.g., radon), whereas if the rate of loss is much lower, then tracers that can estimate ages of old water (e.g., ^{14}C) are more suitable. (Cook (2020) discusses environmental tracers for estimating water ages.

5   Rates of Groundwater Recharge

5.1   Introduction

This Section summarises measured rates of diffuse and focused recharge in different environments. Reviews of diffuse recharge values obtained beneath different land covers, through different soil types and in different climatic zones can be found in Kim and Jackson (2012), Petheram and others (2002), Owuor and others (2016), and Scanlon and others (2006). Owuor and others (2016) and Scanlon and others (2006) focus on arid and semi-arid regions; whereas, Kim and Jackson (2012) and Petheram and others (2002) also include higher precipitation areas. Most studies focus on cropping, rangeland, and native forest areas; only Kim and Jackson (2012) contain a thorough assessment of irrigation recharge. Diffuse recharge values measured beneath forests and woodlands, dryland cropping and grazing, and irrigated crops are described in Sections 5.2, 5.3 and 5.4, based on the aforementioned studies. Focused recharge values measured below rivers and streams are described in Section 5.5 and other forms of focused recharge are discussed in Section 5.6. At the time of writing, there have not been any comprehensive reviews of focused recharge rates. Section 5.7 discusses time lags between changes in land use and changes in groundwater recharge.

5.2   Diffuse Recharge beneath Forests and Woodland

Many of the recharge studies beneath native forests and woodland vegetation have taken place in arid and semi-arid environments. Diffuse recharge beneath native vegetation in these environments can be very low, as these vegetation types are well adapted to low precipitation and typically have deep roots that are extremely efficient at extracting soil water. Rates of diffuse groundwater recharge beneath native vegetation in semi-arid areas of southeastern Australia have been measured at 0.05 to 0.2 mm/y (Allison et al., 1990). Precipitation in these areas averages approximately 300 mm/y; and so, recharge is less than 0.1% of precipitation. Similarly low rates of diffuse groundwater recharge have been measured beneath native vegetation in arid and semi-arid areas of southwestern US (Scanlon et al., 1999; Walvoord and Phillips, 2004) and central Argentina (Santoni et al., 2010).

Petheram and others (2002) reviewed recharge rates beneath forests and woodlands in Australia, including eucalypt, jarrah, banksia, and pine ecosystems. Most of the sites had mean annual precipitation of less than 600 mm/y. A regression analysis indicated that precipitation explained 45% of the variation in recharge beneath forest and woodlands on sandy soils and 51% of the variation in recharge on other soil types. Regression is the process of finding a relationship between data sets and if there is a one-to-one correlation, precipitation would explain all of the of variation in recharge. When the correlation between precipitation and recharge is less than one, other factors contribute to the observed

51

recharge variation. Such factors might include soil type (e.g., different types of sandy soils, for example) and vegetation type.

　　　The best-fit relationship between precipitation and recharge for forests and woodlands indicated recharge rates less than 1% of precipitation in areas with sandy soils and precipitation up to 800 mm per year, with lower recharge rates on other soil types (Figure 27). Based on a global review covering sites with up to 2630 mm/y mean annual precipitation, Kim and Jackson (2012) reported an average recharge of 0.2% of precipitation for forests and woodlands with annual precipitation less than 500 mm/y, and approximately 8% of precipitation for sites with a mean annual precipitation of more than 500 mm/y.
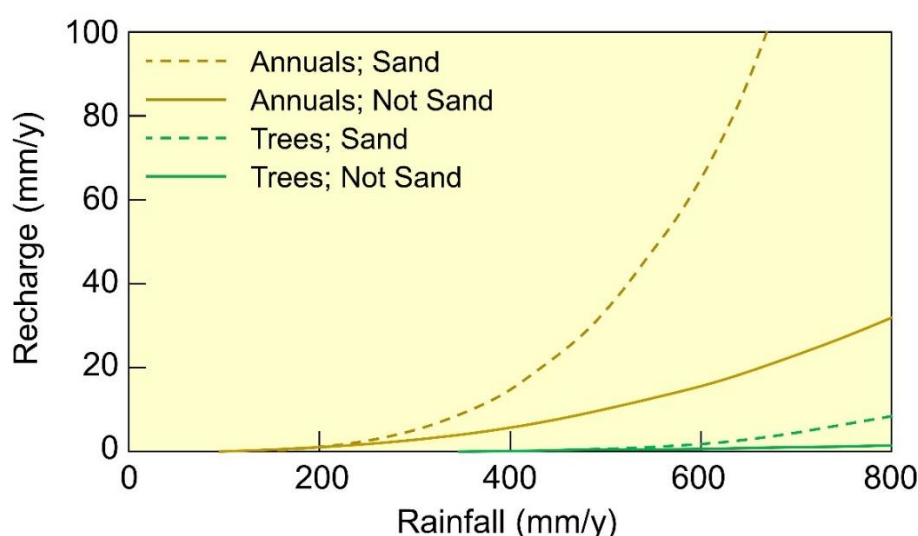
Figure 27 - Empirical relationships between mean annual precipitation and mean annual recharge for tree and annual vegetation types on sands and finer textured soils (non-sand), based on a review of recharge studies in Australia (regression relationships are from Petheram et al., 2002).

5.3　Diffuse Recharge beneath Cropping and Grazing Land

　　　There have been many studies to quantify rates of recharge beneath dryland-agriculture, particularly in semi-arid environments affected by salinization. Petheram and others (2002) reviewed recharge rates in Australia beneath annual vegetation types which included pasture and annual crops, some of which included crop/pasture rotations with periods of fallow. Recharge rates were mostly less than 10% but sometimes up to 40% of precipitation. Recharge was higher on sands than on other soils. A regression relationship indicated that precipitation explained 60% of variation in recharge beneath annuals on sand but only 23% of the variation beneath annuals on other soils. The best-fit relationship indicated recharge through sand of approximately 1% of precipitation where the annual precipitation was 250 mm/y, increasing to 7% of precipitation at 500 mm/y precipitation and 25% of precipitation at 800 mm/y (Figure 27). In the Murray Basin in southeastern Australia, a strong relationship was observed between recharge and clay content in the

upper 2 m of the soil profile, which is the maximum rooting depth of annual crops (Canadell et al., 1996). Mean annual precipitation ranged between 250 and 600 mm/y but was between 300 and 400 mm/y at most sites, and mean annual recharge decreased from approximately 25 mm/y where soils had 3% clay to 3 mm/y for soils with 40% clay (Kennett-Smith et al., 1994).

Owuor and others (2016) conducted a global study across 75 sites, assessing how land use changes affected groundwater recharge in semi-arid regions. They found that changes from native forest to rangelands (i.e., pasture used for stock grazing) caused a lower increase in recharge than conversion to grasslands (i.e., native vegetation with no livestock grazing) or croplands (annual and perennial crops), possibly partly due to compaction of soils by grazing animals. The conversion of forest to rangeland caused an increase in recharge from an average value of approximately 0.13% of precipitation to approximately 0.64% of precipitation. Conversion of forest to grasslands or croplands caused an increase in recharge from an average value of approximately 0.15% of precipitation to approximately 3.7% of precipitation—more than an order of magnitude. The absolute increase in recharge due to clearing forests and woodlands on clay soils was approximately half of that on sands.

Mohan and others (2018) compiled a database of 715 recharge estimates from globally distributed sites and examined the ability of 12 climate and landscape variables to predict groundwater recharge at these sites. Approximately half of the recharge estimates were derived from tracer data—345 of the 715 estimates—with 17% from water balances—123 of 715—and the remainder using other methods. Pasture and cropland were the dominant land uses in the data set. Predictors examined in the study included precipitation, temperature, potential evapotranspiration (PET), number of rain days, land slope, saturated hydraulic conductivity at 0 to 150 cm depth, soil water storage capacity, excess water (monthly precipitation excess over PET), aridity index (precipitation to PET ratio), soil clay content (0 to 150 cm depth), bulk density (0 to 150 cm), and land use. The predictors precipitation, PET, and land use stood out as having the greatest power to explain recharge rate, with soil clay content and saturated hydraulic conductivity the next most important (Figure 28). Other predictors had little explanatory power. However, most predictors were derived from global datasets with spatial resolutions of 0.25 to 0.5 degrees—equivalent to about 500 to 2500 km² at the equator. Thus, some errors would have resulted from the difference between the scale of the predictors (hundreds of square kilometers) and the scale of the recharge measurements—most were point estimates—which may have reduced the apparent importance of predictors that are highly variable at small spatial scales—e.g., soil properties. Nevertheless, based on the derived relationships the authors produced a global recharge map (Figure 29) that shows a similar global recharge distribution to the global map derived from a water balance model as presented in Section 3.2.
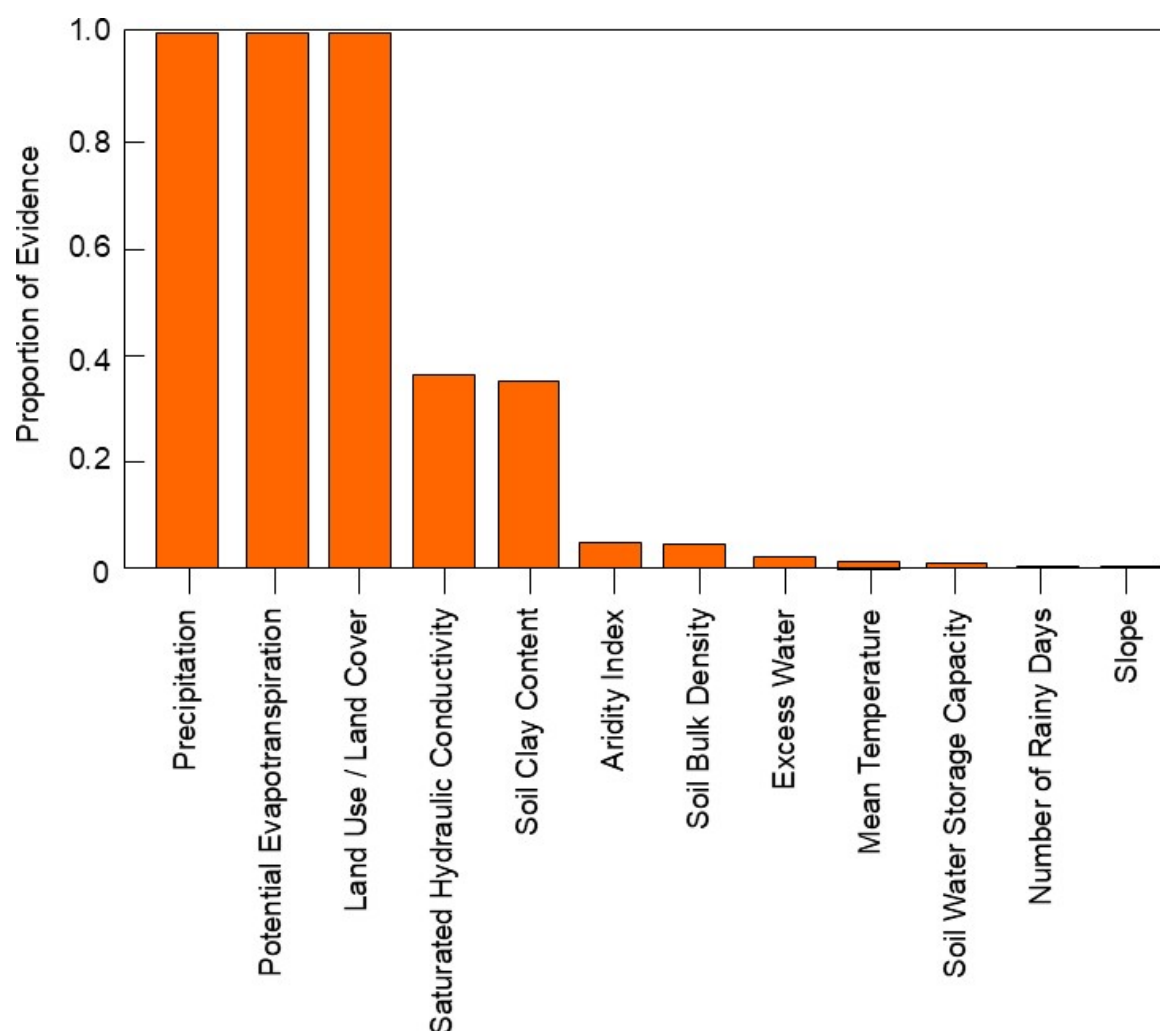
Figure 28 - Relative predictive power of twelve different predictors of groundwater recharge based on a multiple linear regression on groundwater recharge obtained from a global recharge database. Higher values of proportion of evidence indicate increased predictive power (after Mohan et al., 2018).
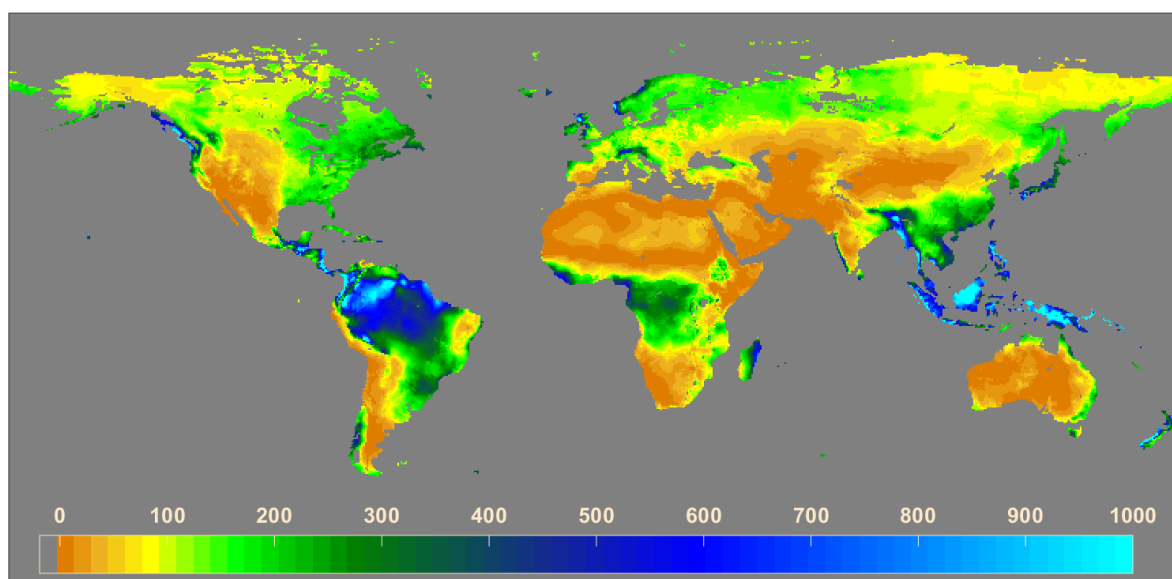
Figure 29 - Annual average groundwater recharge (mm/y) based on a review of recharge estimates and their relationships to soil, climate, and land-use parameters (reproduced from Mohan et al., 2018).

5.4   Diffuse Recharge beneath Irrigated Crops

Recharge rates beneath irrigated areas are a function of soil type and crop type, precipitation and climate, the volume of applied water, as well as the frequency and method of irrigation. Flood irrigation is the application method that is generally considered to produce most recharge with lesser recharge resulting from sprinkler and drip irrigation methods. Liu and others (2012) describe a study in the Mosuowan irrigation district at the southeastern edge of the Gurbantünggüt Desert, northwestern China, where cotton is the main irrigated crop. Annual recharge beneath flood-irrigated fields was estimated to be approximately 110 mm/y, whereas beneath drip irrigation it was approximately half of that value (56 mm/y). Annual precipitation at this site was 117 mm/y, but the volume of irrigated water applied was not stated. In some areas, recharge due to leakage from canals delivering water to farms can be more significant, and sometimes greater, than recharge from leakage beneath irrigated crops (Meredith and Blais, 2019). Vallet-Coulomb and others (2017) describe recharge beneath irrigated agriculture overlying the Crau aquifer in southern France. Precipitation across most of the area is 500 to 600 mm/y, and flood irrigation occurs principally for hay production. Irrigation rates are estimated to be 2000 to 2500 mm/y, mean irrigation recharge is estimated to be 1190 mm/y in addition to natural recharge of 110 to 160 mm/y. The site with the highest irrigation recharge rate was believed to be affected by leakage from irrigation channels.

Perhaps surprisingly, at the time of writing there are not any comprehensive reviews of deep drainage or recharge rates beneath irrigation areas in the scientific literature, although irrigated sites are included in the global review of recharge rates by Kim and Jackson (2012). They developed a relationship between the recharge rate and the total volume of water applied to the soil surface, which was the sum of precipitation and irrigation (Figure 30). Their data showed that the percentage of water input that becomes diffuse groundwater recharge increases with the rate of water input; from approximately 10% of water input at water input rates of less than 1000 mm/y to 20% of water input for rates of 1500 mm. The irrigation method was not considered in their analysis.
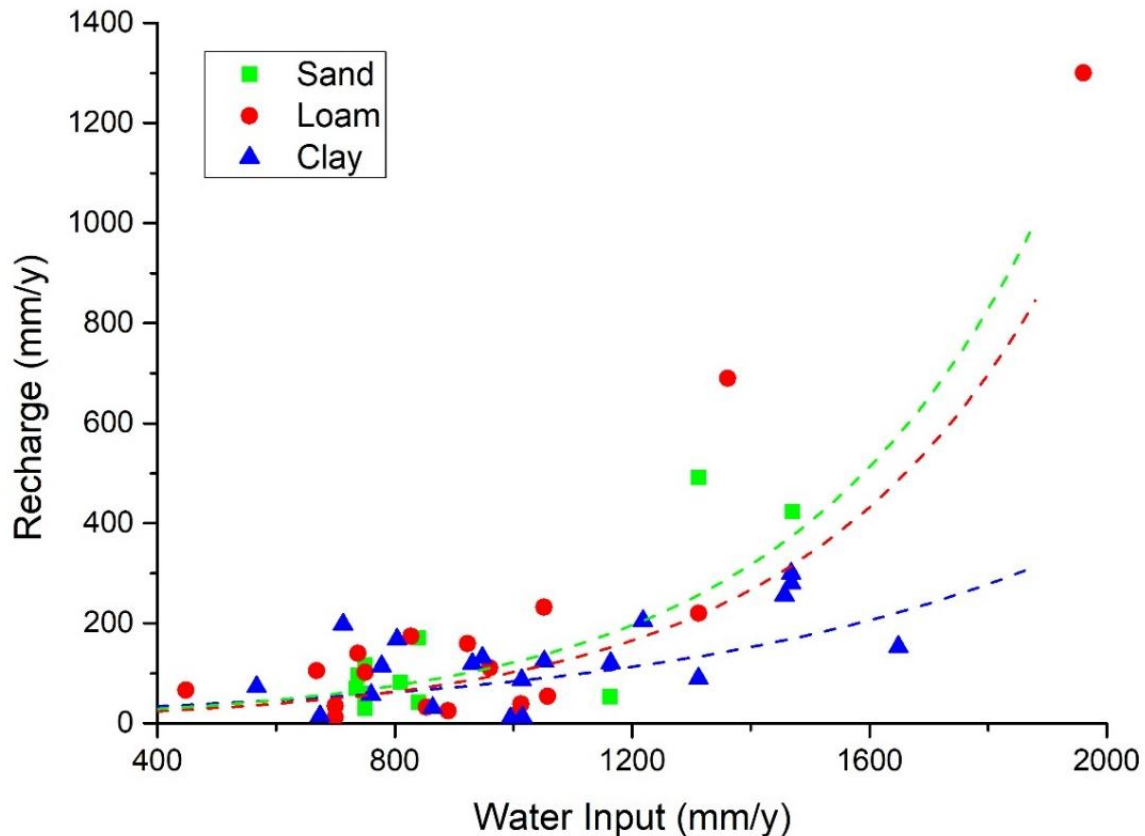
Figure 30 - Relationship between annual water input (precipitation plus irrigation) and recharge rate for irrigated croplands and grasslands based on a global review of recharge rates (Kim & Jackson, 2012). For the purposes of this figure, soil texture classes have been simplified into Sand, Loam (which amalgamates loamy sand, sandy loam, loam, fine sand clay loam and silt loam), Clay (which includes silt, silty clay, and clay). Three sites without soil textural information, but with saturated hydraulic conductivities between 360 and 680 mm/day were included in the Sand category. Broken lines are exponential regression relationships for each category (based on data from Kim & Jackson, 2012).

5.5   Rates of Recharge from Rivers

While there have been several reviews of diffuse recharge rates beneath different land covers and through different soil types, there have not been any comprehensive reviews of recharge rates from rivers, lakes, or other sites of focused recharge. Konrad (2006) examined stream loss rate for six tributaries of the Columbia River draining parts of Idaho, Oregon, and Washington, USA, by measuring changes in river flow rates with distance downstream (as discussed in Section 4.3). Measurements were made at different times during periods of stable flow, and loss rates were calculated for 215 reaches, mostly between 3 to 30 km in length. 74 of the reaches were losing, 116 were gaining and the remainder were neither losing nor gaining. For the losing reaches, loss rates ranged between 0.1 to 6.1 m/day (5.6×10^4 to 2.2×10^8 m^3 per kilometer of river length per year) with a mean loss rate of 0.63 m/day, which is 1.7×10^7 m^3/km/y (Figure 31). For comparison, a mean loss rate near the upper end of the range (6.6×10^7 m^3/km/y) was measured for a losing reach of the Danube River, Hungary (Stute et al., 1997; Cook, 2020; Section 3.5) while a loss rate near the lower end (1.8×10^6 m^3/km/y) was measured for the Namoi River, eastern

56

Australia (McCallum et al., 2014). Key factors determining river loss rates include the hydraulic gradient between the surface water and groundwater, hydraulic conductivity of the river bed, and the cross-sectional area of the flow path between the river and the aquifer. River flow rate is also an important factor, with greater loss rates observed at higher river flow rates (Konrad, 2006). This may be because rivers with higher flow rates will usually be wider and/or have more coarse-textured riverbeds. Groundwater pumping can increase rates of recharge from rivers by lowering water tables and hence increasing hydraulic gradients from connected rivers, until the point when hydraulic disconnection occurs, at which time loss rates reach maximum values as discussed in Section 2.4.
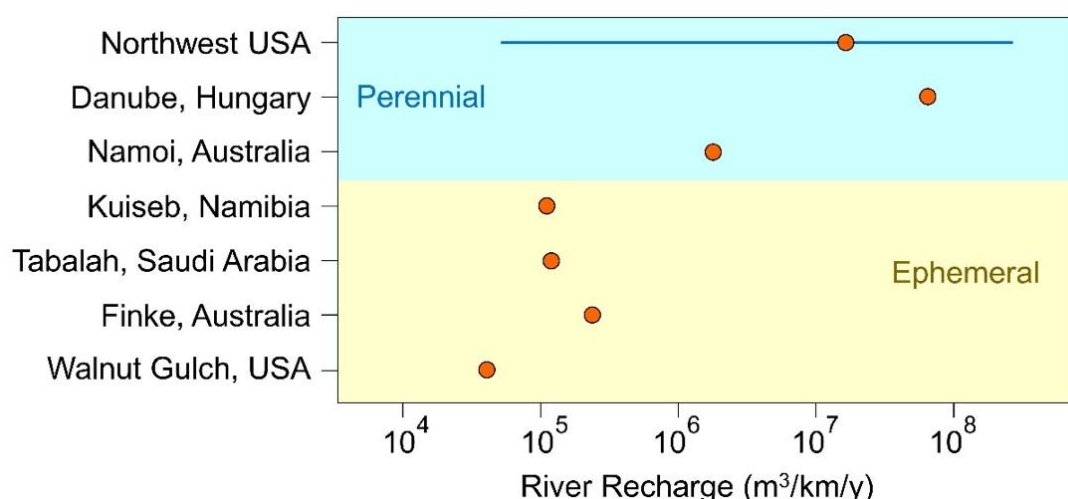
Figure 31 - Rates of groundwater recharge beneath perennial and ephemeral rivers. For ephemeral rivers, data is expressed per year—including no-flow periods—rather than for the duration of flow. Loss rates during flow events are much higher. For the northwest USA, the blue line shows the range of loss rates measured and the circle denotes the mean value. Data for the northwest USA is from Konrad (2006); Danube River is from Stute and others (1997); Kuiseb River is from Benito and others (2010); Wadi Tabalah is from Abdulrazzak (1995), Finke River is from Fulton (2012), and Walnut Gulch is from Goodrich and others (2004).

Similar loss rates have been measured during periods of flow of ephemeral rivers (e.g., 330 m^3/km/h during periods of flow of the Kuiseb River, Namibia; Benito et al., 2010; as discussed in Box 4), although when no-flow periods are included, the average loss rates are much lower (12.6 m^3/km/h or 1.1×10^5 m^3/km/y; Benito et al., 2010). Transmission losses for a 23.8 km reach of Wadi Tabalah, Saudi Arabia, estimated for the three-year period from 1985 to 1987, averaged 0.43×10^6 m^3 per event, with a total loss of 11.6×10^6 m^3 (3.9×10^6 m^3/year) when no-flow periods are included. Based on the estimate that 75% of transmission losses contributed to groundwater recharge, this gives annual recharge of 2.9×10^6 m^3/y, or 1.2×10^5 m^3/km/y (Abdulrazzak, 1995; as discussed in Box 5). The long-term mean recharge rate for the Finke River, central Australia, is between 1.4×10^5 and 3.4×10^5 m^3/km/y (as discussed by Cook (2020) in his Section 3.5). For the much smaller Walnut Gulch, Arizona, recharge for a 7 km reach over a two-year period was estimated to be 560,000 m^3, which is equivalent to 40,000 m^3/km/y.

57

The GROUNDWATER PROJECT   ©The Authors   Free download from gw-project.org

Anyone may use and share gw-project.org links. Direct distribution of the book is strictly prohibited.

5.6   Other Focused Recharge

Apart from rivers, the most-studied focused recharge features are the playas in the High Plains, USA (Gurdak & Roe, 2010; Scanlon & Goldsmith, 1997; Wood & Sanford, 1995). There are more than 75,000 playas overlying the High Plains aquifers (Salley et al., 2022), most of which have surface areas less than 0.2 km^2. The Southern High Plains has the highest density of playas, with an estimated 18,700 playas and density of 4 to 5 per km^2.

Quantifying recharge rates beneath playas is difficult, and estimates can have large error bars (Salley et al., 2022). Mean annual precipitation in the High Plains ranges from approximately 500 to 700 mm/y. Estimates of recharge rates beneath playas in the High Plains vary widely and range from less than 1 mm/y to approximately 600 mm/y, with an average rate of 75 mm/y (Gurdak & Roe, 2010). For comparison, the average recharge rate through inter-playa areas is approximately 12 mm/y. The recharge rate through individual playas is likely to be a function of the catchment area, runoff coefficient, playa soils, land use and vegetation.

The average recharge of playas in the arid Jornada Basin, near Las Cruces, New Mexico, USA ranges from 0.10 to 28 mm/y, with an average of 6 mm/y (McKenna & Sala, 2018). The lower recharge rate compared to the High Plains is probably mostly due to the lower mean annual precipitation of 250 mm/y. Differences in groundwater recharge between playas in this basin were correlated to the size, slope, and soil texture of each catchment with recharge rate increasing with catchment area and catchment slope and decreasing with increasing sand content of soils.

In a semi-arid part of South Australia with mean annual precipitation of 260 mm/y, recharge beneath a single karst sinkhole was estimated to be more than 100 mm/y, while diffuse recharge through calcrete flats was less than 1 mm/y. At another site in South Australia—mean annual precipitation of 400 to 500 mm/y—Herczeg and others (1997) found that water recharging through sinkholes, swamps, and open drainage wells could be identified from its chemical signature only within 150 m of the larger features. The authors thus determined that these focused recharge features accounted for less than 10% of total recharge; although they did not quantify the recharge rates.

5.7   Time Delays Between Changes in Infiltration and Changes in Recharge

Since the land use affects the groundwater recharge rate, changes in land use often lead to changes in diffuse groundwater recharge. However, there is a time delay between a change in land use and a corresponding change in recharge. The magnitude of the time delay is related to the water table depth and is greater when the water table is deeper. For example, when a change in land use leads to a large increase in recharge (e.g., clearing of native vegetation for dryland or irrigated agriculture), infiltration and deep drainage rates increase almost immediately, but it may take several years before the recharge rate

58

The GROUNDWATER PROJECT   ©The Authors   Free download from gw-project.org

Anyone may use and share gw-project.org links. Direct distribution of the book is strictly prohibited.

increases. The time delay is related to the rate of water pressure movement through the unsaturated zone. A pressure pulse is created as the infiltrating water pushes the pre-existing soil water ahead of it (Figure 32). The time for this pressure pulse to propagate through the unsaturated zone can be approximated as shown in Equation (14) (Jolly et al., 1989; Allison et al., 1990).
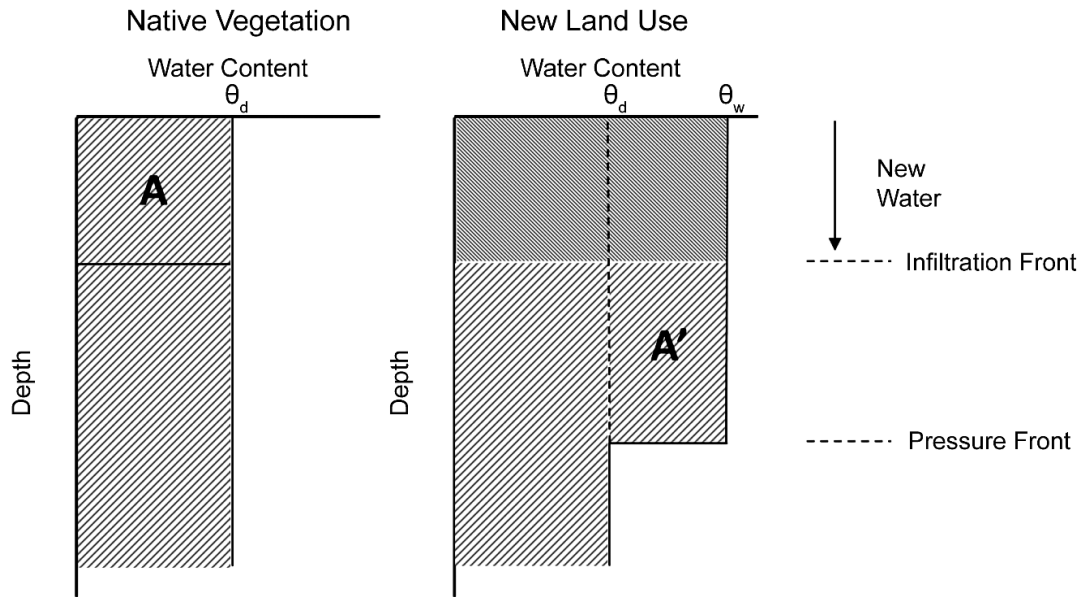

Figure 32 - Schematic of water content of soil under native vegetation following a change in land use, showing the movement of the pressure front in advance of the infiltration front. The pressure front marks the change in soil water velocity (low velocity below, and high velocity above), and the infiltration front marks the boundary between water that infiltrated before the change in land use (below the front) and water that infiltrated after the change in land use (above the front). The schematic shows a homogeneous soil. θ_d is the volumetric water content under native vegetation, which is the same as the water content below the pressure front after the change in land use. θ_w is the volumetric soil water content above the pressure front under the new land use. The water stored in the zone labeled A under native vegetation is pushed ahead of the new infiltrating water. The water volume A and A' must be equal; this allows the relative positions of the infiltrating front and pressure front to be determined from the soil water contents θ_w and θ_d, as described by Equation (14).

$$t_L = \frac{z_{wt}(\theta_w - \theta_d)}{D}$$
(14)

where (parameter dimensions are dark green font with mass as M, length as L, time as T):

t_l　=　time lag from land use change to change in recharge rate (T)

z_{wt}　=　water table depth (L)

θ_w　=　mean volumetric water content of the soil profile before the change in land use (dimensionless)

θ_d　=　mean volumetric water content of the soil profile that will result under the new land use after the pressure has moved through the unsaturated zone and the recharge rate has increased (dimensionless)

D　=　deep drainage rate (LT⁻¹)

The value of θ_w will depend on the new deep drainage and recharge rate and the soil moisture characteristic curve (Hillel, 1982). Where the water table is shallow, the time delay between infiltration and recharge can be very short, but in areas of deeper water tables it can be many years. Figure 33 presents an example from south-eastern Australia where the clearing of native vegetation and development of dryland agriculture has led to an increase in deep drainage that will ultimately cause an increase in recharge. Here, the water table occurs at 60 m below the land surface, and the deep drainage rate under the new land use is approximately 45 mm/y (12% of the mean annual precipitation). In Figure 33, matric potential (discussed in Section 3.2) is used to indicate the depth of the pressure front. In the sandy soils at this site, the mean unsaturated zone water content beneath native vegetation was approximately 0.06, and the water content under dryland agriculture is expected to increase to approximately 0.12, which is the mean water content above the pressure front. Equation (14) gives a time delay between the change in land use and the change in groundwater recharge of approximately 80 years. In practice, the time delay can be determined either from Equation (14), or from observing the velocity of the pressure front through the unsaturated zone. This pressure time delay is different from the travel time for steady infiltration and drainage that is described in Section 2.1.
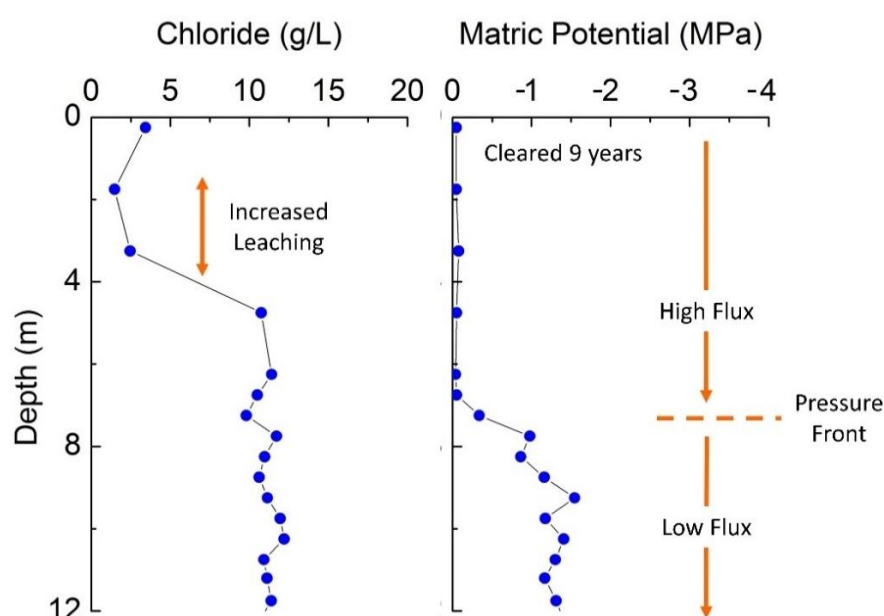
Figure 33 - Conditions associated with an increase in deep drainage leading to an increase in groundwater recharge to a deep groundwater table. The chloride concentration and matric potential of soil water beneath an agricultural field that was cleared of native vegetation 9 years prior to sampling is used to examine the downward movement of soil water that will ultimately result in an increase in recharge. Prior to clearing, high chloride concentrations existed throughout the soil profile. Here, nine years after clearing, the chloride has been leached to approximately 4 m depth (i.e., the infiltration front). This water has displaced the original "pre-clearing" soil water ahead of it, and hence the soil is "wet" (matric potential close to zero) to approximately 7 m depth. Below the pressure front, the soil is drier and soil water is still moving at the pre-clearing rate; the soil water above the pressure front is moving at the new, higher rate. The pressure front has travelled approximately 7 m in 9 years. At this site the water table is approximately 60 m below the land surface, so at the current rate of soil water movement, the pressure front is expected to reach the water table in about 80 years. Recharge to the aquifer will not increase until that time (after Jolly et al., 1989; Allison et al., 1990).

60

There is also a time lag between a decrease in deep drainage and the subsequent decrease in recharge. The decrease in deep drainage might be due to revegetation of previously cleared land, or cessation of irrigation and its replacement with dryland agriculture. The time lag occurs because the water stored within the soil profile under the previous, higher, deep drainage rate will continue to slowly drain to the water table even after the deep drainage rate reduces (Figure 34). Jolly and Cook (2002) carried out numerical simulations to quantify the magnitude of this time lag. They estimated that for a loamy sand soil texture, the time required for recharge to decrease significantly ranges from about 10 years if the water table is 10 m below the land surface to about 50 years for a 50 m water table. The time delays are longer for heavier textured soils, as these soils drain more slowly (Figure 34).
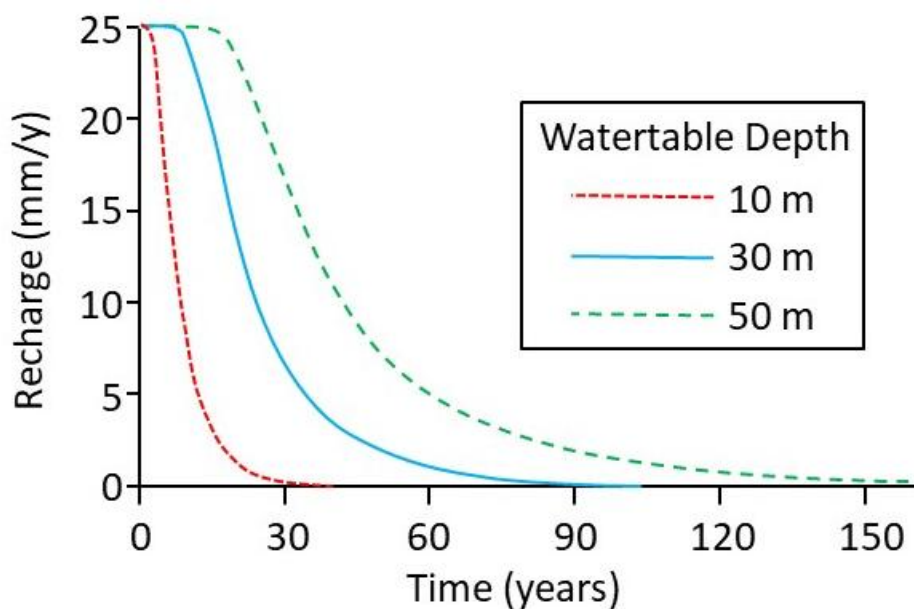

Figure 34 - Predicted changes in recharge over time for three different water table depths following a decrease in infiltration from 25 mm/y to zero. Model simulations are for a loamy sand soil (After Jolly & Cook, 2002).

6   Spatial and Temporal Scales of Recharge Variation

6.1   Introduction

Recharge rates vary with climate, land management practices, vegetation, geology, and soil properties; each of these factors can be spatially variable. Recharge rates are therefore spatially variable. Weather patterns and land management are also temporally variable; hence, recharge rates are temporally variable. These are important considerations in any recharge investigation, and it is important to link the spatial and temporal scales at which recharge is measured with the purpose of the study. Recharge estimation for water resource evaluation tends to rely on long-term estimates of recharge that cover large regions or entire basins. Information on the small-scale spatial variability is usually not required for these studies. However, contaminant transport studies and assessment of aquifer vulnerability to contamination require information on both the spatial and temporal variability of recharge (Scanlon et al., 2006; Dripps & Bradbury, 2010). Spatial variation is important because areas of high recharge will deliver contaminants to the water table more rapidly than other areas.

6.2   Spatial Variability

The spatial variability of recharge is sometimes related to focused recharge and hence linked to geomorphology and surface topography (Scanlon et al., 1999). In other areas, though, there may be no clear link with geomorphology and topography, and variations in recharge may be related to small-scale variations in soil type, variations in fertilizer application in cropped areas, or vegetation structure in open woodlands. The recharge variability over small spatial scales—less than 1 km^2—has been investigated by comparing recharge estimates obtained from measurements on closely spaced soil cores. Johnston (1987) measured chloride profiles on 12 cores obtained within an area of 1000 m^2 near Collie, Western Australia. Eight of the 12 profiles had high chloride concentrations, consistent with recharge rates between 2 to 8 mm/y. However, four profiles, located within a small part of the site, had much lower chloride concentrations, consistent with recharge rates of 50 to 100 mm/y. The area of high recharge was attributed to a discontinuity in the regolith. Cook and others (1989) measured the spatial variability of recharge beneath a 14 hectare agricultural field (annually rotated between dryland crops and pasture) near Adelaide, South Australia. An electromagnetic induction survey was conducted at the site, and 13 cores were taken. Recharge was estimated using a chloride balance approach, and a relationship between apparent electrical conductivity of the earth and recharge rate was used to map recharge across the site. Recharge rate was found to vary between approximately 1 and 50 mm/year (Figure 35) and could be described by a log-normal distribution. The authors concluded that 86% of the recharge occurred through 60% of land

62

area, and 41% of the recharge occurred through 20% of area. The field was selected because large variations in condition of the crop were apparent, which appeared to persist from year-to-year.

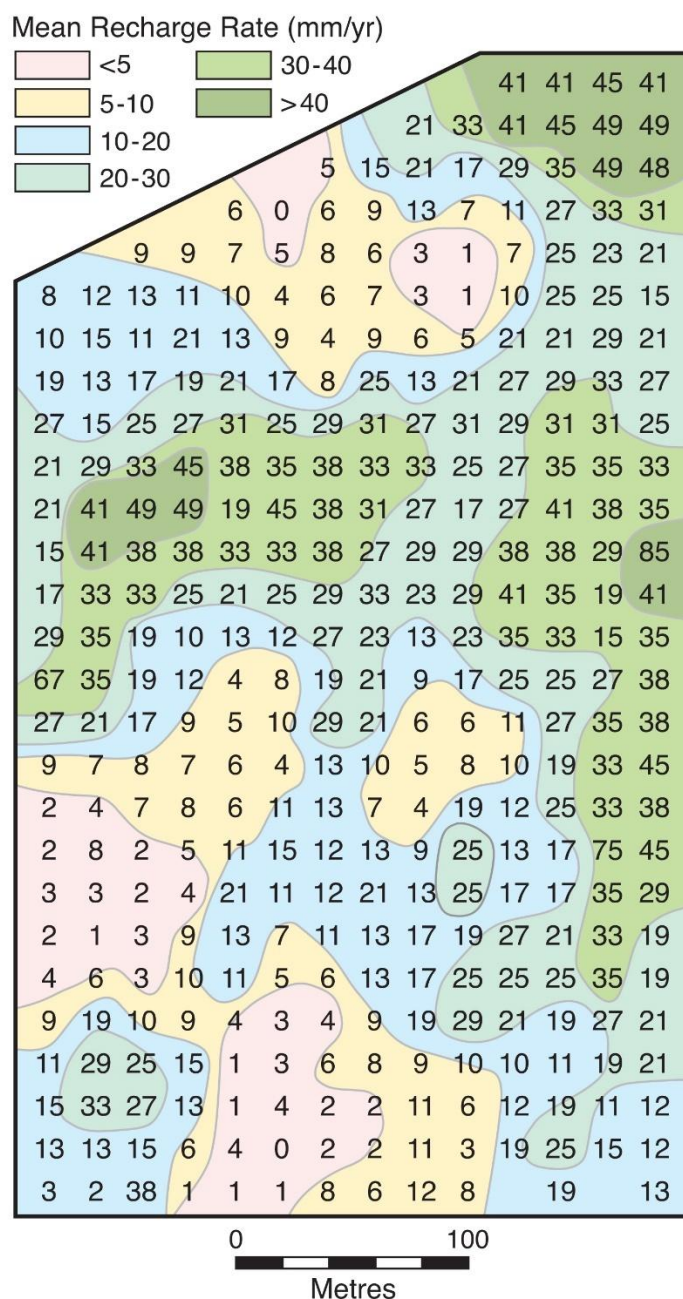**Figure 35** - Spatial variability of groundwater recharge within a 0.14 km^2 agricultural field near Adelaide, South Australia. Numerals represent recharge rates in mm/y, and broad patterns of recharge variability are indicated by color-filled contours. Estimated recharge rates are mean rates since the field was cleared of native woodland for agriculture – a period of approximately 50 years. (Adapted from Cook et al., 1989.)

6.3   Temporal Variability

Recharge is temporally variable due to variations in weather patterns—especially precipitation and air temperature—and seasonal patterns of plant and crop growth and land management. In cropped areas, the period of highest recharge and the magnitude of recharge variability is influenced by climate seasonality, the growing season of crops, whether crop lands are left fallow for part of the year, and the nature and timing of irrigation. In cold climates, timing of snowmelt and ground freezing can be major influences on recharge seasonality. In northern Wisconsin, USA, Dripps and Bradbury (2010) observed low or negligible recharge during the winter months, as the ground is usually frozen, and precipitation occurs mainly as snow. Highest rates of recharge are usually associated with the spring snowmelt, which occurs in March and April in northern Wisconsin. In contrast, recharge is winter-dominant throughout most of Nebraska, USA, despite summer-dominant precipitation, due to high evapotranspiration during the growing season of summer crops. However, some areas in the southeast and southwest of Nebraska show summer-dominant recharge, due to irrigation during the summer growing season (Cherry et al., 2019). In arid and semi-arid climates, recharge is often associated with extreme precipitation events which can also have a seasonal pattern. In the Ti Tree Basin, central Australia, recharge has been linked to extreme precipitation associated with summer monsoon cyclones (Boas & Mallants, 2022).

On a year-to-year basis, the temporal variability of groundwater recharge is usually highest where recharge is low and lowest where recharge is high. Crosbie and others (2012) modeled recharge at 20 sites across the Murray-Darling Basin, Australia, for the period 1895 to 2006 using a water balance model and daily climate data. The site with the highest precipitation had the lowest annual variability in groundwater recharge, and the site with the lowest precipitation had the highest variability (Figure 36). However, even in the high precipitation site, annual precipitation varied over a factor of more than ten.
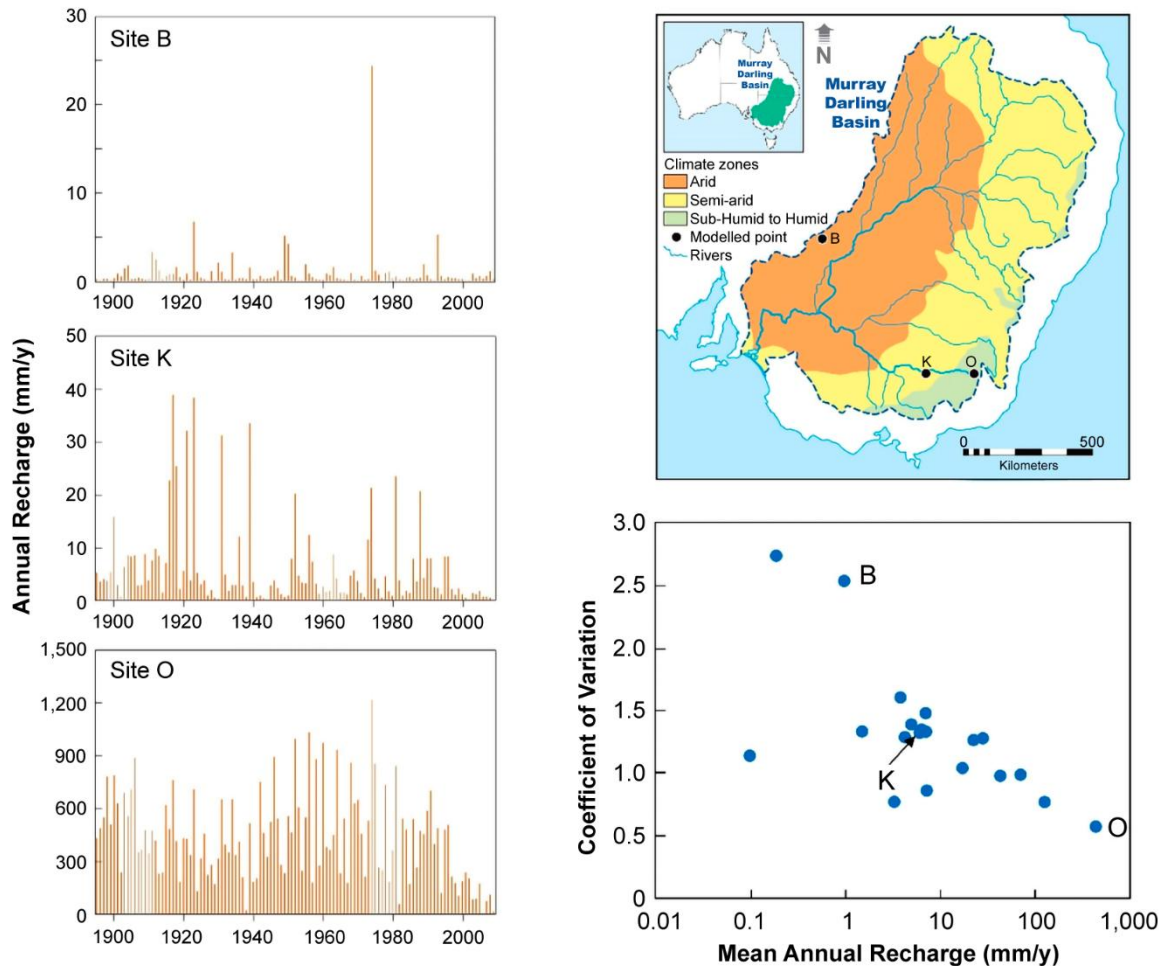
Figure 36 - Simulated variation in annual precipitation at three sites within the Murray-Darling Basin, Australia, together with the relationship between mean annual recharge and coefficient of variation (CV) of annual recharge for these and 17 other sites. Site O has a mean annual precipitation of 1450 mm/y, a mean annual recharge of 435 mm/y and a CV of annual recharge of 0.58. Site K has a mean annual precipitation of 519 mm/y, a mean annual recharge of 6.1 mm/y and a CV of annual recharge of 1.33. Site B has a mean annual precipitation of 205 mm/y, a mean annual recharge of 1.0 mm/y and a CV of annual recharge of 2.54. The data illustrate that temporal variability increases as precipitation and recharge rates decrease (after Crosbie et al., 2012).

The coefficient of variation (CV) is a useful statistic for characterizing the variability of annual groundwater recharge. The CV is calculated by dividing the standard deviation by the mean, with high values denoting increased variability. In the Murray-Darling Basin, the CV of annual recharge increased from 0.58 at a site with mean annual recharge of 435 mm/y to 2.54 at a site with only 1 mm/y of mean annual recharge (Figure 36). In a forested basin in northern Wisconsin, the CV of annual recharge was approximately 0.4, and the mean annual recharge was approximately 280 mm/y (Dripps & Bradbury, 2010). The increase in temporal variability with decreasing recharge is expected, and highlights the need for recharge in arid regions to be measured over long periods of time. Recharge measured over a period of only 1 to 2 years may not be representative of the long-term mean rate.

6.4   Spatial and Temporal Measurement Scales

Each method for estimating recharge has its own temporal and spatial scale (Figure 37). The link between the spatial and temporal scale of the recharge estimate and the spatial and temporal variability of recharge processes is important to understand. The spatial and temporal variability of recharge that occurs on scales that are less than the measurement scale will not be captured in the measurement. Rather, the measurement will provide an average estimate over a period of time and for a particular area of land. These measurement scales differ between the different methods for estimating recharge and between the different environments where the methods are applied.
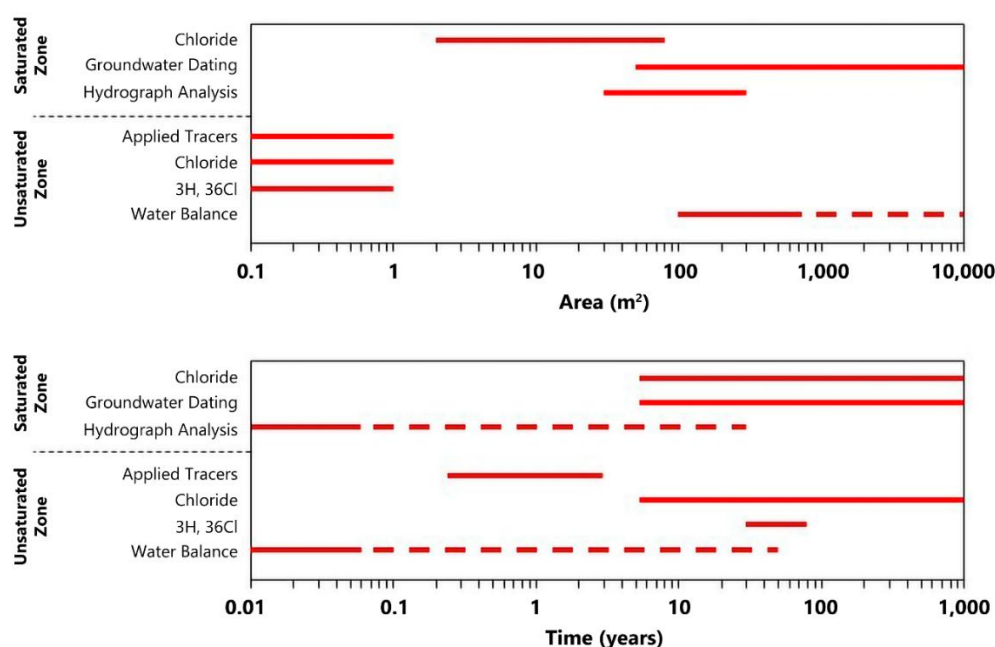

Figure 37 - Approximate spatial and temporal scales of seven methods for estimating diffuse groundwater recharge. Solid lines indicate typical temporal and spatial resolution, whereas broken lines indicate typical coverage. Thus, for example, the water balance is usually applied at a daily timestep, but data is often available to enable deep drainage or recharge to be estimated over several years or decades. It is also usually based on data sets with a spatial resolution of tens or several tens of meters but can provide recharge estimates over very large areas (>10,000 m^2). Similarly, hydrograph analysis can estimate recharge with a resolution of a few days, and these values are typically summed to provide a total recharge over months to tens of years, depending on the length of record. Other methods usually have a fixed spatial and temporal scale (which will depend on environmental parameters) (modified from Scanlon et al., 2002).

Recharge rates based on water chemistry in the unsaturated zone—both applied and environmental tracers—represent relatively small spatial scales, usually less than 1 m^2. The temporal scale varies depending on the method. Applied tracers are usually only observed over periods of months to a few years and so indicate recharge over this time period. Environmental tracers such as ^{3}H and ^{36}Cl estimate recharge over several decades— the period between high concentrations of these tracers in precipitation—1950 to 1965— (Cook et al., 2020; Section 2.5) and the time of measurement in the unsaturated zone. Unsaturated zone chloride profiles can sometimes provide information on changes in deep drainage rates over time (as discussed in Section 3.4). The temporal scale of the method will

66

The GROUNDWATER PROJECT   ©The Authors   Free download from gw-project.org

Anyone may use and share gw-project.org links. Direct distribution of the book is strictly prohibited.

vary depending on the deep drainage flux, and the extent of dispersion within the profile (Cook et al., 1992). Water balance methods estimate recharge over the time period for which data are available. This may be years to several decades, but the method also provides information on temporal variability within this time period. Thus, the measurement scale is relatively short (usually one day), but recharge estimates are available over longer time periods by summing the daily estimates. Of course, some types of calibration data for water balance methods may only be available over shorter periods of time. Such models might then be more accurate over the period with detailed calibration data and less accurate over other times. Similarly, the spatial scale of the water balance method will be the resolution at which the climate, vegetation and soil information is available (usually hundreds of square meters or more), but information can be obtained over very large areas using spatial maps of climate/vegetation/soil parameters, and by performing calculations for the different input parameter combinations.

Recharge estimates based on saturated zone measurements usually represent larger spatial scales. Although measured in individual wells, water table fluctuation measurements reflect a spatial scale of perhaps tens to hundreds of square meters, depending upon the transmissivity of the aquifer. The method usually relies on data with a temporal resolution of minutes to days, and the temporal scale of the method is related to the event duration and travel time through the unsaturated zone (days to weeks). However, the method can estimate recharge over longer periods of time (the time period for which data are available; typically, years to decades) by summing recharge from individual events. The spatial scale represented by chloride mass balance estimates of recharge derived from groundwater samples is determined by the length scale of dispersion during transport through the aquifer, which is probably only a few meters or tens of meters. Importantly, the estimate does not relate to the location where the sample is collected, but rather to the upgradient location where the water first entered the saturated zone (Harrington et al., 2002). The estimate reflects the deep drainage rate at the time the water moved below the root zone—when the chloride concentration was set. This may be many tens or hundreds of years ago, or longer, and may not reflect deep drainage or recharge under conditions prevailing at the time the groundwater sample was collected.

Groundwater dating methods provide an average recharge estimate over a spatial scale representing the length of the groundwater flowline from the point of recharge to the point of sampling (Figure 38), perhaps representing an area hundreds of meters to tens or hundreds of kilometers in length but only tens of meters in width. The length of the characterized area is determined by the flow path whereas the width is determined by dispersion. The temporal scale is determined by the groundwater age. Thus, for example, suppose that the aquifer is 100 m thick, and a groundwater sample collected from 20 m depth has an age of 200 years. If the aquifer porosity is 0.2, then Equation (12) of Section 3.6 gives a recharge rate of 20 mm/y. This recharge rate represents an average over the past 200 years, which is the time since the sampled groundwater entered the aquifer. If the

67

The GROUNDWATER PROJECT   ©The Authors   Free download from gw-project.org

Anyone may use and share gw-project.org links. Direct distribution of the book is strictly prohibited.

groundwater velocity is 5 m/y, then the groundwater would have travelled 1000 m in that 200-year period. Thus, the recharge estimate of 20 mm/y represents the average recharge rate over a 1000 m distance upstream of the sampling location over the past 200 years (Figure 38). Importantly, the method does not provide any information on how recharge may have changed over that 200-year period. If the recharge rate is estimated using the chloride mass balance based on a groundwater sample obtained from the same piezometer, then the estimated recharge rate applies only to the point where the water entered the aquifer and represents the recharge rate approximately 200 years ago.
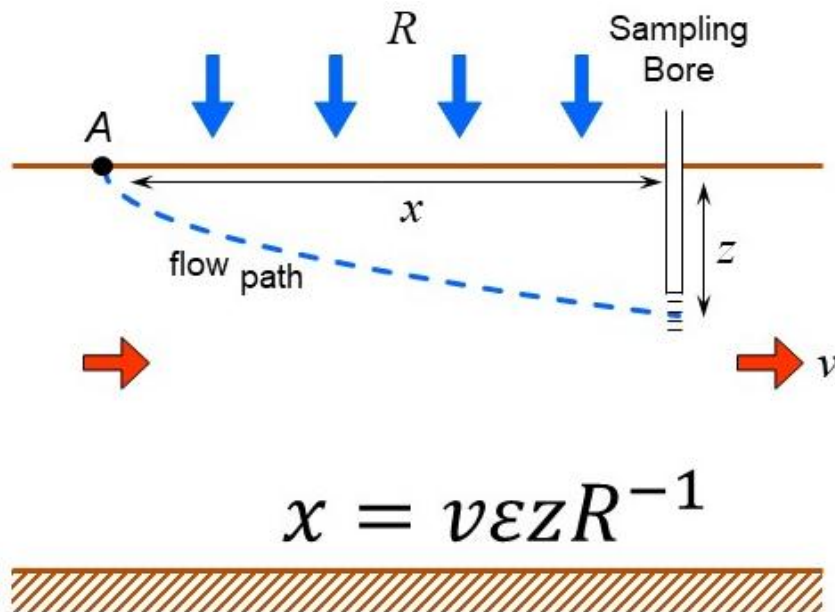

$$x = v\varepsilon z R^{-1}$$

Figure 38 - Schematic representation of the spatial scale of groundwater tracer methods for estimating recharge. Groundwater dating methods estimate recharge over the interval x, between the location of the sampling bore and the point at which the sampled water entered the saturated zone (point A). If sampling takes place in the upper part of the aquifer, then the distance x can be calculated from the horizontal groundwater velocity (v (LT^{-1})), the aquifer porosity (ε; [dimensionless]) the depth that the sample was collected below the water table (z (L)), and the estimated recharge rate (R (LT^{-1})). Chloride mass balance estimates of recharge based on groundwater data represent the recharge at or close to point A, upstream of the bore where the chloride concentration is measured. The equation shown on the figure is calculated by recognizing that x=vt and substituting for t using Equation (12).

6.5   Recharge Maps

For recharge measurements at small spatial scales, replicate sampling is essential if these values are to be applied to larger areas. If enough recharge estimates are available to establish relationships with other environmental parameters, then these surrogate variables can sometimes be used to extrapolate the small-scale measurements and hence construct recharge maps over larger areas. Geophysical measurements—e.g., electromagnetic induction—have proved useful for regionalizing point estimates of diffuse recharge (e.g., Cook et al., 1989; Scanlon et al., 1999). They have also been used for mapping recharge from stream networks using geophysical techniques operated from amphibious vehicles or boats (Khan et al., 2009; Crosbie et al., 2014), or on-foot during periods without

flow in the case of ephemeral streams (Callegary et al., 2007). Thus, deep drainage was mapped across a 0.14 km² agricultural field by eight extrapolating small-scale measurements of deep drainage derived from soil chloride profiles, with soil electrical conductivity data obtained using an electromagnetic induction meter on a 20 m x 20 m grid (Cook et al., 1989). Similarly, seepage from irrigation channels was mapped over 510 km of channels by extrapolating point estimates of channel recharge derived from seepage meters using data on the electrical conductivity of the riverbed derived from an electromagnetic survey conducted from a boat, supplemented with data on hydraulic conductivity, groundwater depth and salinity (Khan et al., 2009).

Efforts have been made to extrapolate point and small-scale recharge estimates over larger spatial scales, by replicate sampling and comparison with soil and land unit maps or by developing empirical relationships between recharge and various environmental parameters (as discussed in Section 5). Two early examples of this approach are provided by Allison and others (1990) and Fayer and others (1996). Allison and others (1990) mapped groundwater recharge across an area of approximately 60,000 km² in the western Murray Basin, Australia based on 56 deep drainage estimates obtained from chloride profiles. The point estimates of deep drainage were extrapolated across the region using land unit and vegetation maps. Fayer and others (1996) estimated deep drainage over approximately 1000 km² in Washington State, USA, based on point estimates of deep drainage obtained from lysimeters, water content monitoring, and unsaturated zone profiles of chloride and ³⁶Cl, supplemented by estimates from one-dimensional unsaturated zone flow models. The deep drainage estimates were extrapolated across the region using available vegetation/land use and soil maps to produce a deep drainage map with a resolution of 50 m x 50 m. In both examples, the recharge maps were used as the upper boundary layer for groundwater flow models. In the former case, the model was used to predict future salinization rates of a major river system, and in the latter case, it was used to understand migration rates of contaminants through the unsaturated zone and groundwater.

Surrogate variables can also be used to extrapolate local estimates of recharge across entire basins and continents. McDonald and others (2021) mapped groundwater recharge across Africa based on statistical upscaling of 134 ground-based recharge estimates (Figure 39). The recharge estimates did not include leakage from large rivers, lakes or from irrigation, although the authors noted that some of the methods used to estimate recharge would have included recharge from small-scale focused recharge features. Statistical analysis of the data found a significant relationship between annual precipitation and recharge, which was used to extrapolate the field data across the continent. There was no clear relationship between recharge and other climate variables, with soil type, or with land cover.
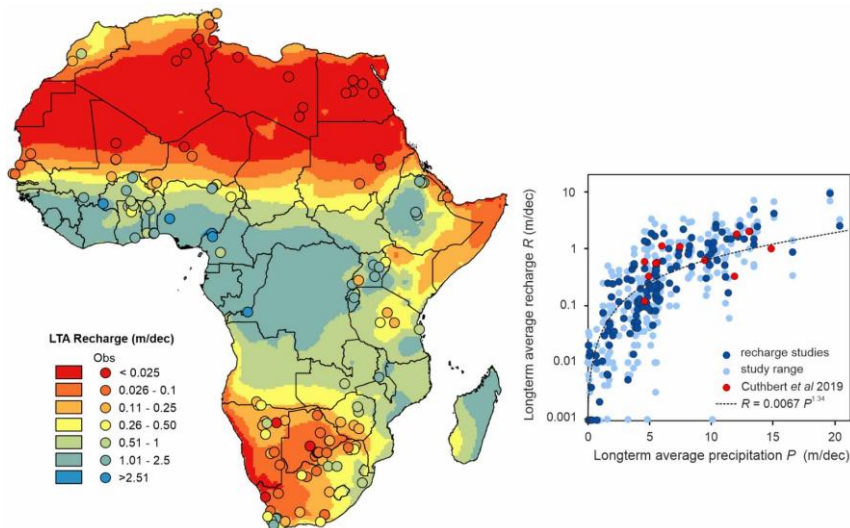
Figure 39 - Long-term average groundwater recharge (meters per decade) across Africa based on a relationship between recharge and precipitation observed in 134 ground-based studies. (reproduced from McDonald et al., 2021).

Water balance models can also be used to construct recharge maps, particularly if reliable maps are available of the climate and soil parameters required by these models. Groundwater recharge was mapped at two sites in semiarid Botswana based on estimates of recharge derived from a chloride mass balance, extrapolated using a simple water balance model with precipitation and actual evaporation estimates derived from satellite imagery (Brunner et al., 2004). Each area was approximately 10,000 km^2 in area, and recharge was mapped with a resolution of approximately 8 km x 8 km. In southern Australia, recharge was mapped at a resolution of 50 m x 50 m across an 8000 km^2 catchment using a water balance model and maps of climate, vegetation/land-use and soil type. Global-scale recharge maps have been developed using water balance models that combine global climate data sets with maps of soil properties and vegetation type. These are described in Section 7.

As an alternative to the above quantitative deep drainage and recharge maps, several studies have developed qualitative recharge maps by mapping the different geomorphic, geological, and climatic factors that are believed to affect recharge, and assigning scores and weights to these different factors. These are sometimes referred to as *recharge potential* maps.

Some of the factors that have been considered when deriving recharge potential maps include:

- Precipitation—Other factors being equal, higher rates of precipitation will result in higher rate of groundwater recharge (as discussed in Section 5).

- Land use or land cover—Areas of forests, farms, and urban areas can be delineated using aerial photography, remote sensing, or other available maps. Land use and vegetation type have been shown to be important determinants of recharge in numerous studies (as discussed in Section 5).

70

- Topographic slope—Recharge is usually assumed to be less likely in areas with high topographic slopes due to an increase in runoff (e.g., Yeh et al., 2009; Maqsoom et al., 2022).

- Soil type—This is an important factor influencing recharge rates (as discussed in Section 5). Where information on soil type is not available across a region, lithology can be used as a surrogate variable (e.g., Yeh et al., 2009).

- Lithology—Different lithological units will have different hydraulic conductivities and hence different recharge potentials. High hydraulic conductivity indicates high recharge potential (Maqsoom et al., 2022).

- Drainage density—Drainage density is often included as a recharge potential factor; although, its relationship to recharge potential is somewhat uncertain. Sometimes a high drainage density is considered to indicate high potential for focused groundwater recharge (e.g., Yeh et al., 2009); whereas in other studies high drainage density is believed to indicate low permeability of rocks and high surface runoff and hence low recharge potential (Magesh et al., 2012; Ponnusamy et al., 2022).

- Fault or Lineament Density—Faults are sometimes assumed to be more permeable than the surrounding host rock; therefore, recharge is more likely to occur in areas close to faults or areas having a high fault density (e.g., Maqsoom et al., 2022). Lineaments are linear structures that are visible on aerial or satellite photos, and may represent faults, fractures, or dykes. Lineament density has been used as a factor to indicate recharge potential in some studies (e.g., Yeh et al., 2009).

For each factor, scores are given to different parameter values or categories, with high scores usually reflecting a high recharge potential. For example, each different soil type within a region will be given a score. Similarly, different scores will be assigned to different fault or lineament densities. Then the different factors are weighted according to their perceived importance in determining the recharge potential. Sometimes the weighting of a factor is based on the number of other factors that it influences. For example, Magesh and others (2012) gave lithology a weighting of four, because this factor was considered to influence four other factors: soil type, drainage density, lineament density, and land use/land cover. In contrast, soil was considered to only influence one other factor—land use/land cover—so was given a weighting of one. Mapping is usually carried out in a GIS framework—where scores for each factor are multiplied by the factor weights—then summed to give an overall value for recharge potential for each model cell. This is then mapped across the region. Recharge potential maps are rarely verified using measured values, so their accuracy is difficult to assess.

An example of this approach is illustrated in Figure 40 for a part of Tamil Nadu, India. Seven factors were considered: precipitation, lithology, soil type, topographic slope, drainage density, lineament density, and land use/land cover. Maps of each of these factors

71

are derived and combined to yield an overall recharge potential assessment. Similar approaches have been widely applied within the past 10 to 20 years. Other examples include southeast Taiwan (Yeh et al., 2009), Pakistan (Maqsoom et al., 2022) and South Africa (Ponnusamy et al., 2022). Choosing different factors to include in the analysis, the scores assigned within each factor—and the weighting between the different factors—can be site-specific and somewhat subjective but this method is nevertheless a useful first step in mapping recharge across a region.
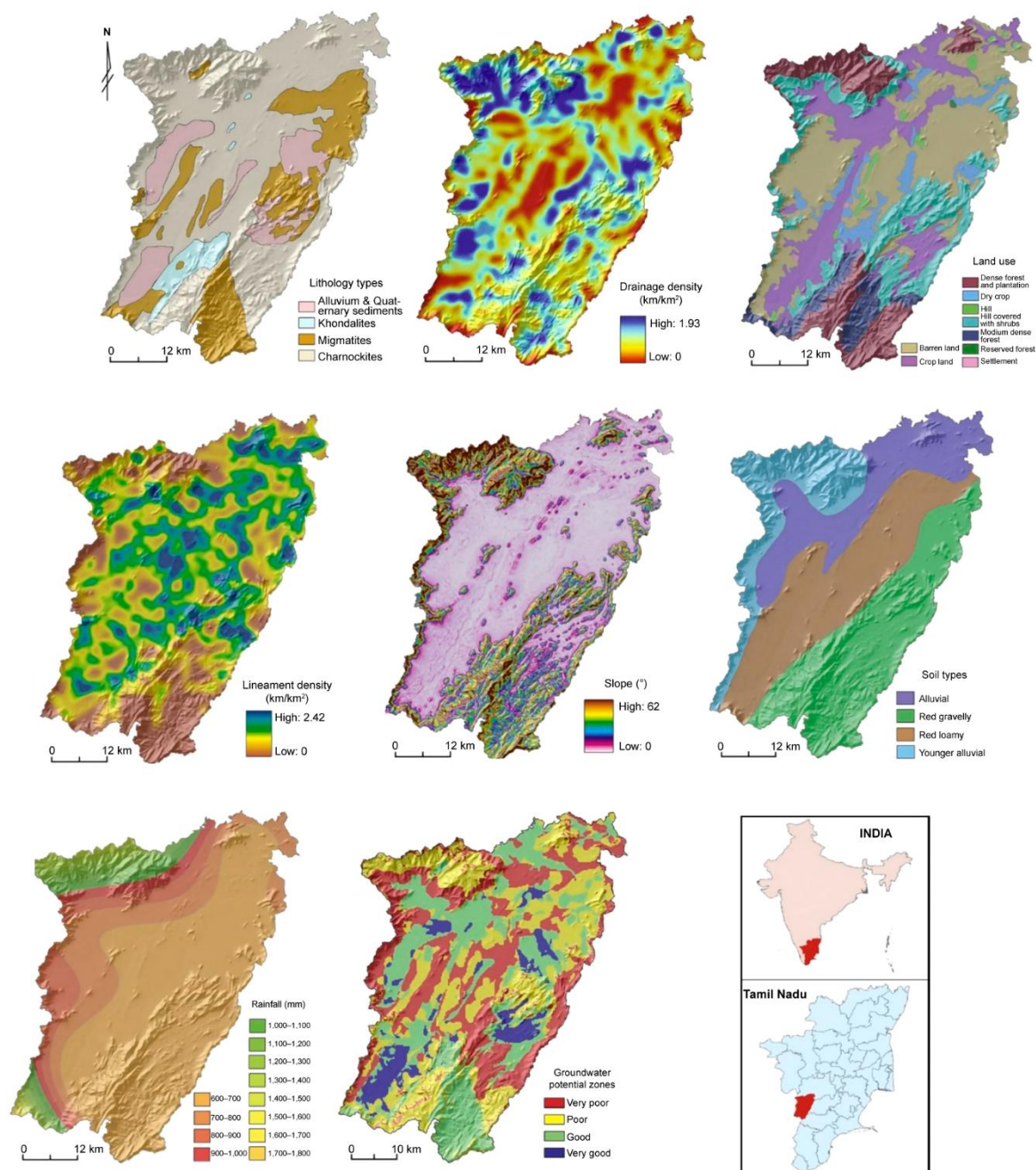

Figure 40 - Recharge potential in Theni district in southwestern Tamil Nadu, India, estimated by considering seven factors that influence groundwater recharge rate: lithology, drainage density, land use/land cover, lineament density, topographic slope, soil type, and rainfall to produce zones of potential groundwater recharge (reproduced from Magesh et al., 2012).

7   Climate Change and Recharge

Climate change causes changes in mean annual precipitation and potential evaporation, induces change in precipitation patterns and intensity of precipitation events, and alters temperature and CO_2 levels. In arid and semi-arid areas, increases in the frequency and intensity of large precipitation events may lead to increases in recharge, while increase in temperatures are likely to increase vapor pressure deficits and hence increase transpiration rates. Increases in atmospheric CO_2 levels generally decrease plant transpiration through stomatal closure. In most locations, the reduction in transpiration through stomatal closure will offset the effect of increased vapor pressure deficits, resulting in a net decrease in transpiration (Kirschbaum & McMillan, 2018). Other factors being equal, this will contribute to an increase in recharge.

In cold regions, global warming lengthens the growing season of plants, so that annual transpiration rates may increase despite decreases in daily transpiration rates. Warming temperatures also change snow storage dynamics and thus can significantly affect the duration and temporal distribution of snow cover and snow melt. Permafrost significantly affects infiltration dynamics (Lemieux et al., 2020). Some of the more important aspects related to a warming climate include a reduced frozen period—thus earlier spring thaw—and a shallower soil-frost penetration depth. The worldwide thawing of permafrost will tend to increase infiltration and thus groundwater recharge rates.

In sum, changes in climate will thus result in changes in mean annual recharge rates as well as the frequency and intensity of recharge events. Climate changes are also likely to change the balance between diffuse and focused recharge. Understanding these changes is important for groundwater management.

Prediction of future impacts of climate change on groundwater recharge can be conducted either by establishing empirical relationships between recharge and climate parameters—such as precipitation—and inferring changes in recharge from changes in these climate parameters predicted by global climate models (e.g., McKenna & Sala, 2018) or by predictive water balance modeling that explicitly uses climate models to derive climate parameters to input to the water balance models. Most of these studies focus on changes in diffuse recharge and only consider some of the processes that ultimately impact groundwater recharge. Only a few studies explicitly consider focused recharge or mountain front/mountain block recharge. Furthermore, most studies only examine the direct effect of changes in climate on the water balance and few also look at indirect effects such as how climate change may influence irrigation rates, cropping patterns or crop types, and how this may affect recharge rates.

Studies of the impact of climate change on recharge have been conducted at the aquifer scale, continental scale, and at the global scale. A recent review of the literature identified 50 such studies published in peer-reviewed English-language journals since 2016

73

(Adhikari et al., 2022). An example of an aquifer-scale study is that for the High Plains aquifer, in the central area of the USA. This aquifer covers parts of eight states, extends across approximately 450,000 km² and is an important source of water for irrigation. The aquifer is already under stress due to over-pumping; so, understanding the possible effects of climate change on recharge is important for future management of the resource. Crosbie and others (2013) used a water balance model to examine recharge under four potential future climate scenarios. Point scale water balance modeling was conducted for 17 climate zones, 10 soil classes and three land use types (dryland cropland, irrigated cropland, and perennial grasses). Recharge was assessed for each of these 510 regimes of combined climate—soil—land use (17 x 10 x 3) under the climate conditions at the time, 1990, and for 48 possible future climates based on predictions for 2050. The future climates were based on 16 global climate models and three climate scenarios—low, medium, and high global warming—to provide information on the uncertainty of future predictions. Under a 2050 climate, the median prediction was for an 8% increase in recharge in the Northern High Plains, a 3% decrease in the Central High Plains, and a 10% decrease in the Southern High Plains. However, there was considerable uncertainty in both the direction and magnitude of these changes due to variation in the climate predictions of the different global climate models.

One of the few studies that considered focused recharge as well as diffuse recharge was that of Meixner and others (2016). This study examined changes in recharge in eight aquifer systems in the western USA, including the High Plains aquifer (Figure 41). For four of these aquifer systems—High Plains, San Pedro, Central Valley, and Columbia Plateau aquifers—quantitative assessments were available from previous studies that had examined the effects of changes in climate on recharge using water balance models (e.g., Crosbie et al. (2013) for the High Plains aquifer). For the other aquifer systems—Death Valley, Wasatch Front, Spokane Valley, and Williston Basin—a qualitative assessment of the likely direction of recharge from the different recharge mechanisms was made based on the author's knowledge of these aquifer systems and by comparison with the four aquifer systems that had been studied in more detail. Mountain system recharge was expected to decrease across most of the region due to a decrease in the snowpack arising principally from higher temperatures. In the San Pedro aquifer, which is dominated by mountain front recharge, the decrease in groundwater recharge in the basin was estimated to be 30% over the next 100 years. Total recharge was also predicted to decrease in other aquifer systems that were dominated by mountain system recharge. Focused recharge was the dominant recharge mechanism in the Spokane Valley, but the authors noted that without quantitative studies, it was difficult to predict whether the effect of projected warmer temperatures—which would tend to decrease recharge—would outweigh the effects of a slight projected increase in precipitation. In general, it was difficult to predict changes in focused recharge that would arise from changes in frequency and intensity of storm events in any of the aquifer systems.
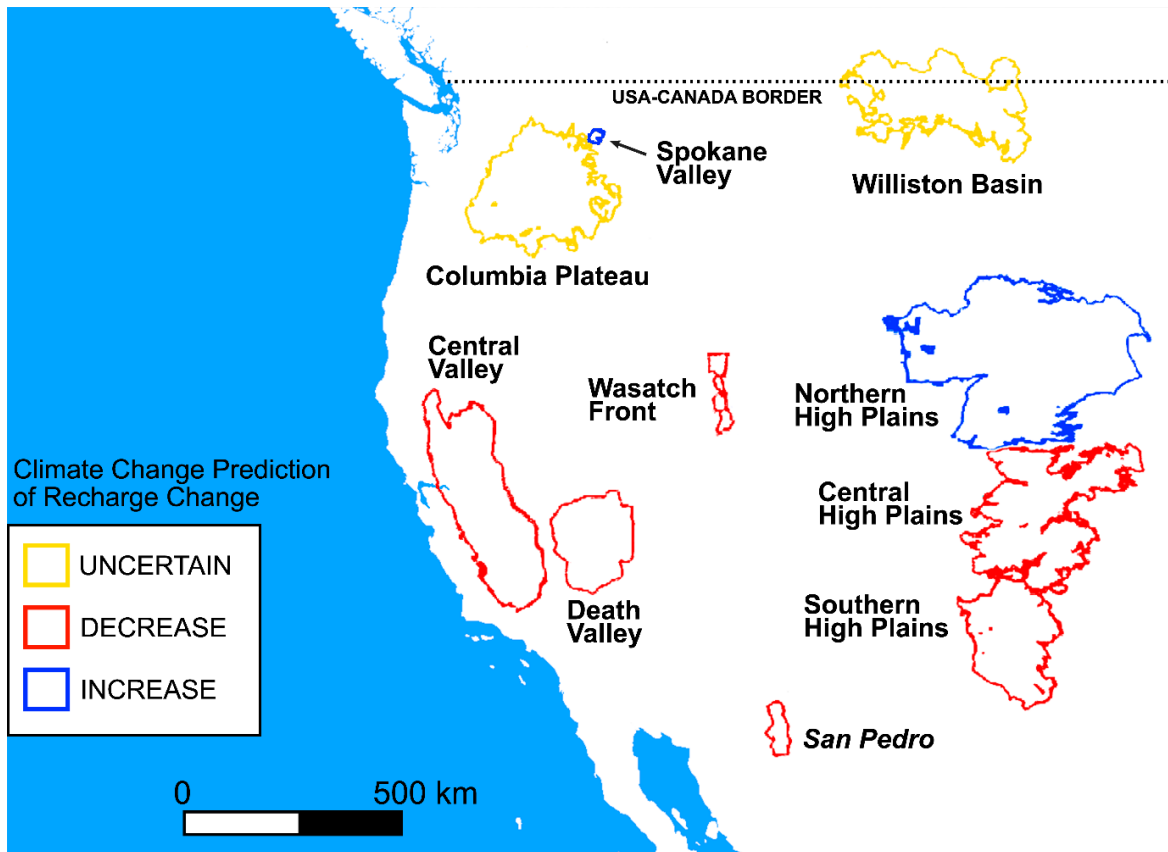
74

Figure 41 - Effect of climate change on recharge in the western USA. Overall, recharge was projected to decrease in San Pedro, Death Valley, Wasatch Front, and Central Valley aquifer systems and increase in the Spokane Valley. The change was variable in the High Plains—an increase in the Northern High Plains and decrease in the Central and Southern High Plains—while the direction of the change was uncertain in the Columbia Plateau and Williston Basin aquifer systems (After Meixner et al., 2016).

A study of climate change impacts on focused recharge through playas was also conducted for the Jornada Basin near Las Cruces, New Mexico, USA (McKenna & Sala, 2018). In the southwestern USA, increased atmospheric temperatures are expected to increase the magnitude of large precipitation events, and this may increase surface water inflows to playas. There are approximately 100 playas in the Jornada Basin, and runoff contributions were modeled for 20 of these to develop an empirical relationship between surface water inflow and event precipitation. The study found that for every 1% decrease in mean annual precipitation, average playa recharge decreased by 5%. It also found that for every 1% increase in inter-annual precipitation variability, there was an 18% increase in playa recharge rate. For the area studied, the effect on recharge of the predicted increase in inter-annual variability of precipitation outweighed the effect of the decrease in mean annual precipitation; therefore, the net effect of climate change was predicted to be an increase in playa recharge.

The effect of climate change on groundwater recharge has also been predicted on a global scale, and the use of several different global climate models and global hydrological models—water balance models—allows assessment of the uncertainty of these predictions. For example, in some cases, some models—or combinations of models—predict increases

75

in recharge whereas others predict decreases. While the High Plains aquifer study discussed above examined uncertainty in recharge predictions by using 16 different climate models, the use of a range of different water balance models as well as different climate models allows a more robust analysis of the uncertainty. On the other hand, the need to use globally available data often means that hydrological models used for these studies are simpler than those used in regional studies and may not include all relevant processes. The study of Reinecke and others (2021) used 4 climate models and 8 global hydrological models. Analysis of the variations in predictions between the different climate models and the different hydrological models allowed significant differences to be separated from those that were not considered significant because there was too much variance in the predictions. Based on their results, the authors predicted that significant decreases in recharge would occur in southern Chile, parts of Brazil, central US, the Mediterranean and southern China (Figure 42). In many areas, however, variation between the results obtained from the different model combinations was too great to make any definitive predictions.
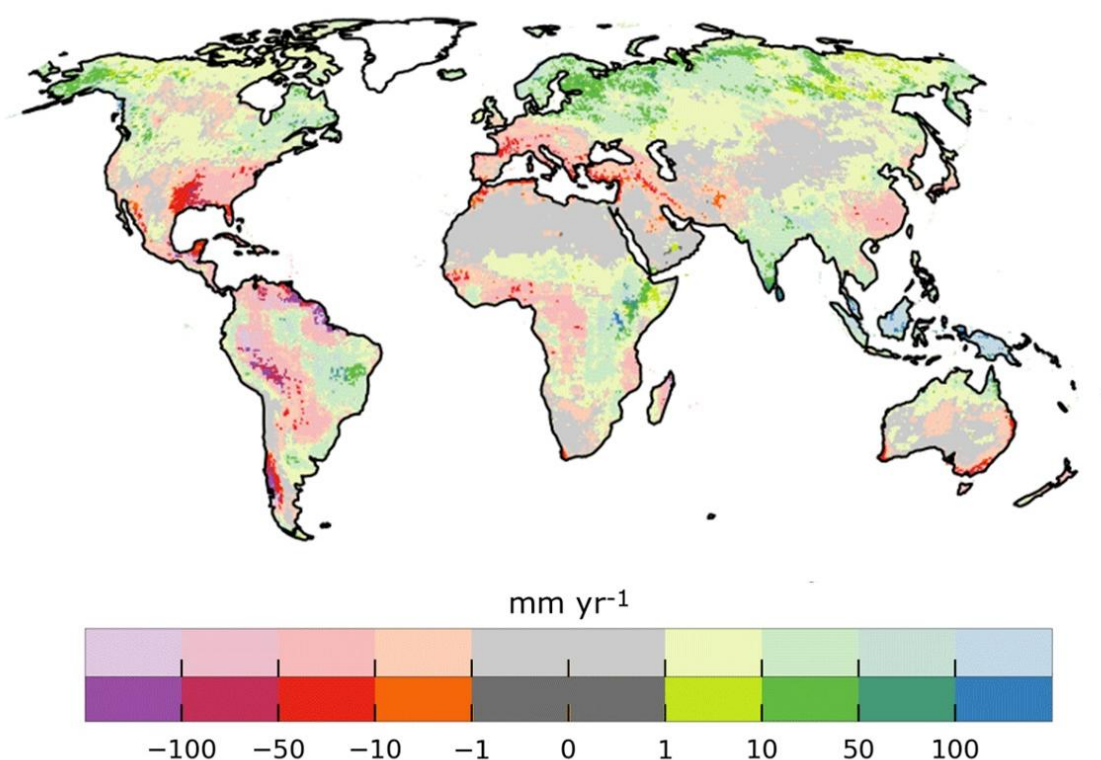
Figure 42 - Predicted global changes in groundwater recharge (in mm/y) due to a 2 °C increase in temperature over present-day levels (3° increase over the pre-industrial period). Results are derived from eight global hydrological models forced by climate change predictions of four global climate models. Different colors indicate the mean predicted change in recharge; areas where predictions are considered significant—due to similarity of predictions from the different combinations of climate and hydrological models—are shown in darker tones—bottom line of scale bar (reproduced from Reinecke et al., 2021).

8   References

Abdulrazzak, M. J. (1995). Losses of flood water from alluvial channels. *Arid Land and Research Management, 9*(1), 15–24. https://doi.org/10.1080/15324989509385870↗.

Adhikari, R. K., Yilmaz, A. G., Mainali, B., Dyson, P., & Imteaz, M. A. (2022). Methods of groundwater recharge estimation under climate change: a review. *Sustainability, 14,* 15619.

Ala-Aho, P., Autio, A., Bhattacharjee, J., Isokangas, E., Kujala, K., Marttila, H., Menberu, M., Meriö, L. J., Postila, H., Rauhala, A., Ronkanen, A. K., Rossi, P. M., Saari, M., Haghighi, A. T., & Kløve, B. (2021). What conditions favor the influence of seasonally frozen ground on hydrological partitioning? A systematic review. *Environmental Research Letters, 16*(4). https://iopscience.iop.org/article/10.1088/1748-9326/abe82c/meta↗.

Allaire, S. E., Roulier, S., & Cessna, A. J. (2009). Quantifying preferential flow in soils: A review of different techniques. *Journal of Hydrology, 378*(1–2), 179–204. https://doi.org/10.1016/j.jhydrol.2009.08.013↗.

Allison G. B., Cook P. G., Barnett S. R., Walker G. R., Jolly I. D. & Hughes M. W. (1990). Land clearance and river salinisation in the Western Murray Basin, Australia. *Journal of Hydrology, 119*(1–4), 1–20. https://doi.org/10.1016/0022-1694(90)90030-2↗.

Allison, G. B., & Hughes, M. W. (1978). The use of environmental chloride and tritium to estimate total recharge to an unconfined aquifer. *Australian Journal Soil Research, 16(2)*, 181–195. https://doi.org/10.1071/SR9780181↗.

Allison, G. B., & Hughes, M. W. (1983). The use of natural tracers as indicators of soil-water movement in a temperate semi-arid region. *Journal of Hydrology, 60*(1–4), 157–173. https://doi.org/10.1016/0022-1694(83)90019-7↗.

Allison, G. B., Stone, W. J., & Hughes, M. W. (1985). Recharge in karst and dune elements of a semi-arid landscape as indicated by natural isotopes and chloride. *Journal of Hydrology, 76*(1–2*)*, 1–25. https://doi.org/10.1016/0022-1694(85)90088-5↗.

Athavale, R. N., Murti, C. S., & Chand, R. (1980). Estimation of recharge to the phreatic aquifers of the Lower Maner Basin, India, by using the tritium (sic) injection method. *Journal of Hydrology, 45*(3–4), 185–202. https://doi.org/10.1016/0022-1694(80)90019-0↗.

Avanzi, F., De Michele, C., Morin, S., Carmagnola, C. M., Ghezzi, A., & Lejeune, Y. (2016). Model complexity and data requirements in snow hydrology: seeking a balance in practical applications. *Hydrological Processes, 30*(13), 2106–2118. https://doi.org/10.1002/hyp.10782↗.

Baquero, J. C., de los Reyes, M. J., Custodio, E., Scheiber, L., & Vázquez-Suñé, E. (2016). Groundwater Management in Mining: The Drainage and Reinjection System in Cobre Las Cruces, Spain. *Modern Environmental Science and Engineering, 2*(10), 631–646. https://www.mdsamericas.com/assets/groundwater-management-in-mining-the-drainage-and-reinjection-system-in-cobre-las-cruces.pdf↗.

Baron, O. V., Crosbie, R. S., Charles, S. P., Dawes, W. R., Ali, R. Evans, W. R., Cresswell, R., Pollock, D., Hodgson, G., Currie, D., Mpelasoka, D., Pickett, T., Aryal, S., Donn, M., & Wurcker, B. (2011). Climate change impact on groundwater resources in Australia: summary report. CISRO Water for a Healthy Country Flagship, Australia.

Bayard, D., Stähli, M., Parriaux, A., & Flühler, H. (2005). The influence of seasonally frozen soil on the snowmelt runoff at two Alpine sites in southern Switzerland. *Journal of Hydrology, 309*(1–4), 66–84. https://doi.org/10.1016/j.jhydrol.2004.11.012↗.

Bazuhair, A. S., & Wood, W. W. (1996). Chloride mass-balance method for estimating ground water recharge in arid areas: examples from western Saudi Arabia. *Journal of Hydrology, 186*(1–4), 153–159. https://doi.org/10.1016/S0022-1694(96)03028-4↗.

Benito, G., Rohde, R., Seely, M., Külls, C., Dahan, O., Enzel, Y., Todd, S., Botero, B., Morin, E., Grodek, T., & Roberts, C. (2010). Management of alluvial aquifers in two southern African ephemeral rivers: Implications for IWRM. *Water Resources Management, 24*, 641–667. https://doi.org/10.1007/s11269-009-9463-9↗.

Bertin, C., & Bourg, A. C. M. (1994). Radon-222 and chloride as natural tracers of the infiltration of river water into an alluvial aquifer in which there is significant river/groundwater mixing. *Environmental Science & Technology, 28*(5), 794–798. https://doi.org/10.1021/es00054a008↗.

Beyer, M., Gaj, M., Hamutoko, J. T., Koeniger, P., Wanke, H., & Himmelsbach, T. (2015). Estimation of groundwater recharge via deuterium labelling in the semi-arid Cuvelai-Etosha Basin, Namibia. *Isotopes in Environmental and Health Studies, 51*(4), 533–552. https://doi.org/10.1080/10256016.2015.1076407↗.

Boas. T., & Mallants, D. (2022). Episodic extreme rainfall events drive groundwater recharge in arid zone environments of central Australia. *Journal of Hydrology: Regional Studies, 40*, 101005. https://doi.org/10.1016/j.ejrh.2022.101005↗.

Böhlke, J. K. (2002). Groundwater recharge and agricultural contamination. *Hydrogeology Journal, 10(1),* 153-179.

Boreux, M. P., Lamoureux, S. F., & Cumming, B. F. (2021). Use of water isotopes and chemistry to infer the type and degree of exchange between groundwater and lakes in an esker complex of northeastern Ontario, Canada. *Hydrol. Earth Syst. Sci., 25,* 6309-6332.

Bredehoeft, J. D. (1997). Safe yield and the water budget myth. *Ground Water, 35*(6), 929.

Bresciani, E., Cranswick, R. H., Banks, E. W., Batlle-Aguilar, J., Cook, P. G., & Batelaan, O. (2018). Using hydraulic head, chloride and electrical conductivity data to distinguish between mountain-front and mountain-block recharge to basin aquifers, *Hydrology and Earth System Sciences, 22*(2), 1629–1648. https://doi.org/10.5194/hess-22-1629-2018↗.

Brunner, P., Bauer, P., Eugster, M., & Kinzelbach, W. (2004). Using remote sensing to regionalize local precipitation recharge rates obtained from the Chloride Method. *Journal of Hydrology, 294*, 241-250.

Brunner, P., Cook, P. G., & Simmons, C. T. (2009). Hydrogeologic controls on disconnection between surface water and groundwater. *Water Resources Research, 45*(1). https://doi.org/10.1029/2008WR006953↗.

Callegary, J. B., Leenhouts, J. M., Paretti, N. V., & Jones, C. A. (2007). Rapid estimation of recharge potential in ephemeral-stream channels using electromagnetic methods, and measurements of channel and vegetation characteristics. *Journal of Hydrology, 344*(1–2), 17–31. https://doi.org/10.1016/j.jhydrol.2007.06.028↗.

Canadell, J., Jackson, R. B., Ehleringer, J. R., Mooney, H. A., Sala, O. E., & Schulze, E. D. (1996). Maximum rooting depth of vegetation types at the global scale. *Oecologia, 108*, 583–595. https://doi.org/10.1007/BF00329030↗.

Calver, A., 2001. Riverbed permeabilities: information from pooled data. *Groundwater 39*(4), 546–533. https://doi.org/10.1111/j.1745-6584.2001.tb02343.x↗.

Cey, E. E. & Rudolph, D. L. (2009) Field study of macropore flow processes using tension infiltration of a dye tracer in partially saturated soils. *Hydrological Processes, 23*, 1768–1779. https://doi.org/10.1002/hyp.7302↗.

Cey, E. E., Rudolph, D. L., Parkin, G. W., & Aravena, R. (1998). Quantifying groundwater discharge to a small perennial stream in southern Ontario, Canada. *Journal of Hydrology, 210*(1–4), 21–37. https://doi.org/10.1016/S0022-1694(98)00172-3↗.

Chen, X., Song, J., Cheng, C., Wang, D., & Lackey, S.O. (2009). A new method for mapping variability in vertical seepage flux in streambeds. *Hydrogeology Journal, 17*, 519–525.

Cherry, M., Gilmore, T., Mittelstet, A., Gastmans, D., Santos, V., & Gates, J. B. (2019). Recharge seasonality based on stable isotopes: Nongrowing season bias altered by irrigation in Nebraska. *Hydrological Processes, 34*(7), 1575–1586. https://doi.org/10.1002/hyp.13683↗.

Conant, B. (2004). Delineating and quantifying ground water discharge zones using streambed temperatures. *Groundwater, 42*(2), 243–257. https://doi.org/10.1111/j.1745-6584.2004.tb02671.x↗.

Constantz, J. (1998). Interaction between stream temperature, streamflow, and groundwater exchanges in alpine streams. *Water Resources Research, 34*(7), 1609–1615. https://doi.org/10.1029/98WR00998↗.

Cook, P. G. (2015). Quantifying river gain and loss at regional scales. *Journal of Hydrology, 532*, 102–121. https://doi.org/10.1016/j.jhydrol.2015.10.052↗.

Cook, P. G. (2020). *Introduction to Isotopes and Environmental Tracers as Indicators of Groundwater Flow*. The Groundwater Project. https://gw-project.org/books↗.

Cook, P. G., & Bohlke, J. K. (1999). Determining timescales for groundwater flow and solute transport. In P.G. Cook and A.L. Herczeg (Ed.), *Environmental Tracers in Subsurface Hydrology* (pp. 1–30). Kluwer, Boston.

Cook, P. G., Edmunds, W. M., & Gaye, C. B. (1992). Estimating paleorecharge and paleoclimate from unsaturated zone profiles. *Water Resources Research, 28(10)*, 2721-2731.

Cook P. G., Jolly I. D., Leaney F. W., Walker G. R., Allan G. L., Fifield L. K., & Allison G. B. (1994). Unsaturated zone tritium and chlorine-36 profiles from southern Australia: their use as tracers of soil water movement. *Water Resources Research, 30*(6), 1709–1719. https://doi.org/10.1029/94WR00161↗.

Cook, P. G., Shanafield, M., Andersen, M. S., Bourke, S., Cartwright, I., Cleverly, J., Currell, M., Doody, T. M., Hofmann, H., Hugmann, R., Irvine, D. J., Jakeman, A., McKay, J., Nelson, R., & Werner, A. D. (2022). Sustainable management of groundwater extraction: An Australian perspective on current challenges. *Journal of Hydrology: Regional Studies, 44*, 101262. https://doi.org/10.1016/j.ejrh.2022.101262↗.

Cook, P. G., Walker, G. R., & Jolly, I. D. (1989). Spatial variability of groundwater recharge in a semi-arid region. *Journal of Hydrology, 111*(1–4), 195–212. https://doi.org/10.1016/0022-1694(89)90260-6↗.

Costelloe, J. F., Irvine, E. C., Watson, A. W. & Herczeg, A. L. (2009). Groundwater recharge and discharge dynamics in an arid-zone ephemeral lake system, Australia. *Limnol. Oceanogr., 54*(1), 86–100.

Crosbie, R. S., McCallum, J. L., Walker, G. R., & Chiew, F. H. S. (2012). Episodic recharge and climate change in the Murray-Darling Basin, Australia. *Hydrogeology Journal, 20*, 245–261. https://doi.org/10.1007/s10040-011-0804-4↗.

Crosbie, R. S., Taylor, A. R., Davis, A. C., Lamontagne, S., & Munday, T. (2014). Evaluation of infiltration from losing-disconnected rivers using a geophysical characterization of the riverbed and a simplified infiltration model. *Journal of Hydrology, 508*, 102–113. https://doi.org/10.1016/j.jhydrol.2013.07.045↗.

Crosbie, R. S., Binning, P., & Kalma, J. D. (2005). A time series approach to inferring groundwater recharge using the water table fluctuation method. *Water Resources Research, 41*, W01008, https://doi.org/10.1029/2004WR003077↗.

Crosbie, R. S., Scanlon, B. R., Mpelasoka, F. S., Reedy, R. C., Gates, J. B., & Zhang, L. (2013). Potential climate change effects on groundwater recharge in the High Plains Aquifer, USA. *Water Resources Research, 49*, 3936–3951. https://doi.org/10.1002/wrcr.20292↗.

Dahan, O., Tatarsky, B., Enzel, Y., Kulls, C., Seely, M., & Benito, G. (2008). Dynamics of flood water infiltration and ground water recharge in hyperarid desert. *Groundwater, 46*(3), 450–461. https://doi.org/10.1111/j.1745-6584.2007.00414.x↗.

Devlin, J. F., & Sophocleous, M. (2005). The persistence of the water budget myth and its relationship to sustainability. *Hydrogeology Journal, 13*, 549–554. https://doi.org/10.1007/s10040-004-0354-0↗.

Diamond, R.E. (2022*). Stable Isotope Hydrology*. The Groundwater Project, Guelph, Ontario, Canada.

Díaz-Cruz, M. S., & Barceló, D. (2008). Trace organic chemicals contamination in ground water recharge. *Chemosphere, 72*, 333-342.

Dillon, P., Stuyfzand, P., Grischek, T., Lluria, M., Pyne, R. D. G., Jain, R. C., Bear, J., Schwarz, J., Wang, W., Fernandez, E., Stefan, C., Pettenati, M., van der Gun, J., Sprenger, C., Massmann, G., Scanlon, B. R., Xanke, J., Jokela, P., Zheng, Y., Rossetto,

R., Shamrukh, M., Pavelic, P., Murray, E., Ross, A., … Sapiano, M. (2019). Sixty years of global progress in managed aquifer recharge. *Hydrogeology Journal, 27*, 1–30. https://doi.org/10.1007/s10040-018-1841-z↗.

Dodson, W. J. (2008). *Groundwater recharge from the Gascoyne River, Western Australia*. Department of Water, Hydrogeological record series HG 32.

Döll, P., & Fiedler, K. (2008). Global-scale modelling of groundwater recharge. *Hydrology and Earth System Sciences*, 863–885. https://doi.org/10.5194/hess-12-863-2008↗.

Dozier, J., Bair, E. H., & Davis, R. E. (2016). Estimating the spatial distribution of snow water equivalent in the world's mountains. *WIREs Water 3*(3), 461–474. https://doi.org/10.1002/wat2.1140↗.

Dripps, W. R., & Bradbury, K. R. (2007). A simple daily soil-water balance model for estimating the spatial and temporal distribution of groundwater recharge in temperate humid areas. *Hydrogeology Journal, 15*, 433–444. https://doi.org/10.1007/s10040-007-0160-6↗.

Dripps, W. R., & Bradbury, K. R. (2010) The spatial and temporal variability of groundwater recharge in a forested basin in northern Wisconsin. *Hydrological Processes, 24*, 383–392. https://doi.org/10.1002/hyp.7497↗.

Drury, L., Calf, G., Dharmasiri, J., 1984. Radiocarbon dating of groundwater in tertiary sediments of the Eastern Murray basin. *Australian Journal of Soil Research, 22*(4), 379–387. https://doi.org/10.1071/SR9840379↗.

Dubois, E., Larocque, M., Gagné, S., & Meyzonnat, G. (2021). Simulation of long-term spatiotemporal variations in regional-scale groundwater recharge: contributions of a water budget approach in cold and humid climates. *Hydrology and Earth System Sciences, 25*, 6567–6589. https://doi.org/10.5194/hess-25-6567-2021↗.

Duke, H. R. (1972). Capillary properties of soils—influence upon specific yield. *Transactions of the ASAE, 15*(4), 688–691. https://doi.org/10.13031/2013.37986↗.

Edmunds, W. M. & Tyler, S. W. (2002). Unsaturated zones as archives of past climates: Toward a new proxy for continental regions. *Hydrogeology Journal, 10*, 216–228. https://doi.org/10.1007/s10040-001-0180-6↗.

Edwards, E. C., Nelson, C., Harter, T., Bowles, C., Li, X., Lock, B., Fogg, G. E., & Washburn, B. S. (2022). Potential effects on groundwater quality associated with infiltrating stormwater through dry wells for aquifer recharge. *Journal of Contaminant Hydrology, 246*, 103964.

Faunt, C. C. (2009). *Groundwater availability of the Central Valley aquifer, California*. USGS Professional Paper 1766. https://pubs.usgs.gov/pp/1766/PP_1766.pdf↗.

Fayer, M. J., Gee, G. W., Rockhold, M. L., Freshley, M. D., & Walters, T. B. (1996). Estimating recharge rates for a groundwater model using a GIS. *J. Environ. Qual., 25*, 510–518.

Finch, J. W. (2001) Estimating change in direct groundwater recharge using a spatially distributed soil water balance model. *Quarterly Journal of Engineering Geology and Hydrogeology, 34*(1), 71–83.

81

Fox, G. A., & Durnford, D. S. (2003). Unsaturated hyporheic zone flow in stream/aquifer conjunctive systems. *Adv. Water Resour., 26*, 989–1000. https://doi.org/10.1016/S0309-1708(03)00087-3↗.

Freydier, R., Dupre, B., & Lacaux, J. P. (1998). Precipitation chemistry in intertropical Africa. *Atmospheric Environment, 32*(4), 749–765.

Fryar, A. E., Currens, B. J., & Alvarez Villa, C. S. (2023). Hydrochemical delineation of spring recharge in an urbanized karst basin, central Kentucky. *Environmental and Engineering Geoscience, 29(3)*, 203–216.

Fulton, S. A. (2012). *Technical Report: Great Artesian Basin Resource Assessment* (Report 14). Department of Land Resource Management, Darwin.

Genereux, D. P., Leahy, S., Mitasova, H., Kennedy, C. D., & Corbett, D. R. (2008) Spatial and temporal variability of streambed hydraulic conductivity in West Bear Creek, North Carolina, USA. *Journal of Hydrology, 358*(3–4), 332–353. https://doi.org/10.1016/j.jhydrol.2008.06.017↗.

Goodrich, D. C., Williams, D. G., Unkrich, C. L., Hogan, J. F., Scott, R. L., Hultine, K. R., Pool, D., Coes, A. L., & Miller, S. (2004). Comparison of methods to estimate ephemeral channel recharge, walnut gulch, San Pedro river basin, Arizona. In J. F. Hogan, F. M. Phillips, B. R. Scanlon (Eds.), *Groundwater Recharge in a Desert Environment: The Southwestern United States* (pp. 77–99). Water Science and Application Series, Vol. 9, American Geophysical Union. https://doi.org/10.1029/009WSA06↗.

Gotkowitz, M. B., Attig, J. W., & McDermott, T. (2014). Groundwater flood of a river terrace in southwest Wisconsin, USA. *Hydrogeology Journal, 22*, 1421-1432.

Government of Western Australia. (2021). *Managed aquifer recharge.* Department of Water and Environmental Regulation, Government of Western Australia. https://www.wa.gov.au/system/files/2021-01/Brochure_Managed_aquifer_recharge.pdf↗.

Gurdak, J. J., & Roe, C. D. (2010). Review: Recharge rates and chemistry beneath playas of the High Plains aquifer, USA. *Hydrogeology Journal, 18*(8), 1747–1772.

Harder, P., Pomeroy, J. W., & Helgason, W. D. (2020). Improving sub-canopy snow depth mapping with unmanned aerial vehicles: lidar versus structure-from-motion techniques. *The Cryosphere 14*(6), 1919–1935. https://doi.org/10.5194/tc-14-1919-2020↗.

Harrington, G. A., Cook, P. G., & Herczeg, A. L. (2002). Spatial and temporal variability of ground water recharge in central Australia: a tracer approach. *Groundwater, 40*(5), 518–527. https://doi.org/10.1111/j.1745-6584.2002.tb02536.x↗.

Harte, P. T., & Kiah, R. G. (2009). Measured river leakages using conventional streamflow techniques: the case of Souhegan River, New Hampshire, USA. *Hydrogeology Journal, 17(2)*, 409–424.

Hartmann, A., Jasechko, S., Gleeson, T., et al. (2021). Risk of groundwater contamination widely underestimated because of fast flow into aquifers. *PNAS, 118(20),* e2024492118.

Harvey, F. E., & Sibray, S. S. (2001) Delineating ground water recharge from leaking irrigation canals using water chemistry and isotopes. Ground Water, 39(30), 408-421.

Healy, R. W. (2010). *Estimating Groundwater Recharge*. Cambridge University Press.

Healy, R. W., & Cook, P. G. (2002), Using groundwater levels to estimate recharge. *Hydrogeology Journal, 10*(1), 91–109. https://doi.org/10.1007/s10040-001-0178-0↗.

Herczeg, A. L., Leaney, F. W. J., Stadler, M. F., Allan, G. L., & Fifield, L. K. (1997). Chemical and isotopic indicators of point-source recharge to a karst aquifer, South Australia. *Journal of Hydrology, 192*(1–4), 271–299. https://doi.org/10.1016/S0022-1694(96)03100-9↗.

Herczeg, A. L., Dogramaci, S.S., & Leaney, F. W. J. (2001). Origin of dissolved salts in a large, semi-arid groundwater system: Murray Basin, Australia. *Mar. Freshwater Res., drology, 52*, 41–52.

Hillel, D. (1982). *Introduction to Soil Physics.* Academic Press.

Hoehn, E., & Von Gunten, H. (1989). Radon in groundwater: a tool to assess infiltration from surface waters to aquifers. *Water Resources Research, 25* (8), 1795–1803. https://doi.org/10.1029/WR025i008p01795↗.

Howard, K. (2023). Urban groundwater. The Groundwater Project. https://doi.org/10.21083/978-1-77470-038-9↗.

Huang, Y., Evaristo, J., & Li, Z. (2019). Multiple tracers reveal different groundwater recharge mechanisms in deep loess deposits. *Geoderma, 353*, 204–212. https://doi.org/10.1016/j.geoderma.2019.06.041↗.

Ingraham, N. L. (1998). Isotopic variations in precipitation. In C. Kendall & J. J. McDonnell (Eds.), *Isotope Tracers in Catchment Hydrology* (pp. 87–118). Elsevier, Amsterdam.

Isiorho, S. A., Matisoff, G., & Wehn, K. S. (1996) Seepage relationships between Lake Chad and the Chad aquifers. Ground Water, 34(5), 819-826.

Iwata, Y., Hayashi, M., Suzuki, S., Hirota, T., & Hasegawa, S. (2010). Effects of snow cover on soil freezing, water movement, and snowmelt infiltration: A paired plot experiment. *Water Resources Research 46*(9). https://doi.org/10.1029/2009WR008070↗.

Johnson, A. C., Besien, T. J., Lal Bhardwaj, C., Dixon, A., Gooddy. D. C., Haria, A. H., & White, C. (2001). Penetration of herbicides to groundwater in an unconfined chalk aquifer following normal soil applications. *Journal of Contaminant Hydrology, 53*(1–2), 101–117. https://doi.org/10.1016/S0169-7722(01)00139-5↗.

Johnson, A. I. (1967). *Specific yield: compilation of specific yields for various materials*. (USGS Water-Supply Paper 1662-D). US Government Printing Office.

Johnston, C. D. (1987). Preferred water flow and focussed recharge in a variable regolith. *Journal of Hydrology, 94*, 129–142. https://doi.org/10.1016/0022-1694(87)90036-9↗.

Jolly, I. D., & Cook, P. G. (2002). Time lags in salinity control: controlling recharge and halting watertable rise. *Natural Resource Management, 5*(2), 16–21.

Jolly, I. D., Cook, P. G., Allison, G. B., & Hughes, M. W. (1989). Simultaneous water and solute movement through an unsaturated soil following an increase in recharge. *Journal of Hydrology, 111*(1–4), 391–396. https://doi.org/10.1016/0022-1694(89)90270-9↗.

Jonas, T., Marty, C., & Magnusson, J. (2009). Estimating the snow water equivalent from snow depth measurements in the Swiss Alps. *Journal of Hydrology 378*(1–2), 161–167. https://doi.org/10.1016/j.jhydrol.2009.09.021↗.

Junge, C. E., & Werby, R. T. (1958). The concentration of chloride, sodium, potassium, calcium, and sulfate in rain water over the United States. *Journal of Meteorology, 15*(5), 417–425. https://doi.org/10.1175/1520-0469(1958)015%3C0417:TCOCSP%3E2.0.CO;2↗.

Jurado, A., Bofill-Mas, S., Vázquez-Suñe, E., Pujades, E., Girones, R., & Rusiñol, M. (2019). Occurrence of pathogens in the river-groundwater interface in a losing river stretch (Besòs River Delta, Spain). *Science of the Total Environment, 696*, 134028.

Kalbus, E., Reinstorf, F., & Schirmer, M. (2006). Measuring methods for groundwater–surface water interactions: a review. *Hydrol. Earth Syst. Sci., 10*(6), 873–887. https://doi.org/10.5194/hess-10-873-2006↗.

Katz, B.S., Stotler, R.L., Hirmas, D., Ludvigson, G., Smith. J.J., & Whittemore, D.O. (2016). Geochemical recharge estimation and the effects of a declining water table. Vadose Zone Journal, https://doi.org/10.2136/vzj2016.04.0031↗.

Keese, K. E., Scanlon, B. R., & Reedy, R. C. (2005). Assessing controls on diffuse groundwater recharge using unsaturated flow modeling. *Water Resources Research, 41*, W06010. https://doi.org/10.1029/2004WR003841↗.

Kendy, E., Gérard-Marchant, P., Walter, M. T., Zhang, Y., Liu, C., & Steenhuis, T. S. (2003). A soil-water-balance approach to quantify groundwater recharge from irrigated cropland in the North China Plain. *Hydrological Processes, 17*, 2011–2031. https://doi.org/10.1002/hyp.1240↗.

Kennedy, C. D., Genereux, D. P., Corbett, D. R., & Mitasova, H. (2009). Spatial and temporal dynamics of coupled groundwater and nitrogen fluxes through a streambed in an agricultural watershed. *Water Resources Research, 45*, W09401. http://dx.doi.org/10.1029/2008WR007397↗.

Kennedy, C. D., Murdoch, L. C., Genereux, D. P., Corbett, D. R., Stone, K., Pham, P., & Mitasova, H. (2010). Comparison of Darcian flux calculations and seepage meter measurements in a sandy streambed in North Carolina, United States. *Water Resources Research, 46*(9), W09501. http://dx.doi.org/10.1029/2009WR008342↗.

Kennett-Smith, A., Cook, P. G., & Walker, G. R. (1994). Factors affecting groundwater recharge following clearing in the south western Murray Basin. *Journal of Hydrology, 154*(1–4), 85–105. https://doi.org/10.1016/0022-1694(94)90213-5↗.

Khan, S., Rana, T., Dassanayake, D., Abbas, A., Blackwell, J., Akbar, S., & Gabriel, H. F. (2009). Spatially distributed assessment of channel seepage using geophysics and artificial intelligence. *Irrigation and Drainage, 58*(3), 307–320. https://doi.org/10.1002/ird.415↗.

84

Kim, J. H., & Jackson, R. B. (2012). A global analysis of groundwater recharge for vegetation, climate, and soils. *Vadose Zone Journal*, *11*(1). https://doi.org/10.2136/vzj2011.0021RA↗.

Kirschbaum, M. U. F., & McMillan, A. M. S. (2018). Warming and elevated CO2 have opposing influences on transpiration. Which is more important? *Current Forestry Reports*, *4*, 51–71. https://doi.org/10.1007/s40725-018-0073-8↗.

Konrad, C. P. (2006). Location and timing of river-aquifer exchanges in six tributaries to the Columbia River in the Pacific Northwest of the United States. *Journal of Hydrology, 329*(3–4), 444–470. https://doi.org/10.1016/j.jhydrol.2006.02.028↗.

Koutantou, K., Mazzotti, G., & Brunner, P. (2021). UAV-based lidar high-resolution snow depth mapping in the Swiss Alps: Comparing flat and steep forests. *International Archives of the Photogrammetry, Remote Sensing and Spatial Information Sciences, XLIII-B3-2021*, 477–484. https://doi.org/10.5194/isprs-archives-XLIII-B3-2021-477-2021↗.

Koutantou, K., Mazzotti, G., Brunner, P., Webster, C., & Jonas, T. (2022). Exploring snow distribution dynamics in steep forested slopes with UAV-borne LiDAR. *Cold Regions Science and Technology, 200*, 103587. https://doi.org/10.1016/j.coldregions.2022.103587↗.

Kuniansky, E. L., Taylor C. J., Williams J.H., & Paillet F. (2022). Introduction to Karst Aquifers. The Groundwater Project. doi.org/10.21083/978-1-77470-040-2

Leaney, F. W., & Allison, G. A. (1986). Carbon-14 and stable isotope data for an area in the Murray Basin: Its use in estimating recharge. *Journal of Hydrology, 88*(1–2), 129–145. https://doi.org/10.1016/0022-1694(86)90201-5↗.

Lee, D. R. (1977). A device for measuring seepage flux in lakes and estuaries. *Limnology. Oceanography. 22*(1), 140–147. https://doi.org/10.4319/lo.1977.22.1.0140↗.

Lee, L. J. E., Lawrence, D. S. L., & Price, M. (2006). Analysis of water-level response to rainfall and implications for recharge pathways in the Chalk aquifer, SE England. *Journal of Hydrology, 330*(3–4), 604–620. https://doi.org/10.1016/j.jhydrol.2006.04.025↗.

Lemieux, J-M., Fortier, R., Murray, R., Dagenais, S., Cochand, M., Delottier, H., Therrien, R., Molson, J., Pryet, A., & Parhizkar, M. (2020). Groundwater dynamics within a watershed in the discontinuous permafrost zone near Umiujaq (Nunavik, Canada). *Hydrogeology Journal, 28*(3), 833–851. https://doi.org/10.1007/s10040-020-02110-4↗.

Lerner, D. N. (1990). Groundwater recharge in urban areas. *Atmospheric Environment. Part B. Urban Atmosphere, 24*(1), 29–33. https://doi.org/10.1016/0957-1272(90)90006-G↗.

Lerner, D. N. (2002). Identifying and quantifying urban recharge: a review. *Hydrogeology Journal, 10*, 143–152. https://doi.org/10.1007/s10040-001-0177-1↗.

Li, Z., Chen, X., Liu, W., & Si, B. (2017). Determination of groundwater recharge mechanism in the deep loessial unsaturated zone by environmental tracers. *Science of The Total Environment, 586*, 827–835. https://doi.org/10.1016/j.scitotenv.2017.02.061↗.

Liu, H.-L., Chen, X., Bao, A., Wang, L., Pan, X., & He, X. (2012). Effect of irrigation methods on groundwater recharge in alluvial fan area. *Journal of Irrigation and Drainage Engineering, 138*(3), 266–273.

Magesh, N. S., Chandrasekar, N., & Soundranayagam, J. P. (2012). Delineation of groundwater potential zones in Theni district, Tamil Nadu, using remote sensing, GIS and MIF techniques. *Geoscience Frontiers*, *3*(2), 189–196. https://doi.org/10.1016/j.gsf.2011.10.007↗.

Manna, F., Cherry, J. A., McWhorter, D. B., & Parker, B. L. (2016). Groundwater recharge assessment in an upland sandstone aquifer of southern California. *Journal of Hydrology, 541*(Part B), 787–799. https://doi.org/10.1016/j.jhydrol.2016.07.039↗.

Manna, F., Walton, K. M., Cherry, J. A., & Parker, B. L. (2017). Mechanisms of recharge in a fractured porous rock aquifer in a semi-arid region. *Journal of Hydrology, 555*, 869–880. https://doi.org/10.1016/j.jhydrol.2017.10.060↗.

Manning, A. H., & Solomon, D. K. (2005). An integrated environmental tracer approach to characterizing groundwater circulation in a mountain block. *Water Resources Resesach, 41*(12), W12412. https://doi.org/10.1029/2005WR004178↗.

Maqsoom, A., Aslam, B., Khalid, N., Ullah, F., Anysz, H., Almaliki, A. H., Almaliki, A. A., & Hussein, E. E. (2022). Delineating groundwater recharge potential through remote sensing and geographic information systems. *Water*, *14*(11), 1824. https://doi.org/10.3390/w14111824↗.

Marei, A., Khayat, S., Weise, S., Ghannam, S., Sbaih, M., & Geyer, S. (2010). Estimating groundwater recharge using the chloride mass-balance method in the West Bank, Palestine. *Hydrological Sciences Journal*, *55*(5), 780–791. https://doi.org/10.1080/02626667.2010.491987↗.

Marrero-Diaz, R., Alcalá, F. J., Pérez, N. M., López, D. L., Melián, G. V., Padrón, E., & Padilla, G. D. (2015). Aquifer recharge estimation through atmospheric chloride mass balance at Las Cañadas Caldera, Tenerife, Canary Islands, Spain. *Water*, *7*(5), 2451–2471. https://doi.org/10.3390/w7052451↗.

McCallum, A. M., Andersen, M. S., Rau, G. C., Larsen, J. R., & Acworth, I. (2014). River-aquifer interactions in a semiarid environment investigated using point and reach measurements. *Water Resources Research*, *50*(4), 2815–1829. https://doi.org/10.1002/2012WR012922↗.

McDonald, A. M., Lark, R. M., Taylor, R. G., Abiye, T., Fallas, H. C., Favreau G., Goni I. B., Kebede S., Scanlon B., Sorensen J. P. R., Tijani M., Kirsty A Upton, K. A., & West, C. (2021). Mapping groundwater recharge in Africa from ground observations and implications for water security. *Environmental Research Letters*, *16*(3*)*. https://iopscience.iop.org/article/10.1088/1748-9326/abd661↗.

McKenna, O. P., & Sala, O. E. (2018). Groundwater recharge in desert playas: current rates and future effects of climate change. *Environmental Research Letters, 13*, 014025. https://doi.org/10.1088/1748-9326/aa9eb6↗.

MDBA (2020). Murray-Darling Basin Plan Groundwater Methods Report: Determining the groundwater baseline and sustainable diversion limits. MDBA Publication no. 42/20, November 2020, Murray-Darling Basin Authority, Australian Government.

Meeks, J., Moeck, C., Brunner, P., & Hunkeler, D. (2017). Infiltration under snow cover: Modeling approaches and predictive uncertainty. *Journal of Hydrology, 546*, 16-27.

Meixner, T., Manning, A. H., Stonestrom, D. A., Allen, D. M., Ajami, H., Blasch, K. W., Brookfield, A. E., Castro, C. L., Clark, J. F., Gochis, D. J., Flint, A. L., Neff, K. L., Niraula, R., Rodell, M., Scanlon, B. R., Singha, K., & Michelle A. Walvoord, M. A. (2016). Implications of projected climate change for groundwater recharge in the western United States. *Journal of Hydrology, 534*, 124–138. https://doi.org/10.1016/j.jhydrol.2015.12.027.

Meredith, E., & Blais, N. (2019). Quantifying irrigation recharge sources using groundwater modelling. *Agriultural Water Management, 214*, 9–16. https://doi.org/10.1016/j.agwat.2018.12.032.

Meyland, S. J. (2011). Examining safe yield and sustainable yield for groundwater supplies and moving to managed yield as water resource limits become a reality. *WIT Transactions on Ecology and the Environment 145*, 813–823. https://doi.org/10.2495/WRM110731.

Moeck, C., Radny, D., Popp, A., Brennwald, M., Stoll, S., Auckenthaler, A., Berg, M., & Schirmer, M. (2017). Characterization of a managed recharge system using multiple tracers. *Science of The Total Environment, 609*, 701–714. https://doi.org/10.1016/j.scitotenv.2017.07.211.

Mohan, C., Western, A. W., Wei, Y., & Saft, M. (2018). Predicting groundwater recharge for varying land cover and climate conditions—a global meta-study. *Hydrology and Earth System Sciences, 22*(5), 2689–2703. https://doi.org/10.5194/hess-22-2689-2018.

Murdoch, L. C., & Kelly, S. E. (2003). Factors affecting the performance of conventional seepage meters. *Water Resources Research, 39 (6)*, 1163. http://dx.doi.org/10.1029/2002WR001347.

Noorduijn, S. L., Harrington, G. A., & Cook, P. G. (2014). The representative stream length for estimating surface water – groundwater exchange using Darcy's Law. *Journal of Hydrology, 513*, 353–361. https://doi.org/10.1016/j.jhydrol.2014.03.062.

Owuor, S. O., Butterbach-Bahl, K., Guzha, A. C., Rufino, M. C., Pelster, D. E., Díaz-Pinés, E., & Breuer, L. (2016). Groundwater recharge rates and surface cover runoff response to land use and land cover changes in semi-arid environments. *Ecological Processes, 5*(16). https://doi.org/10.1186/s13717-016-0060-6.

Peters, E., Visser, A., Esser, B. K., & Moran, J. E. (2018) Tracers reveal recharge elevations, groundwater flow paths and travel times on Mount Shasta, California. *Water, 10*(2), 97. https://doi.org/10.3390/w10020097.

Petheram, C., Walker, G., Grayson, R., Thierfelder, T., & Zhang, L. (2002). Towards a framework for predicting impacts of land-use on recharge: 1. A review of recharge studies in Australia. *Aust. J. Soil Res., 40*(3), 397–417.

Phillips, F. M., Mattick, J. L., Duval, T. A., Elmore, D., & Kubik, P. W. (1988). Chlorine 36 and tritium from nuclear weapons fallout as tracers for long-term liquid and vapor movement in desert soils, *Water Resources Research*, *24*(11), 1877–1891. https://doi.org/10.1029/WR024i011p01877.

Pomeroy, J. W., Gray, D. M., Hedstrom, N. R., & Janowicz, J. R. (2002). Prediction of seasonal snow accumulation in cold climate forests. *Hydrological Processes 16*(18), 3543–3558. https://doi.org/10.1002/hyp.1228.

Ponnusamy, D., Rajmohan, N., Li, P., Thirumurugan, M., Chidambaram, S., & Elumalai, V. (2022). Mapping of potential groundwater recharge zones: a case study of Maputaland plain, South Africa. *Environmental Earth Sciences*, *81*, 418. https://doi.org/10.1007/s12665-022-10540-4.

Qi, J., Vermeer, P., Cheng, G. (2006). A review of the influence of freeze-thaw cycles on soil geotechnical properties. *Permafrost and Periglacial Processes*, 17: 245-252. https://doi.org/10.1002/ppp.559

Reinecke, R., Schmied, H. M., Trautmann, T., Andersen, L. S., Burek, P., Flörke, M., Gosling, S. N., Grillakis, M., Hanasaki, N., Koutroulis, A., Pokhrel, Y., Thiery, W., Wada, Y., Yusuke, S., & Döll, P. (2021). Uncertainty of simulated groundwater recharge at different global warming levels: a global-scale multi-model ensemble study. *Hydrology and Earth System Sciences*, *25*(2), 787–810. https://doi.org/10.5194/hess-25-787-2021.

Rosenberry, D. O., & LaBaugh, J. W. (2008). Field techniques for estimating water fluxes between surface water and ground water: U.S. Geological Survey Techniques and Methods 4–D2. https://doi.org/10.3133/tm4D2.

Rugh, D. F., & Burbey, T. J. (2008). Using saline tracers to evaluate preferential recharge in fractured rocks, Floyd County, Virginia, USA. *Hydrogeology Journal, 16*, 251–262. https://doi.org/10.1007/s10040-007-0236-3.

Ruland, W. W., Cherry, J. A., & Feenstra, S. (1991). The depth of fractures and active ground-water flow in a clayey till plain in southwestern Ontario. *Groundwater, 29*(3), 405–417. https://doi.org/10.1111/j.1745-6584.1991.tb00531.x.

Rushton, K. R., & Ward, C. (1979). The estimation of groundwater recharge. *Journal of Hydrology, 41*, 345–361. https://doi.org/10.1016/0022-1694(79)90070-2.

Salley, K.A., Stotler, R.L., Johnson, W.C., Burt, D.J., Hirmas, D.R., Fifield, K., Bowen, M.W., Kastens, J.H., & Ryuh, Y.-G. (2022) Hydrology of a hydroperiod: Assessing recharge to the High Plains aquifer through a playa in western Kansas. *Journal of Hydrology, 612*, 128141.

Sanchez-Rodriguez, I., Ireson, A., Brannen, R., & Brauner, H. (2025). Insights into freeze–thaw and infiltration in seasonally frozen soils from field observations. *Vadose Zone Journal*, 24, e20396. https://doi.org/10.1002/vzj2.20396.

Santoni, C. S., Jobbágy, E. G. & Contreras, S. (2010). Vadose zone transport in dry forests of central Argentina: Role of land use. *Water Resources Research*, *46*(10), W10541. https://doi.org/10.1029/2009WR008784.

Scanlon, B. R. (1992). Evaluation of liquid and vapor water flow in desert soils based on chlorine 36 and tritium tracers and nonisothermal flow simulations. *Water Resources Research, 28*(1), 285–297. https://doi.org/10.1029/91WR02200↗.

Scanlon, B. R., & Goldsmith, R. S. (1997). Field study of spatial variability in unsaturated flow beneath and adjacent to playas. *Water Resources Research, 33*(10), 2239–2252. https://doi.org/10.1029/97WR01332↗.

Scanlon, B. R., Healy, R. W., & Cook, P. G. (2002). Choosing appropriate techniques for quantifying groundwater recharge. *Hydrogeology Journal, 10*(1), 18–39. https://doi.org/10.1007/s10040-001-0176-2↗.

Scanlon, B. R., Keese, K. E., Flint, A. L., Flint, L. E., Gaye, C. B., Edmunds, W. M., & Simmers, I. (2006). Global synthesis of groundwater recharge in semiarid and arid regions. *Hydrological Processes, 20*(15), 3335–3370. https://doi.org/10.1002/hyp.6335↗.

Scanlon, B. R., Langford, R. O., & Goldsmith, R. S. (1999). Relationship between geomorphic settings and unsaturated flow in an arid setting. *Water Resources Research, 35*(4), 983–999. https://doi.org/10.1029/98WR02769↗.

Scanlon, B. R., Reedy, R. C., & Tachovsky, J. A. (2007). Semiarid unsaturated zone chloride profiles: Archives of past land use change impacts on water resources in the southern High Plains, United States. *Water Resources Research, 43*, W06423.

Seiler, K-P., & Gat, J. R. (2007). *Groundwater Recharge from Run-Off, Infiltration and Percolation*. Springer, Dordrecht.

Shanafield, M. & Cook, P. G. (2014). Transmission losses, infiltration and groundwater recharge through ephemeral and intermittent streambeds: A review of applied methods. *Journal of Hydrology, 511*, 518–529. https://doi.org/10.1016/j.jhydrol.2014.01.068↗.

Slater, L., Zaidman, M. D., Binley, A. M., & West, L. J. (1997). Electrical imaging of saline tracer transport migration for the investigation of unsaturated zone transport mechanisms. *Hydrology and Earth System Sciences, 1*(2), 291–302. https://doi.org/10.5194/hess-1-291-1997↗.

Smith, D. B., Wearn, P. L., Richards, H. J., & Rowe, P. C. (1970). *Water movement in the unsaturated zone of high and low permeability strata by measuring natural tritium* (pp. 73–87). Isotope Hydrology 1970, Proceedings of a Symposium Vienna, 9–13 March 1970. IAEA, Vienna.

Solomon, D. K., Poreda, R. J., Cook, P. G., & Hunt, A. (1995). Site characterization using $^{3}H/^{3}He$ ground water ages, Cape Cod, MA. *Groundwater, 33*(6), 988–996. https://doi.org/10.1111/j.1745-6584.1995.tb00044.x↗.

Sorman, A. U., & Abdulrazzak, M. J. (1993). Infiltration-recharge through wadi beds in arid regions. *Hydrological Sciences Journal, 38*(3), 173–186. https://doi.org/10.1080/02626669309492661↗.

Standen, K., Costa, L. R. D., & Monteiro, J-P. (2020). In-channel managed aquifer recharge: A review of current development worldwide and future potential in Europe. *Water, 12*(11), 3099. https://doi.org/10.3390/w12113099↗.

Stone, A. E. C., & Edmunds, W. M. (2016). Unsaturated zone hydrostratigraphies: A novel archive of past climates in dryland continental regions. *Earth-Science Reviews, 157*, 121–144. https://doi.org/10.1016/j.earscirev.2016.03.007↗.

Storck, P., Lettenmaier, D. P., & Bolton, S. M. (2002). Measurement of snow interception and canopy effects on snow accumulation and melt in a mountainous maritime climate, Oregon, United States. *Water Resources Research 38*(11), 5-1–5-16. https://doi.org/10.1029/2002WR001281↗.

Stute, M., Deak, K., Revesz, K., Böhlke, J. K., Deseo, E., Weppernig, R., & Schlosser, P. (1997). Tritium/^{3}He dating of river infiltration: an example from the Danube in the Szigetkoz area, Hungary. *Groundwater, 35*(5), 905–911. https://doi.org/10.1111/j.1745-6584.1997.tb00160.x↗.

Suariz, D. L. (1989). Impact of agricultural practices on groundwater salinity. *Agriculture, Ecosystems and Environment, 26*, 215-227.

Sun, Q., Miao, C., Duan, Q., Ashouri, H., Sorooshian, S., & Hsu, K-L. (2018). A Review of Global Precipitation Data Sets: Data Sources, Estimation, and Intercomparisons. *Reviews of Geophysics 56*(1), 79–107. https://doi.org/10.1002/2017RG000574↗.

Theis, C. V. (1940). The source of water derived from wells: Essential factors controlling the response of an aquifer to development. *Civil Eng., 10*, 277–280.

Tobin, C., Schaefli, B., Nicótina, L., Simoni, S., Barrenetxea, G., Smith, R., Parlange, M., & Rinaldo, A. (2013). Improving the degree-day method for sub-daily melt simulations with physically-based diurnal variations. *Advances in Water Resources 55*, 149–164. https://doi.org/10.1016/j.advwatres.2012.08.008↗.

Tyler, S. W., & Walker, G. R. (1994). Root zone effects on tracer migration in arid zones. *Soil Science Society of America Journal, 58*(1), 25–31. https://doi.org/10.2136/sssaj1994.03615995005800010004x↗.

Vallet-Coulomb, C., Séraphin, P., Golçalvès, J., Radakovitch, O., Cognard-Plancq, A-L., Crespy, A., Babic, M., & Charron, F. (2017). Irrigation return flows in a Mediterranean aquifer inferred from combined chloride and stable isotope mass balances. *Applied Geochemistry, 86*, 92–104. https://doi.org/10.1016/j.apgeochem.2017.10.001↗.

Vásquez-Sũné, E., Carrera, J., Tubau, I., Sánchez-Vila, X., & Soler, A. (2010). An approach to identify urban groundwater recharge. *Hydrology and Earth System Sciences, 14*(10), 2085–2097. https://doi.org/10.5194/hess-14-2085-2010↗.

Villeneuve, S., Cook, P.G., Shanafield, M., Wood, C., & White, N. (2015). Groundwater recharge via infiltration through an ephemeral riverbed, central Australia. *Journal of Arid Environments, 117*, 47-58.

Visser, A., Moran, J. E., Singleton, M. J., & Esser, B. K. (2018). Importance of river water recharge to the San Joaquin Valley groundwater system. *Hydrological Processes, 32*(9), 1202–1213. https://doi.org/10.1002/hyp.11468↗.

Vogel, J. C. (1967). *Investigation of groundwater flow with radiocarbon* (pp. 355–369). Isotopes in Hydrology Conference. IAEA, Vienna.

Vogt, M.-L. A., Zwahlen, F., Pera, S., Mahamat, H. B., Hunkeler, D., & Brunner, P. (2024) Infiltration and recharge dynamics in the Nubian Sandstone Aquifer System of northern Chad. Hydrogeology Journal, 32, 417-431. https://link.springer.com/article/10.1007/s10040-024-02765-3↗.

Wada, Y., van Beek, L. P. H., van Kempen, C. M., Reckman, J. W. T. M., Vasak, S., & Bierkens, M. F. P. (2010). Global depletion of groundwater resources. *Geophysical Research Letters, 37*(20), L20402. https://doi.org/10.1029/2010GL044571↗.

Wakode, H. B., Baier, K., Jha, R., & Azzam, R. (2018). Impact of urbanization on groundwater recharge and urban water balance for the city of Hyderabad, India. *International Soil and Water Conservation Research, 6*(1), 51–62. https://doi.org/10.1016/j.iswcr.2017.10.003↗.

Walker, G. R., Jolly, I. D., & Cook, P. G. (1991). A new chloride leaching approach to the estimation of diffuse recharge following a change in land use. *Journal of Hydrology, 128*(1–4), 49–67. https://doi.org/10.1016/0022-1694(91)90131-Z↗.

Walvoord, M. A., & Phillips, F. M. (2004). Identifying areas of basin-floor recharge in the Trans-Pecos region and the link to vegetation. *Journal of Hydrology, 292*(1–4), 59–74. https://doi.org/10.1016/j.jhydrol.2003.12.029↗.

Wilson, J. L., & Guan, H. (2004). Mountain-block hydrology and mount-front recharge. In F. M. Philips, J. Hogan, & B. Scanlon (Eds.), *Groundwater Recharge in a Desert Environment: The Southwestern United States* (pp. 113–137). Water Science and Application Series, Vol. 9, American Geophysical Union. https://doi.org/10.1029/009WSA08↗.

Wood, W. W., & Sanford, W. E. (1995). Chemical and isotopic methods for quantifying ground-water recharge in a regional, semiarid environment. *Groundwater, 33*(3), 458–468. https://doi.org/10.1111/j.1745-6584.1995.tb00302.x↗.

Wood, W. W., Rainwater, K. A., & Thompson, D. B. (1997). Quantifying macropore recharge: Examples from a semi-arid area. *Groundwater, 35*(6), 1097–1106. https://doi.org/10.1111/j.1745-6584.1997.tb00182.x↗.

Yeh, H-F., Lee, C-H., Hsu, K-C., & Chang, P-H. (2009). GIS for the assessment of the groundwater recharge potential zone. *Environmental Geology, 58*, 185–195. https://doi.org/10.1007/s00254-008-1504-9↗.

Young, N. L., Lemieux, J.-M., Delottier, H., Fortier, R., & Fortier, P. (2020). A Conceptual Model for Anticipating the Impact of Landscape Evolution on Groundwater Recharge in Degrading Permafrost Environments. Geophysical Research Letters, 47, e2020GL087695. https://doi.org/10.1029/2020GL087695↗.

Zhang, L., Hume, I. H., O'Connell, M. G., Mitchell, D. C., Milthorpe, P. L., Yee, M., Dawes, W. R., & Hatton, T. J. (1999). Estimating episodic recharge under different crop/pasture rotations in the mallee region. Part 1. Experiments and model calibration. *Agricultural Water Management, 42*(2), 219–235. https://doi.org/10.1016/S0378-3774(99)00034-7↗.

Zhang, H., Xu, Y., & Kanyerere, T. (2020). A review of the managed aquifer recharge: Historical development, current situation and perspectives. *Physics and Chemistry of the Earth, Parts A/B/C, 118–119*, 102887. https://doi.org/10.1016/j.pce.2020.102887↗.

Zlotnik, V. A., Olaguera, F., & Ong, J. B. (2009). An approach to assessment of Flow regimes of groundwater-dominated lakes in arid environments. *Journal of Hydrology, 371(1-4)*, 22-30.

9   Exercises

Exercise 1 - Diffuse and Focused Recharge Volumes

The main recharge area of an aquifer covers 600 km². The mean annual precipitation rate is 500 mm/y, and the average diffuse recharge rate across this area has been estimated to be 25 mm/y. However, focused recharge also occurs. There are 30 shallow lakes, that recharge the aquifer. The leakage rate beneath these lakes has been estimated to be 200 mm/year. The size of the lakes vary, but the average size is approximately 20000 m². The area is also drained by a river, which is approximately 30 km long and averages 30 m width. The leakage rate beneath the base of the river has been estimated to be 2 mm/day.

Estimate the total volume of diffuse and focused recharge within the recharge area, and hence the proportion of diffuse and focused—lake and river—recharge.

Exercise 2 - Chloride Mass Balance

The goal is to estimate recharge in a semi-arid region with mean annual precipitation of 370 mm/y. Chloride data is available from 14 wells within the study area, and the chloride mass balance approach can be used to estimate the recharge rate. Chloride concentrations of water obtained from these wells are given in the first table. Monthly precipitation depth measurements and chloride concentrations of the samples are available as shown in the second table. What is the mean volume-weighted chloride concentration in precipitation and what is the estimated mean annual recharge, assuming that surface runoff is negligible? What is the spatial variability of the recharge rate?

Chloride concentrations (mg/L) measured for water samples from 14 wells within the study area..

210	312	345	297	354	179	245
274	102	473	425	303	186	243

Monthly rain depth and chloride concentration.

Month	Precipitation water equivalent (mm)	Chloride (mg/L)
Jan	47	3.2
Feb	36	3.5
Mar	39	4.1
Apr	24	3.9
May	27	5.4
Jun	17	6.5
Jul	12	6.8
Aug	19	6.1
Sep	29	5.3
Oct	27	4.9
Nov	30	5.8
Dec	44	3.9

Exercise 3 - Travel Time from Surface

Suppose that a water-borne contaminant is released to the soil surface. How long would it take for the contaminant to reach a depth of 10 m in the aquifer?

To accomplish this, one needs to calculate and sum three travel times: the time for water to move through 1) the plant root zone, 2) the unsaturated zone below the root zone, and 3) the top 10 m of the aquifer

The following assumptions should be made: a mean annual precipitation of 750 mm/y and recharge of 150 mm/y, root zone depth of 5 m, water table depth of 20 m, aquifer thickness of 50 m, porosity of 0.4, and volumetric water content in the unsaturated zone (including the root zone) of 0.2.

For the root zone, assume that plant roots extract water from the soil uniformly with depth, hence the uniform root extraction function of Tyler and Walker (1994) can be used. This is the equation that was used to calculate travel time through the root zone shown in Figure 2. This is equation 9 of Tyler & Walker (1994) and is shown here.

$$t(z) = \frac{z_R \theta}{R - P}\left[\ln\left(\frac{z(P - R)}{z_R P}\right)\right]$$

where (parameter dimensions are dark green font with mass as M, length as L, time as T):

P	=	precipitation rate (LT^{-1})
R	=	recharge rate (LT^{-1})
θ	=	volumetric water content (dimensionless)
z_R	=	depth of the plant root zone (L)
$t(z)$	=	time for water to travel to depth z ($z \leq z_R$) (T)

Equation (1) of Section 2.1 gives the travel time through the unsaturated zone below the root zone, and Equation (11) of Section 3.6 gives the travel time in the saturated zone.

Solution to Exercise 3↧

Return to where text linked to Exercise 3↧

10   Boxes

Box 1 - Groundwater Recharge in the West Bank, Palestine

Three groundwater basins have been identified in the West Bank, Palestine, based on the direction of groundwater flow (Figure Box 1-1). Groundwater in the Western Basin flows from east to west, from the mountains towards the Mediterranean Sea. Groundwater in the Northeastern Basin flows towards the north, and groundwater in the Eastern Basin flows from the mountains in the west towards the Dead Sea and the border with Jordan. Mean annual precipitation is 500–600 mm/y in the Northeastern Basin, and 450–650 mm/y in the Western Basin, but in the Eastern Basin it decreases from 650 mm/y in the mountains to less than 200 mm/y in parts of the Jordan Valley. Recharge in the drier areas is dominated by transmission losses from wadis. To estimate recharge across the West Bank, Marei and others (2010) used the chloride mass balance approach and assumed that the mean chloride concentration in groundwater could be used to assess recharge across the region, even in areas dominated by focused recharge. Chloride concentration in precipitation was measured at five sampling sites, with samples at one site collected over a period of four years to examine temporal variability. The average chloride concentration across all five sites was 9.3 mg/L. After also considering values measured in a previous study, the authors adopted a precipitation chloride value of 9.0 mg/L for the analysis. Fifty-seven groundwater samples were collected, with chloride concentrations ranging between 19 and 60 mg/L. Applying Equation (8), the recharge rates were thus estimated to range between 95 and 330 mm/y (Figure Box 1-1).
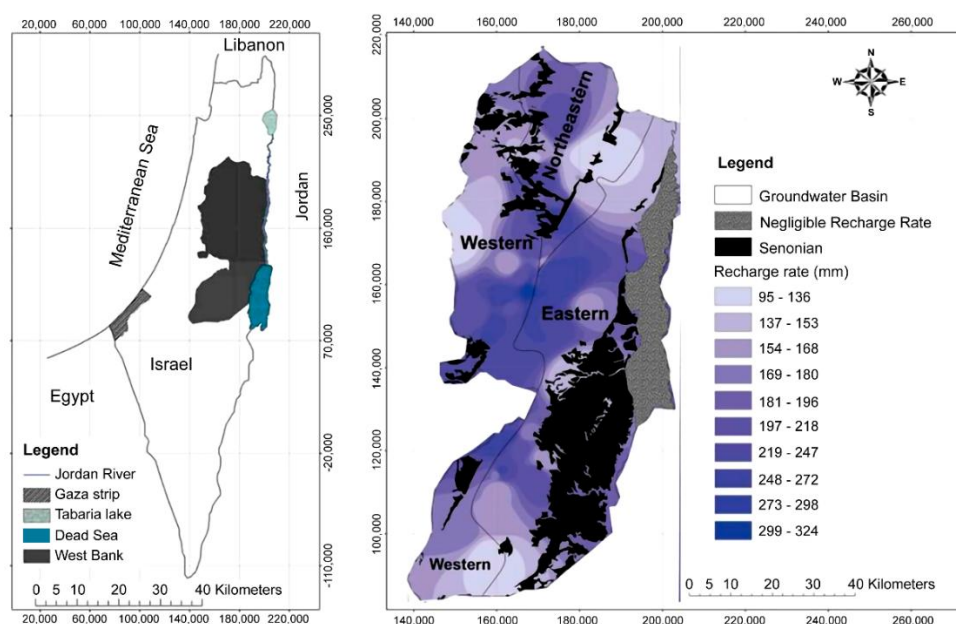

Figure Box 1-1 - Recharge rates across the West Bank, Palestine, obtained by contouring chloride mass balance recharge estimates obtained from 57 groundwater samples distributed across the area (reproduced from Marei et al., 2010).

Back to where text linked to Box 1⤴

96

Box 2 - Recharge processes in the English Chalk aquifer

A good early example of the use of ^{3}H to estimate recharge comes from the Lambourne catchment, which overlies the English Chalk aquifer, Berkshire, UK (Smith et al., 1970). ^{3}H concentrations in soil water were measured between 0.5 m depth and the water table at 27 m depth. A well-defined ^{3}H peak of approximately 550 TU was observed at 4 m (Figure Box 2-1), which was attributed to precipitation from 1963–64 when ^{3}H concentrations were highest. Sampling took place in 1968, 4–5 years after the period of highest ^{3}H levels in precipitation. A mean vertical water velocity of approximately 0.9 m/yr (900 mm/yr) is thus calculated from the position of the peak (4 m in 4.5 years). The mean volumetric soil water content was approximately 0.38, giving an estimated recharge rate of 340 mm/y, which is the average linear velocity calculated as $\left(\frac{900\frac{mm}{yr}}{0.388} \right)$. The smaller ^{3}H peak between 7 and 9 m depth is attributed to precipitation from 1958–1959 which also had high ^{3}H concentrations, although lower than in 1963–64.
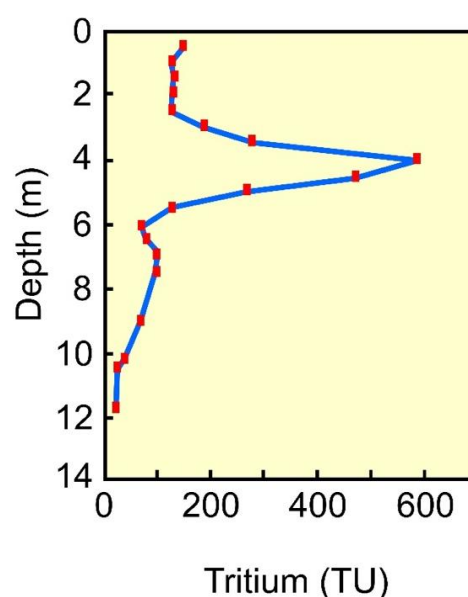

Figure Box 2-1 - Tritium concentrations measured in the upper 12 m of the unsaturated zone in Lambourn catchment, Berkshire, UK. The maximum ^{3}H concentration occurs at approximately 4 m depth and is attributed to high ^{3}H concentrations that occurred 4 to 5 years earlier in 1963–64 due to atmospheric testing of thermonuclear bombs. Although not shown here, ^{3}H concentrations between 10 and 40 TU were measured between 13 m and the water table at 27 m depth (redrawn from Smith et al., 1970).

Although not shown in Figure Box 2-1, ^{3}H concentrations between 12 m and the water table at 27 m range between 10 and 40 TU but showed no systematic trend with depth. Nevertheless, these values indicated some input of ^{3}H deep in the soil profile. The total ^{3}H within the soil profile is 863 TU m and is calculated by multiplying the measured ^{3}H concentration in soil water by the soil water content at each depth and summing over

97

the entire profile depth. At this site, about 15% of the total ^{3}H in the profile occurs below 13 m depth, which the authors attributed to transport of water through cracks within the chalk. Nevertheless, the existence of the well-defined ^{3}H peaks in the upper part of the profile suggests that most of the flow occurs by piston flow. After correcting for radioactive decay to 1968 (the time of sampling), the total ^{3}H that would have fallen as rain was calculated to be 2400 TU m. The total ^{3}H in the soil profile (863 TU m) is 36% of this value, which provides an estimate of the deep drainage fraction. Based on a mean annual precipitation of approximately 720 mm/y, this gives a mean deep drainage rate of 260 mm/y.

Back to where text linked to Box 2⤴

Box 3 - Recharge from the Gascoyne River, Western Australia

The Gascoyne River, northwestern Australia, is ephemeral and drains a catchment of approximately 75,000 km^2. The river extends over 700 km inland, but in its lower reaches (Figure Box 3-1), the river has a bed gradient of approximately 10^{-4}, a channel width of up to 1200 m, and is incised 3 to 5 m into the floodplain. Mean annual precipitation within the catchment is approximately 230 mm/y, and pan evaporation is 2900 mm/y. Surface water flow occurs for about 120 days each year, with large flow events triggered by cyclones. Mean annual flow is approximately 680 GL (giga-liters). Recharge from the river into the regional aquifer is indicated by the hydraulic head contours (Figure Box 3-1), which indicate flow away from the river to the north and south. Hydraulic gradients range from approximately 1×10^{-3} to 5×10^{-3}. Regional groundwater in this area is mostly brackish (chloride concentrations above 1000 mg/L), but fresh groundwater (less than 100 mg/L chloride) occurs within the sediments beneath and adjacent to the river due to aquifer recharge that occurs when the river flows (Figure Box 3-1). This fresh groundwater provides a resource that is used for municipal water supply and irrigation of horticultural crops. Recharge varies annually depending on precipitation and hence river flows, but a mean recharge rate of approximately 17 GL/y has been estimated (Dodson, 2008).
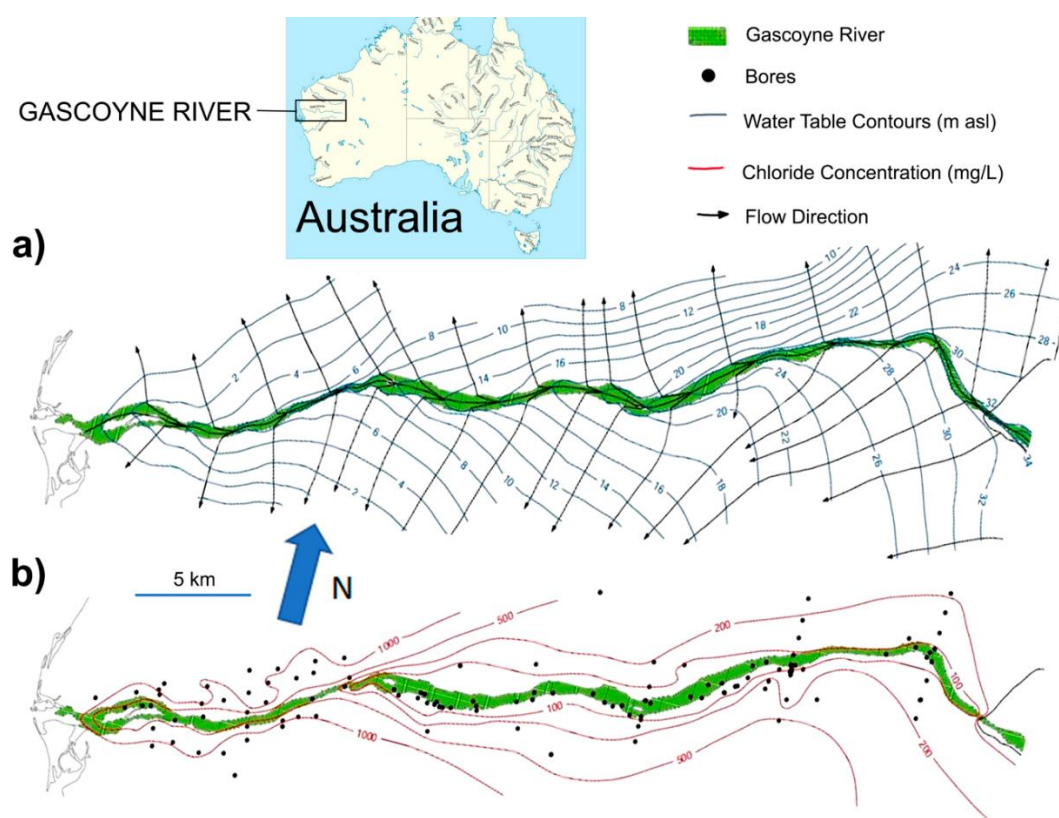

Figure Box 3-1 - The Gascoyne River, Western Australia. a) Water table contours and flownet (contour labels are m above sea level). b) Chloride concentration in groundwater (mg/L; blue circles denote well locations) (after Dodson, 2008).

Back to where text linked to Box 3

99

Box 4 - Recharge from the ephemeral Kuiseb River, Namibia

The Kuiseb River, one of the longest ephemeral rivers in Namibia, drains a catchment of more than 15,000 km^2. The river originates in a semi-arid (250–300 mm/y), high elevation (~1700 m) plateau, and flows across the arid Namib Desert. Most years, the headwaters of the river generate floods in the braided alluvial channel, which recharge the underlying alluvial aquifer. The river ultimately flows to the Atlantic Ocean, but most of the flow does not reach the ocean—discharge to the ocean has occurred only nine times over the last 120 years. Floods that produce channel flows less than 15 cm depth do not produced deep infiltration, but floods greater than this depth produce infiltration fluxes of 0.5 to 1.5 cm/h. Figure Box 4-1 shows two flow events recorded at the upstream Schlesien gauging station. Only one of these flows reached the Gobabeb gauging station, located 157 km downstream. Discharge records show that a minimum flood volume of 1.2 million m^3 at the upstream Schlesien gauging station is required for flow to reach the Gobabeb station. The average infiltration rate along the length of river channel connected to the alluvial aquifer is estimated to be about 330 m^3/km/h during periods of river flow (Benito et al., 2001). The relatively shallow water table (5 to 7 m depth) allows relatively rapid recharge beneath the river channel, with water table increases observed within 2 to 3 days. Very large floods that inundate floodplain areas produce large transmission losses, but proportionally less aquifer recharge due to lower infiltration rates and greater evapotranspiration losses. The water depth and duration of flows within the active streambed seem to determine the aquifer recharge rate from the river (Dahan et al., 2008; Benito et al., 2010). Riparian vegetation can, however, access the shallow aquifer so groundwater discharge is enhanced when the water table rises after flood events.
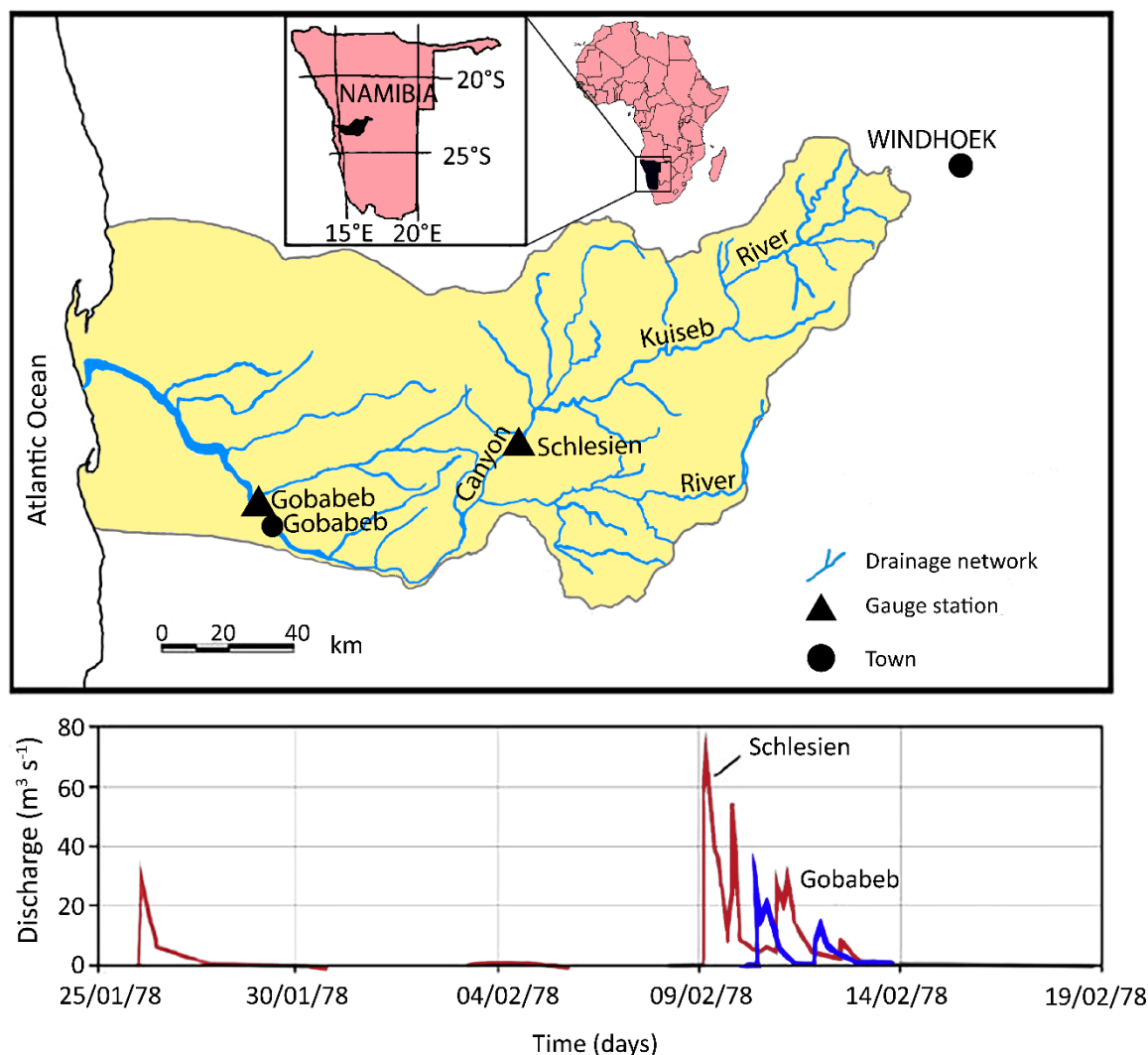
Figure Box 4-1 - Location of the Kuiseb River, Namibia, and flood hydrograph for summer 1978 recorded at the Schlesien and Gobabeb gauging stations shown as triangles, with town locations shown as circles (redrawn from Benito et al., 2010).

Back to where text linked to Box 4

101

Box 5 - Recharge from Tabalah Wadi, Saudi Arabia

Tabalah basin in the southwest of Saudi Arabia was heavily instrumented in the 1980s with precipitation and runoff monitoring stations and groundwater observation wells. Elevation in the basin ranges from 1200 to 2440 m above sea level, and the annual precipitation ranges from 100 mm/y at lower elevations to more than 300 mm/y along the ridges. Annual potential evapotranspiration is 2500 to 3200 mm/y. Wadi Tabalah drains an area of approximately 1270 km^2 and only flows after large rain events. Transmission losses have been estimated between two gauging stations located 23.8 km apart on the wadi (Abdulrazzak, 1995). The water table depth beneath the wadi between these gauging stations ranges between approximately 4 and 8 m.

Transmission loss was estimated as the difference between flow at the upstream and downstream gauging stations, with allowances made for tributary runoff contributions that enter the main channel between the gauging stations and evaporation losses during the flow event. Tributary runoff contributions were estimated using a runoff coefficient approach. Evaporation losses were estimated from pan evaporation data but were negligible for all flow events. Twenty-seven flow events that occurred between 1985 and 1987 were analyzed, and the water balances for three of these events are shown in Figure Box 5-1. In the flow event on May 21, flow at the downstream river gauging station was significantly less than upstream flow. For this event, storms were focused on the upper part of the catchment; so, the runoff input between the two gauging stations was relatively small. After subtracting for a small amount of surface runoff, the difference is attributed to transmission loss. However, for the flow events on April 10 and December 19, downstream flow exceeded upstream flow. For both these events, storms contributed a significant amount of water between the gauging stations. The calculated transmission loss is therefore relatively sensitive to calculation of the runoff inflow. The author observed that transmission losses were higher when a long period of time had elapsed since the last flow event, and hence the soil was drier and more able to accept infiltration. Approximately 75% of transmission losses in this section of Wadi Tabalah becomes groundwater recharge, with the remainder lost to evapotranspiration (Sorman & Abdulrazzak, 1993).
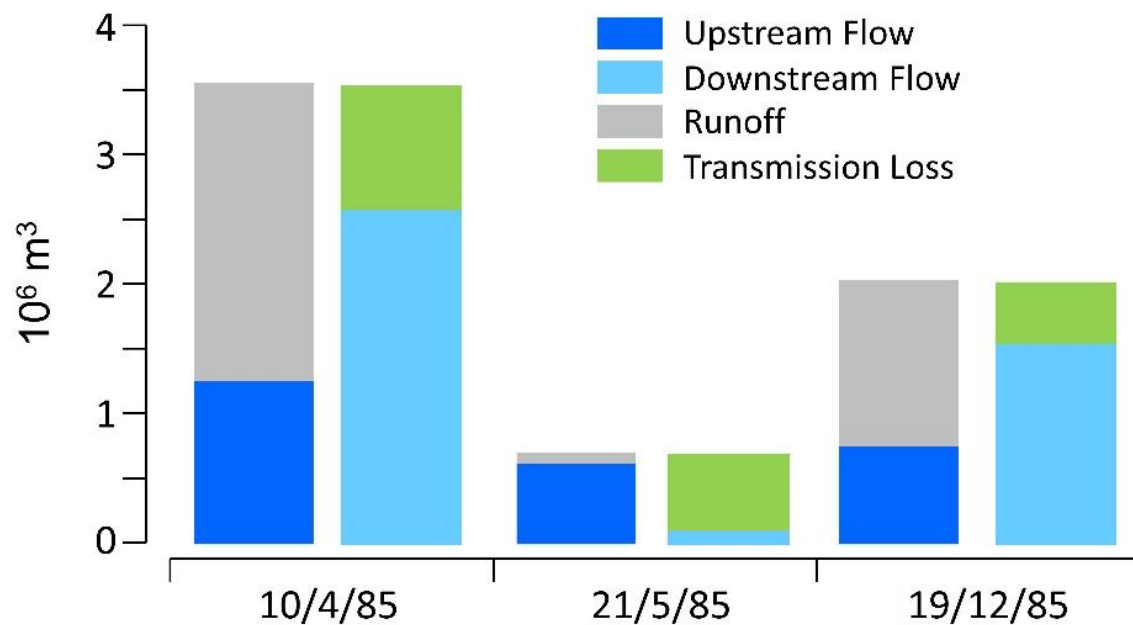
Figure Box 5-1 - Water balance of three flow events in Wadi Tabalah, Saudi Arabia. For two of the three flow events, flow at the downstream gauge exceeds that at the upstream gauge due to runoff that enters the wadi between the two gauging stations (Data from Abdulrazzak,1995).

11   Exercise Solutions

Solution Exercise 1

Area of lakes and rivers does not receive diffuse recharge, but is an insignificant portion of the total area and does not make a significant difference in the total recharge:

$$\text{Area Lakes and Rivers} = (30)\,20{,}000\ \text{m}^2 + \left(30\ \text{km}\frac{1000\ \text{m}}{1\ \text{km}}\right)30\ \text{m} = 1.5\text{x}10^6 \text{m}^2$$

The diffuse recharge volume:

$$\text{Diffuse recharge Volume} = (\text{Area Basin} - \text{Area Lakes and Rivers})\,(\text{Recharge Rate})$$

$$= \left(600\ \text{km}^2\,\frac{1\text{x}10^6\ \text{m}^2}{\text{km}^2} - 1.5\text{x}10^6 \text{m}^2\right)\left(25\ \frac{\text{mm}}{\text{y}}\frac{1\ \text{m}}{1000\ \text{mm}}\right)$$

$$= 1.5\text{x}10^7\,\frac{\text{m}^3}{\text{y}}$$

The volume of focused recharge from lakes:

$$\text{Focused recharge Volume} = (\text{Number Lakes})\,(\text{Average Area})(\text{Leakage Rate})$$

$$= (30)\,20{,}000\ \text{m}^2\left(200\ \frac{\text{mm}}{\text{y}}\frac{1\ \text{m}}{1000\ \text{mm}}\right) = 1.2\text{x}10^5\,\frac{\text{m}^3}{\text{y}}$$

The volume of focused recharge from rivers:

$$\text{Focused River Recharge Volume} = \text{Area (Leakage Rate)}$$

$$= \left(30\ \text{km}\frac{1000\ \text{m}}{1\ \text{km}}\right)30\ \text{m}\left(2\ \frac{\text{mm}}{\text{day}}\frac{1\ \text{m}}{1000\ \text{mm}}\frac{365\ \text{d}}{1\ \text{y}}\right) = 6.57\text{x}10^5\,\frac{\text{m}^3}{\text{y}}$$

The total recharge is the sum of these three quantities, which is $1.5\text{x}10^8\,\frac{\text{m}^3}{\text{y}}$.

Thus, diffuse recharge contributes 95% of the total, and focused recharge is 5%, with lake recharge approximately 1% and river recharge approximately 4%. Focused recharge usually only contributes a large fraction of total recharge when diffuse recharge is very low, or where there is a very high density of focused recharge features.

<div align="right">

Return to Exercise 1↰

Return to where text linked to Exercise 1↰

</div>

Solution Exercise 2

The chloride mass balance equation can be written:

$$R = \frac{C_P P}{C_R}$$

where R is the recharge rate (mm/y), P is the precipitation rate (mm/y), and C_R and C_P are chloride concentrations in recharge and precipitation, respectively (Equation (8) of Section 3.4).

To determine the volume-weighted average chloride concentration in groundwater, we first calculate the total chloride mass in each sample. This is calculated by multiplying the precipitation depth by the chloride concentration and is shown in column four of the table below in units of (mm mg/L). These units could be converted to mg per square meter of land surface—a more commonly used unit for chloride fallout—but there is no need to do this. These monthly values are then summed, and the result is divided by the total amount of precipitation. The amount weighted mean chloride concentration is thus 1617/351 = 4.6 mg/L. Given that we left the units for chloride mass as "mm mg/L", it was easy to calculate the average concentration in units of mg/L. The mean chloride concentration in groundwater is 282 mg/L. Using C_P = 4.6 mg/L, P = 370 mm/y and C_R = 282 mg/L gives a mean recharge rate of R = 6.0 mm/y. The mean annual precipitation is used, rather than the total precipitation over the one-year period with precipitation chemistry data because the concentration in the groundwater reflects the arrival of water over a longer period than one year.

The spatial variability of recharge is indicated by the variability of the chloride concentration in groundwater. Using the maximum and minimum measured concentrations in groundwater (473 and 102 mg/L, respectively) in the chloride mass balance equation, produces minimum and maximum recharge rates respectively of 3.6 and 16.7 mm/y. Spatial variability may be greater than this because of the small number of wells that were sampled, and because dispersion within the aquifer and mixing during sampling is likely to smooth out the original variability of chloride concentration in recharge. Thus, recharge at some locations would have been less than 3.6 mm/y, and at other locations it would have been greater than 16.7 mm/y.

Month	Precipitation Depth (mm)	Chloride Concentration (mg/L)	Product of Precipitation Depth and Chloride Concentration (mm mg/L)
Jan	47	3.2	150
Feb	36	3.5	126
Mar	39	4.1	160
Apr	24	3.9	94
May	27	5.4	146
Jun	17	6.5	111
Jul	12	6.8	82
Aug	19	6.1	116
Sep	29	5.3	154
Oct	27	4.9	132
Nov	30	5.8	174
Dec	44	3.9	172
TOTAL	**351**		**1617**

.

Solution Exercise 3

Travel times are calculated separately for the root zone, the unsaturated zone below the root zone, and the saturated zone.

Root Zone

Using Equation (9) of Tyler and Walker (1994) with the same value of 5 m for both z and z_R allows calculation of the travel time to the bottom of the root zone ($z = z_R$).

$$t(z) = \frac{z_R \theta}{R - P} \left[\ln \left(1 - \frac{z(P - R)}{z_R P} \right) \right]$$

$$t(z) = \frac{5 \text{ m } 0.2}{\left(0.15 \frac{\text{m}}{\text{y}} - 0.75 \frac{\text{m}}{\text{yr}} \right)} \left[\ln \left(1 - \frac{5 \text{ m} \left(0.75 \frac{\text{m}}{\text{y}} - 0.15 \frac{\text{m}}{\text{y}} \right)}{5 \text{ m } 0.75 \frac{\text{m}}{\text{y}}} \right) \right] = 2.7 \text{ y}$$

Using the same value for both z and z_R allows calculation of travel time to the bottom of the root zone ($z = z_R$). Substituting these values into the equations gives a total travel time to the base of the root zone $t(z_R)$ of 2.7 years.

Unsaturated Zone below the root zone

The travel time of water from the base of the plant root zone is calculated using Equation (1).

$$t = \frac{(z_{WT} - z_R)\theta}{R}$$

$$t = \frac{(20 \text{ m} - 5 \text{ m})0.2}{0.15 \frac{\text{m}}{\text{y}}} = 20 \text{ y}$$

Another way to envision this is: the recharge rate is $R = 0.15$ m/year. Since the volumetric water content is 0.2, the water velocity is $R/\theta = 0.15$ m/year/0.2 = 0.75 m/year. Given the thickness of the unsaturated zone below the root zone is $z_{WT} - z_R = 20 - 5 = 15$ m, the travel time is (15 m)/(0.75 m/year) = 20 years.

Groundwater age (or travel time)

Travel time in the saturated zone is given by Equation (11).

$$t = \frac{H\varepsilon}{R} \ln \left(\frac{H}{H-z} \right)$$

$$t = \frac{50 \text{ m } 0.4}{0.15 \frac{\text{m}}{\text{y}}} \ln \left(\frac{50 \text{ m}}{50 \text{ m} - 10 \text{ m}} \right) = 29.8 \text{ y}$$

This calculation assumes a uniform aquifer of constant thickness, receiving constant recharge. If the simpler Equation 12 was used here, the calculated groundwater travel time would be 26.7 y. This is only about 10% different to that obtained using Equation 11.

Total travel time for water-borne contaminant.

Summing the root zone, unsaturated zone below the root zone, and groundwater travel times, gives a total travel time of 2.7 + 20.0 + 29.8 = 52.5 y.

Return to Exercise 3⤴

Return to where text linked to Exercise 3⤴

12 Notations

C_P	=	chloride concentration of precipitation (including dust particles (ML^{-3})
C_R	=	chloride concentration of groundwater recharge (ML^{-3})
$\Delta\Sigma$	=	change in moisture storage per unit area (LT^{-1})
D eq(6)	=	vertical discharge rate per unit area for the region of interest (e.g., evapotranspiration loss of groundwater (LT^{-1})
D eq(14)	=	deep drainage rate (LT^{-1})
ΔS eq(2)	=	change in moisture storage per unit area above the water table (LT^{-1})
ΔS eq(6)	=	change in moisture storage per unit area in the saturated zone (LT^{-1})
E_a	=	evapotranspiration (L^3T^{-1})
ET	=	actual evapotranspiration (LT^{-1})
ε	=	porosity (dimensionless)
h	=	water table height (L)
H	=	aquifer thickness (L)
P	=	precipitation rate (LT^{-1})
$PAWC$	=	plant available water capacity (L)
Q_d	=	downstream flow (L^3T^{-1})
Q_f	=	surface water—groundwater exchange (L^3T^{-1})
Q_{gwin}	=	horizontal groundwater flow per unit area into the region of interest (LT^{-1})
Q_{gwout}	=	horizontal groundwater flow per unit area out of the region of interest (LT^{-1}))
Q_{in}	=	inflow from surface *runoff* (LT^{-1})
Q_{out}	=	outflow from surface *runoff* (LT^{-1})
Q_p	=	diversions from the stream (L^3T^{-1})
Q_t	=	inflow from tributaries or surface runoff (L^3T^{-1})
Q_u	=	upstream flow (L^3T^{-1})
R	=	recharge rate (LT^{-1})
Sy	=	specific yield (dimensionless)
dt	=	derivative of time (T)

109

t	=	groundwater age (T)
t_1 eq(9)	=	application time (T)
t_1 eq(14)	=	time lag from land use change to change in recharge rate (T)
t_2	=	observation time (T)
θ	=	average volumetric soil water content between these two depths (dimensionless)
θ_d	=	mean water content of the soil profile that will result under the new land use after the pressure has moved through the unsaturated zone and the recharge rate has increased (dimensionless)
θ_{FC}	=	volumetric soil water content at field capacity (dimensionless) - often defined as the content to which an initially saturated soil drains after 1 to 2 days
θ_w	=	mean water content of the soil profile before the change in land use (dimensionless)
θ_{WP}	=	volumetric soil water content at the wilting point (dimensionless) - content at which the osmotic pressure in plant roots no longer exceeds the surface tension of water held on soil particles
z	=	depth below the water table (L)
z_1	=	application depth of the tracer (L)
z_2	=	observed tracer depth at time t_2 (L)
z_R	=	thickness of the plant root zone (L)
z_{wt}	=	water table depth (L)

13   About the Authors

Peter Cook is a Professorial Research Fellow at Flinders University, South Australia, and Director of the Australian National Centre for Groundwater Research and Training. He previously spent more than 20 years as Research Scientist with CSIRO. With more than 30 years of experience, Dr. Cook has worked on groundwater investigations in Australia, Europe, North America, and Africa. He regularly advises Australian and international governments on water management and has consulted for attorneys, industries, engineering companies, government agencies and citizen groups on groundwater issues. He has conducted projects on a broad range of groundwater topics many of which have involved the application of environmental tracers and isotopes. These have included assessment of rates of groundwater recharge and discharge, surface water-groundwater interactions, groundwater-dependence of vegetation, impacts of mining, and unconventional gas on groundwater and regional groundwater management. He has written or co-written books on environmental tracers and ecohydrology and was the NGWA Darcy Lecturer in 2009.

Philip Brunner is a full professor at the Centre for Hydrogeology and Geothermics (CHYN) at the University of Neuchâtel in Switzerland. He received his PhD from ETH in Zurich and spent three years as a postdoctoral researcher at Flinders University in Australia. Since 2012, he has headed the "Hydrogeological Processes" group. From 2018 to 2022 he was Institute Director of the CHYN. The overall aim of his research is to develop quantitative tools for the sustainable management of surface and subsurface water resources. His research is highly interdisciplinary, and his group develops and applies methods from a wide range of research fields, including physically based numerical modeling, remote sensing, scientific computing, and isotopic chemistry. His work has applications in fields outside classical hydrogeology, such as agriculture, ecohydrology, engineering, or sustainable use of water and soil resources.

Please consider signing up to the GW-Project mailing list to stay informed about new book releases, events, and ways to participate in the GW-Project. When you sign up for our email list it helps us build a global groundwater community. Sign up↗.